Cape Peninsula
University of Technology

MODELLING AND DESIGN ISSUES OF MODEL PREDICTIVE CURRENT CONTROL OF A VOLTAGE SOURCE CONVERTER

by

PENELOPE SUKE

Dissertation submitted in partial fulfillment of the requirements for the degree

Master of Engineering: Energy

in the Faculty of Engineering and the Built Environment

at the Cape Peninsula University of Technology

Supervisor: **Dr. Ali-Mustafa-Ali Almaktoof**
Co-supervisor: **Prof. Atanda Raji**

Bellville Campus

Date submitted: June 2023

DECLARATION

I, Penelope Suke, declare that the contents of this dissertation/thesis represent my own unaided work and that the dissertation/thesis has not previously been submitted for academic examination towards any qualification. Furthermore, it represents my opinions, not necessarily those of the Cape Peninsula University of Technology.

03/06/2023

Signed **Date**

ABSTRACT

This research implements a Model Predictive Current Control scheme to monitor the output current for a three-phase, two-level VSC. A Finite State-Model Predictive Current Control technique will be presented for a three-phase, two-level VSC. Finite State Model Predictive Current Control proved to be a viable control method for power converters. One of several key benefits is the ability to monitor several system parameters with a single control rule by combining the system parameters with correct weighting factors. Nevertheless, these coefficients are determined through empirical calculations in the present leading-edge research. Thus far, no analytical or numerical method has been devised to obtain an ideal resolution. Furthermore, the empirical technique is not often concise, and no processes have already been identified. The whole research presents a method to a set of instructions that reduces the unpredictability of this process. Firstly, FS-MPCC will be introduced to decrease the computation effort for Model Predictive Current Control as well as to forecast future load current value for all eight generated potential switching states produced by the converter. secondly, this study classifies various cost functions and compares the performance of a system using delay compensation to a system without delay compensation. The objective is to assess the influence of delay compensation on the desired outcome and overall system performance. The various phases of the empiric process are then described. Lastly, the performance assessment of the FS-MPCC for a three-phase, two-level voltage source converter is reviewed in terms of power quality, dynamic performance, and tracking behavior. Modeling and simulation will be performed using the programs MATLAB / Simulink.

Keywords - Voltage Source Converter, Delay Compensation, Finite Set-Model predictive Current Control, weighting factors, cost functions, MATLAB/Simulink

ACKNOWLEDGEMENTS

I would like to extend my heartfelt gratitude to the individuals and institutions listed below for their invaluable support in the successful completion of this dissertation:

- My supervisors, Dr. Ali-Mustafa-Ali Almaktoof and Dr. Atanda Raji, for their guidance and expertise.
- The Engineering and the Built Environment faculty members at the Cape Peninsula University of Technology for their encouragement and knowledge sharing.
- The management and staff of the CPUT Library for their exceptional assistance and willingness to provide me with the essential information required for this research project. Your diligence and assistance have been indispensable to the completion of my thesis.
- My family and friends for their unwavering love and encouragement.

Thank you all for your contributions to this work.

TABLE OF CONTENTS

TABLE OF FIGURES

TABLE OF TABLES

GLOSSARY

Cost Function refers to a mathematical formulation that quantifies the intended control objectives and captures the trade-offs between different system variables.

Voltage Vector refers to a set of voltage values applied to the control inputs of a power electronic converter, typically a voltage source converter, to accomplish the desired control goals.

A Switching State refers to the combination of the on and off phases of the power electronic switches in a converter system.

Switching Frequency refers to the rate at which the on/off phases of the power electronic switches in a converter system change.

A power converter refers to an electronic device or circuit that converts electrical power between different forms.

LIST OF ABBREVIATIONS

PV	Photovoltaic
VSCs	Voltage Source Converters
CSI	Current Source Inverter
MPC	Model Predictive Control
MPCC	Model Predictive Current Control
CS-MPC	Continuous Set Model Predictive Control
FS-MPCC	Finite Set Model Predictive Current Control
GPC	Generalized Predictive Control
Ts	Sampling Time
PWM	Pulse Width Modulation
SVPWM	Space Vector pulse width modulation
HVDC	High Voltage Direct Current
EMI	Electromagnetic Interference
WTS	Wind Turbine system
2L-BTB	2 Level Back-to-Back
SEIG	Self-Excited Induction Generator
PMSG	Permanent Magnet Synchronous Generator
DFIG	Doubly Fed Induction Generator
2L-PWM-VSC	Pulse Width Modulation-Voltage Source Converter
IGBTs	Insulated Gate Bipolar Transistors
GTOs	Gate turn-off thyristors
THD	Total Harmonic Distortion
AC	Alternating Current
DC	Direct Current
RESs	Renewable energy systems
LHB	Lower Band Hysteresis
UHB	Upper Band Hysteresis
PID	Proportional-Integral-Derivative
PI	Proportional-Integral
RMS	Root-Mean-Square

CHAPTER ONE

INTRODUCTION

1.1. Introduction

According to recent estimates, global energy usage is expected to increase by approximately 28% from 2015 to 2040 (Hannan *et al.*, 2019), (Zhang *et al.*, 2022). The majority of this energy is obtained through the combustion of fossil fuels such as coal, natural gas, and nuclear resources. The usage of these sources has caused a significant threat to the environment and human lives. Renewable energy sources like wind and photovoltaic (PV) energy are long-term energy supply solutions that can dramatically reduce dependency on fossil fuels while meeting rapidly rising energy demand. Renewable energy sources are becoming the best options for generating electricity because of the harmful effects of emissions from fossil-fuel power stations, increased energy demand, and the increasing depletion of conventional energy (Tamrakar *et al.*, 2018), (Al-Shetwi, 2022).

In recent years, there has been a notable rise in the use of power converters within renewable energy conversion systems. This growth can be attributed primarily to the escalating energy demands and growing environmental consciousness. Electricity and heat production, for example, account for 42% of world emissions (Hannan *et al.*, 2019). As a result, Renewable energy systems (RESs) based on power electronic converters incorporating "clean" power production can be used as a replacement for power plants that rely on fossil fuels. Photovoltaic generation systems serve as a compelling example of power converter applications, as they necessitate a converter for the transmission of electricity from the PV panel to the grid (M. H. Rashid, 2007), (Rodriguez and Cortes, 2012), (Rodriguez and Cortes, 2015), (Verbytskyi *et al.*, 2022). The incorporation of power converters into electrical grids to promote the use of renewable energy is a new method for solving stability problems.

Power converters, such as Voltage Source Converters (VSCs), have managed to gain recognition during the last years. VSCs are used in most industrial sectors due to their excessive ability to improve grid quality and reliability, enhance performance, and increase efficiency leading to higher production rates (Rodriguez and Cortes, 2015), (Pandey, Purwar and Sharma, 2017). The first voltage source converter was tested on March 10, 1997, between Hellsjön and Grängesberg in central Sweden. During the last decades of the VSCs, many control schemes have been suggested. Moreover, the Model Predictive Current Control (MPCC) has gained considerable appeal over the years due to its robustness, ease of inclusion of non-linearity and constraints, and rapid

dynamic response compared to other control schemes (Rameshkumar *et al.*, 2014), (Shiravani *et al.*, 2022).

Early implementations of predictive control schemes in control electronics started in the 1980s (Rodriguez and Cortes, 2015), (Almaktoof *et al.*, 2017). The predictive control techniques are based on a predictive model of the system under control, which is utilized to predict the plant's behavior and select an ideal value for the control variables.

Because power converters consist of a limited set of switching states, the approach used is the Finite Set Model Predictive Current Control (FS-MPCC) technique. FS-MPCC utilizes the converter model to anticipate the current behavior associated with each specific switching state of the converter (Cortes *et al.*, 2012), (Han *et al.*, 2016). The cost function analyzes and assesses all conceivable switching states. A description of the cost function in Model Predictive Current Control is feasible by taking into account several variables and weighting factors. Consideration of these factors enables the converter to supply the current load close to the reference current, thus reducing total harmonic distortion and switching frequency (Kumar *et al.*, 2014), (Abbaszadeh *et al.*, 2017), (Sandre-Hernandez, De Jesus Rangel-Magdaleno and Morales-Caporal, 2019).

The cost function is not confined to monitoring a given value and to regulating the device. MPCC's key benefits are that the cost function embraces any essential term needed that may reflect a forecast of another device element, device restriction, or device necessity (Cortes *et al.*, 2012), (Ławryńczuk and Nebeluk, 2021). As such terms are also more probable to be of a distinctly physical nature (voltage, current, reactive force, flux, lack of switching, and torque), their measures and magnitudes can often vary significantly (Rodriguez and Cortes, 2015). In MPCC, this issue is commonly discussed by using weighting factors for every cost-function term. The approach to weighting factor adjustment can differ based on what kind of terms are available in the cost function. For example, a compromise reach is necessary between the following reference and control effort in a control system. In a three-phase, two-level VSC, the control effort can be characterized by the displacement of the voltage vector applied to the load. This displacement can be incorporated as an additional term in the cost function to quantify the cumulative discrepancy between the previously implemented voltage vector and the intended voltage vector for implementation (Rodriguez and Cortes, 2015). By amplifying the weighting factor within the cost function, the control effort can be effectively reduced or minimized.

1.2. Power converters

Power converters are electronic devices dealing with electrical power transfer, control, and conditioning, using electronic power drives. Thanks to its improved implementation and higher capacity, which results in higher output speeds, the utilization of power converters has gained popularity in numerous applications over the past several years (Rodriguez and Cortes, 2015), (Lipu *et al.*, 2022). Power converters have been an enabling technology commonly used in residential and industrial applications to allow consistent and efficient power control between source and load.

The first power converter produced was a transformer in 1885 (Zhang *et al.*, 2018), (Allerhand, 2021), which was used to Boost or reduce the voltage (AC-AC) of AC systems and to transfer energy over a significant distance through transmission lines at the same frequency at a lower loss from power plants to customers. In practical implementations, it was anticipated that electrical energy would be transferred from one type to another, for example, between AC and DC, or even to various voltages or frequencies, or any variations of those demands that transformers could not completely satisfy. To solve these problems, semi-conductor switches, and power electronics were introduced. The history of power electronics is related to the production of power semiconductor devices and breakthroughs. The first control electronics system developed in 1900 (Zhang *et al.*, 2018), was a mercury arc rectifier. Thereafter several power electronics devices and numerous control strategies were created to perform specific applications. There are several types of power transfer schemes that are classified by combining sources and forms of loads (DC or AC). Several of the many common forms of power transmission systems are discussed below.

1.2.1. Various categories of power converters

Figure 1.1 illustrates various categories of power converters commonly employed in numerous industrial applications for different purposes. Discussed below are descriptions of these power converters.

a. AC – DC transform current or unmonitored DC voltage from AC.

b. The DC-DC converter transforms the input voltage from DC to DC, including output voltage regulation and insulation control.

c. DC-AC transforms voltage from DC to AC voltage.

d. AC - AC transforms AC waveforms with a similar frequency and magnitude to AC waveforms with a different frequency at a different magnitude.

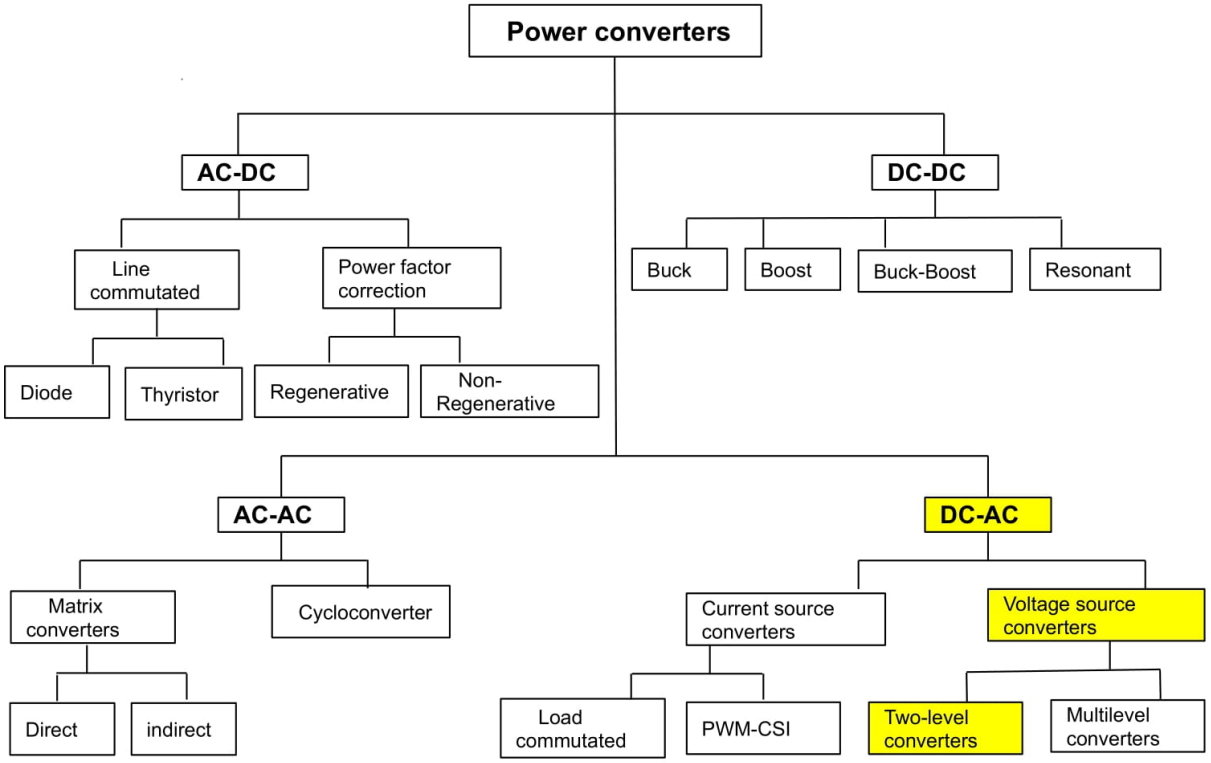

Figure 1. 1: Categorization of power converters.

1.2.2. Power Converter Applications

i. Power electronic converters play a substantial role in the realm of implementing renewable energy solutions. They facilitate the establishment of DC microgrids, enabling the efficient utilization of renewable energy and ensuring reliable connections between energy storage systems and renewable energy sources. Furthermore, they contribute to the electrification of remote villages and rural areas, thereby promoting sustainable energy access and development in underserved regions (Rodriguez and Cortes, 2015).

ii. Power converters, specifically three-phase, two-level VSCs, find extensive application in transportation systems, particularly electric trains. These converters are employed to transmit electricity from overhead lines to the motors by generating the necessary voltages for monitoring the torque and speed of the electric motors.

1.2.3. The three-phase, two-level VSC

For several applications, 3-phase, 2-level, voltage source converters are being extensively studied as the main connectors among power sources and loads in distribution networks in certain industrial and domestic industries (Almaktoof *et al.*, 2014), (Patel and Sood, 2018). However, there are various kinds of grid or load disturbances that pose significant challenges to the regular functioning of the VSC. Grid or load unbalance is one of the few abnormal states that on the DC link can contribute to broad double-frequency current/voltage ripples (Tang *et al.*, 2018). The efficiency of the output voltage produced by VSC relies on the control scheme employed (Seetharamaiah, 2008), (Bi *et al.*, 2022). The primary purpose of the control method is to produce an output voltage similar to the sinusoidal waveforms. Most control methods are designed to minimize total harmonic loss and switch loss. The number of control schemes introduced for the three-phase, two-level VSC, are listed below are shown in Figure 1.2.

1.3. Approaches and Methods for Controlling Power Converters

To achieve the desired performance of a power converter system in the presence of nonlinearities and disturbances, an effective control system is necessary. This control system interacts with the converter using sampled inputs and predicted outputs. Control methods for power converters and drives, including the one depicted in Figure 1.2, have continuously evolved to keep pace with advancements in semiconductor devices and the emergence of new control platforms. The widespread adoption of power converters across diverse applications over the past few decades has

contributed to their popularity. Some of the control strategies that have been employed in the past and continue to be used now will be covered in the following discussion.

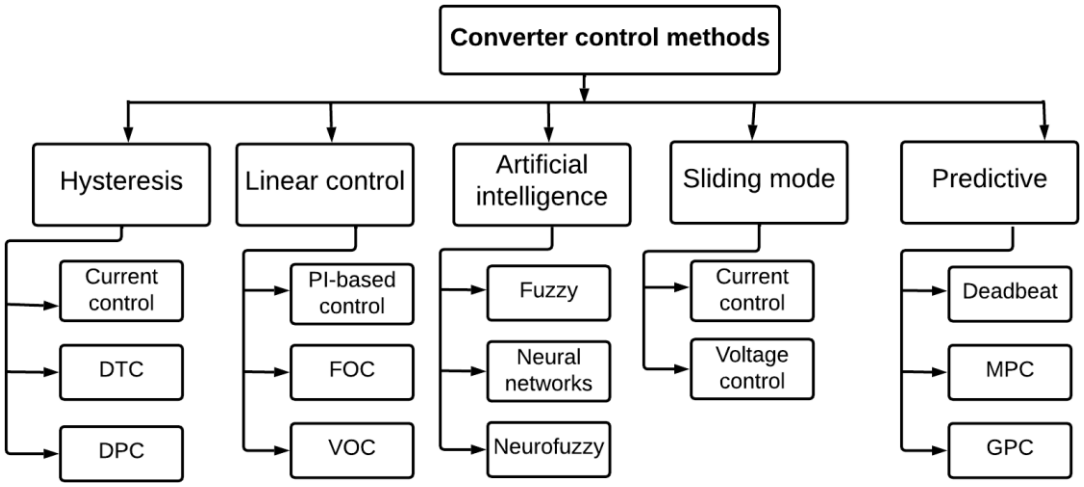

Figure 1. 2: Control methods for power converters and drives

1.3.1. Historical Control Approaches for Power Converters

Control schemes were first implemented using analog circuits consisting of active amplifiers and passive components in the 1960s (Rodriguez and Cortes, 2015), (Hassanein et al., 2022). The purpose of these control circuits is to manage the firing angle of thyristor-based rectifiers. Analog control circuits were utilized from the beginning with the development of power transistors with quicker switching frequency and were eventually supplanted by digital control platforms with the ability to execute more complicated control schemes throughout the 1970s (Rodriguez and Cortes, 2015). Nevertheless, many ideas that were created for analog control circuits are now digitally reproduced.

In analog control circuits for power converters, controlling the time-average voltages or currents is one of the key ideas. These average values are derived based on a base time, which may be a basic cycle for thyristor rectifiers or the period of the triangle waveform for modulated converters. This concept, which is the foundation of most standard control techniques employed today, enables the converter's model to be represented by a linear system. However, the converter's nonlinear features are overlooked. Hysteresis control is another analog circuit-based control system. Classical Current Control Methods are one of the most researched topics in power converter control, and two traditional control approaches have been intensively investigated over the past several decades: hysteresis control and linear control utilizing pulse width modulation (PWM).

1.3.1.1. Hysteresis current control

Hysteresis control, also known as a two-level Hysteresis current control technique, is a method of controlling power converters such as voltage source converters to transmit output current to a reference current waveform (Qian Ping and Zhang Yong, 2011), (Wang *et al.*, 2021). This approach is nonlinear and is based on current error. This approach consists of a contrast between the current of the load and the limit of the band provided to it. This is the simplest approach to implement for power converters. The downside, though, is that there is no limit on the number of flips. A very high sampling frequency is needed when applied in a digital control platform to maintain the constant regulated factors inside the hysteresis band (Patel and Baria, 2016).

The present monitoring technique for hysteresis involves a nonlinear feedback loop along with a comparator for hysteresis. Comparator hysteresis comprises two stages of this technique: lower band hysteresis (LHB) and upper band hysteresis (UHB). These bands function on the error of the constant state. The real current and the reference current are measured to give rise to any current error. The error would then be passed to the hysteresis comparator (Roselyn *et al.*, 2020). If the error current approaches UHB, the inductor current reduces, and the switches are turned ON. Similarly, once the error current approaches LHB, the top switches are switched off and the intervals of the inductor that controls the current are not above the limits (Seetharamaiah, 2008). This cycle is repeated. Switches work ON and OFF at random to track and retain the reference present.

In 3-phase VSC, hysteresis comparators are used to compare the measured load currents of every phase to the appropriate references, as illustrated in Figure 1.3. To keep the load currents inside the hysteresis band, each comparator selects the switching state of the corresponding inverter leg (Sa, Sb, and Sc) (Davoodnezhad, Holmes and McGrath, 2014), (Rodriguez and Cortes, 2015). The hysteresis width, load parameters, and operating settings all affect the switching frequency. This is one of the significant disadvantages of hysteresis control since fluctuating switching frequency may lead to resonance issues. Hysteresis control can only be used at lower power levels due to switching losses (Durna, 2018). To regulate the hysteresis controller's switching frequency, a few changes have been suggested. Hysteresis control used on a digital control platform necessitates a high sampling frequency to maintain controlled variables inside the hysteresis band.

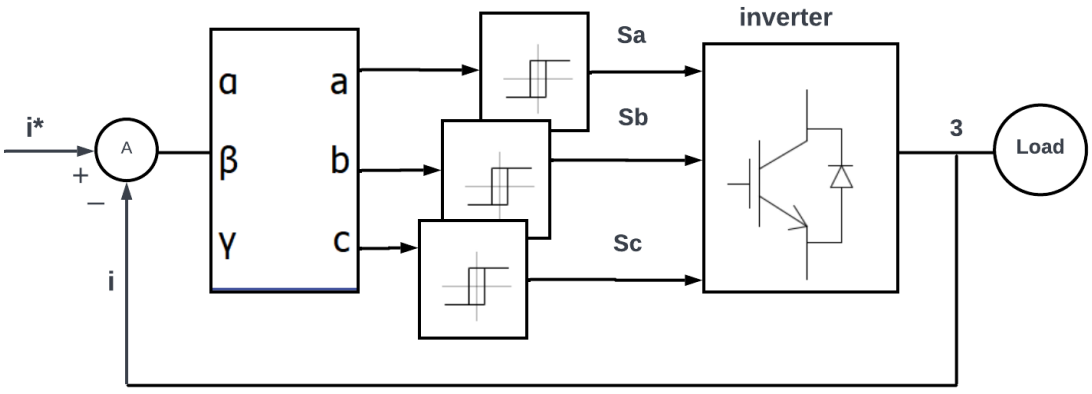

Figure 1. 3: 3-phase hysteresis current control technique

1.3.1.2. Linear Control Using Pulse Width Modulation.

PWM methods have been the center of intensive study since the 1970s (Rao *et al.*, 2014), (Firdoush *et al.*, 2016). Switching techniques for pulse width modulation are widespread in the market for power electronics and drive systems. PWM is widely used in devices such as motor velocity sensors and audio amplifier converters, it helps to modify the voltage implemented in the generator. There is no single PWM solution that will suit all applications. Different PWM methods were built for various industrial applications according to the modern technology of solid-state control electronic devices and microprocessors (Singh *et al.*, 2014).

The employment of a pulse width modulator in a single-phase inverter involves comparing a sinusoidal reference voltage to a triangle carrier signal, therefore creating a pulsed voltage waveform at the inverter's output. This voltage's basic component is proportional to the reference voltage. In a 3-phase inverter, the switching states for each corresponding inverter leg are generated by comparing the reference voltage of each phase to the triangular waveform. The primary focus of the PWM is to regulate the output voltage of the converter as well as to lessen the harmonic value of the output voltage. The PWM solution's advantages are lower dissipation, simple integration, and control, compliance with current digital microprocessors, the output voltage can be achieved without extra elements, and the lesser harmonics function can be reduced together with output voltage management (Singh *et al.*, 2014). Below are a few of the various PWM techniques.

1.3.1.3. Space Vector Pulse Width Modulation

The Space Vector pulse width modulation (SVPWM) method was initially established as a vector strategy for modulation of the pulse width for three-phase converters. The SVPWM strategy is popularly utilized in vector control devices. This technique is used in vector-driven applications to produce reference voltage while the current power is being applied. It's a much more sophisticated, new, computationally vigorous method for sine wave processing, providing higher voltage with lesser overall harmonic distortion, and seems to be the best of all pulse width modulation methods (Singh *et al.*, 2014), (Katyara, Hashmani and Chowdhry, 2020). The primary goal of every modulation technique is to attain an adjustable output voltage with minimal harmonics while maintaining a predefined fundamental component (Rao *et al.*, 2014). Several PWM techniques have mostly been developed to allow the inverters to have different desired performance features to accomplish the broad linear modulation range, fewer switching errors, and lesser harmonic distortion.

Figure 1.4 illustrates a traditional current control strategy based on SVM. In this approach, a PI controller compares the reference load currents with the measured load currents to generate the reference load voltages. The strategy maintains a constant switching frequency determined by the carrier signal. The effectiveness of this control method depends on the controller settings and the frequency of the reference current. The PI controller ensures zero steady-state error for continuous references, however, it may introduce significant inaccuracies when sinusoidal references are used. These inaccuracies become more pronounced with increasing reference current frequency, which is undesirable for certain applications. To address the limitations of PI controllers with sinusoidal references, the conventional approach is to transform the original control scheme into a rotating reference frame with predetermined reference currents.

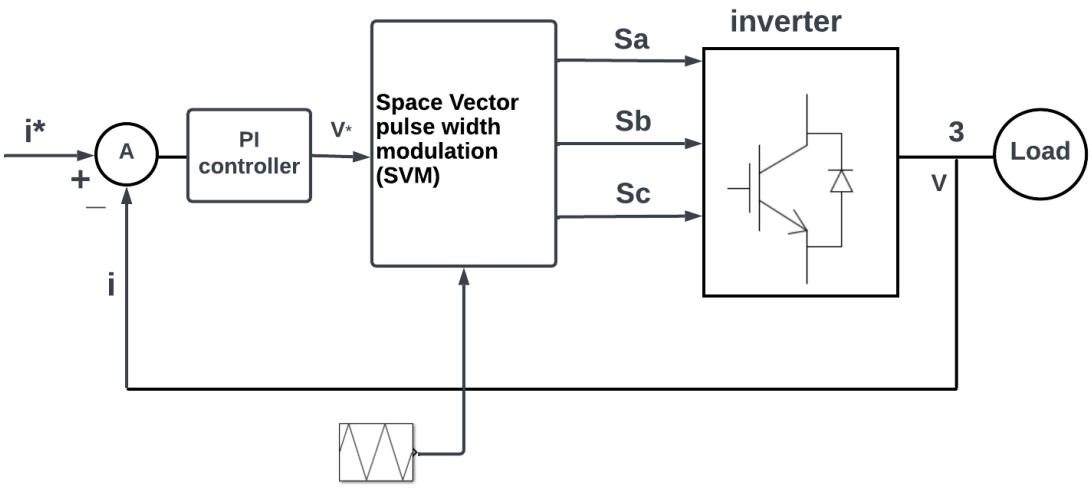

Figure 1. 4: SVM-based classical control approach.

1.3.2. Predictive Control Methods

Predictive control refers to a large group of controls commonly used in power converters. Figure 1.5 demonstrates traditional predictive controller architecture. The fundamental aspect of predictive control lies in utilizing a system model that forecasts the future behavior of the controlled variables based on input information. The performance of this model plays a crucial role in predicting and optimizing the behavior of the controlled variables (Hu and Cheng, 2017). The controller utilizes this knowledge to achieve the desired actuation, based on a predefined principle of optimization. Mentioned below are some examples of predictive control.

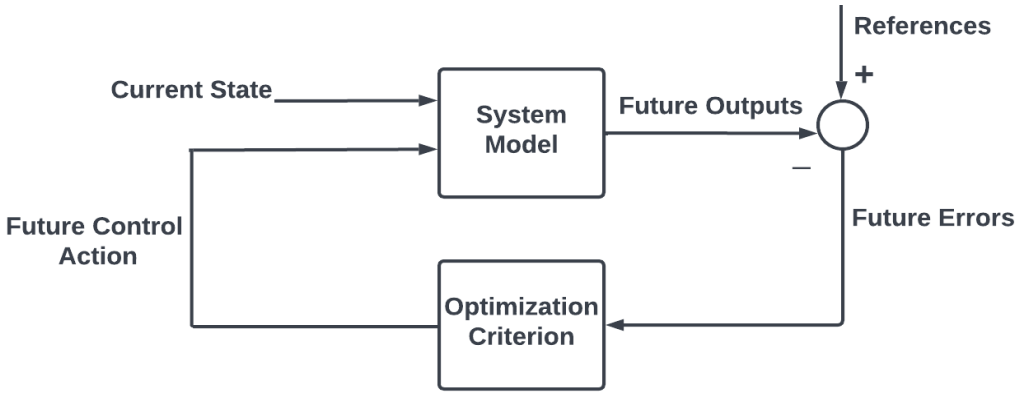

Figure 1. 5: Fundamental principle of predictive control.

1.3.2.1. Model Predictive Current Control Strategy

MPCC also recognized as receding horizon control, is the first of the alleged advanced control methods (normally translated as more complex than traditional PID control techniques), which have become widely used in practical uses in recent years and have had a profound impact on research and innovation of industrial control systems (Balaji and Rajaji, 2013). Early implementation of MPCC ideas in control electronics can be seen from the 1980s (Rodriguez and Cortes, 2015), (Almaktoof *et al.*, 2017) in the light of high-power devices with low switching frequency. It is important to implement new steps in controller design to tackle current challenges such as non-linearity and lack of response.

Owing to the advent of efficient microprocessors, predictive current control has been implemented in previous decades. Many essential restrictions such as THD, current restriction, and frequency switching can be regulated by utilizing predictive current control (Alhasheem *et al.*, 2018). Control modeling approaches based on the MPCC concept are widely accepted in industrial applications and are studied in academia. It is perhaps the most widely used in industrial applications among all specialized control methodologies. The reason for this success is the ability of MPCC architecture to create high-performance control systems that can work without expert interference for long periods (Rodriguez and Cortes, 2015).

The model predictive current control approach is built on the assumption that a static power converter can only yield a limited set of possible switching states and device designs should be used to simulate the variable behavior for each switching state (Rodriguez and Cortes, 2015), (Gu *et al.*, 2023). Because of its robustness, ease of integrating non-linearity and restrictions, and rapid dynamic response, predictive control was widely debated as an appropriate option for control strategies for Voltage Source Converters (Alhasheem *et al.*, 2018). The cost function in MPC tests each dynamic state. Its goal is to minimize the discrepancy between the calculated values and the initial values, thus reducing uncertainty. In addition, the cost function may include secondary objectives, although they may be different. The weighting factors applied to these objectives determine their relative importance. Currently, there are no established guidelines for effectively managing these variables. (Shen *et al.*, 2019).

Continuous control set MPCC and finite state-model current predictive control as shown in Figure 1.6, can be defined as the MPCC techniques used to control the converter. A modulator produces switching conditions for continuous control set MPC, depending on the predictive controller's continuous output (Shen *et al.*, 2019). Because power converters have a limited number of switching states, the MPCC optimization

issue can be conveniently conceived, generalized, and minimized explicitly for such possible switching states to predict the system's behavior. This control strategy is well known as an introduction to Finite State-Model Predictive Current Control (Almaktoof *et al.*, 2017).

MPCC Continuous Control Set Properties.

i. Modulator Required
ii. Set frequency changeover.
iii. Include restrictions.

Finite State-Model Predictive Current Control Properties.

i. No Modulator
ii. Variable frequency transition
iii. Optimization online
iv. Lower complexity (N=1)
v. Include restrictions

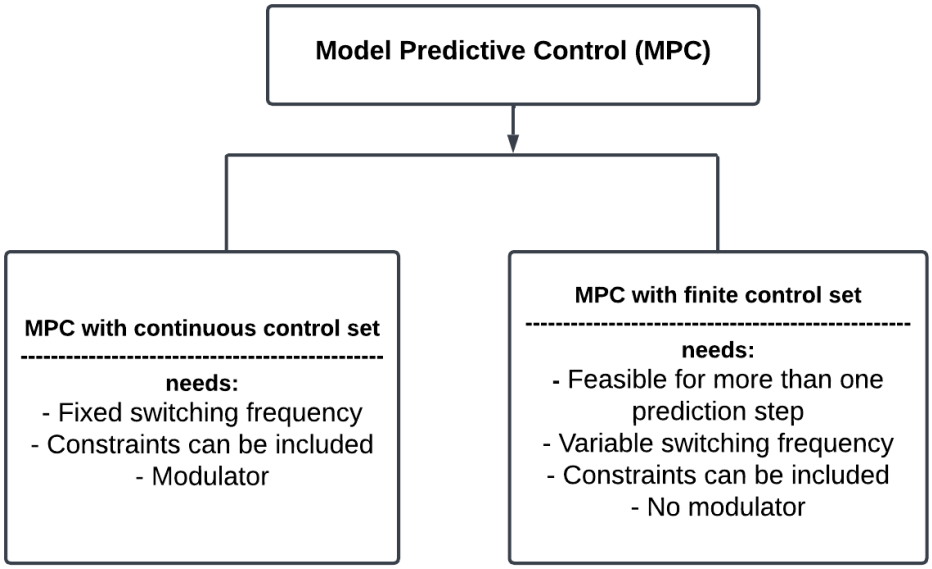

Figure 1. 6: Categories of MPC Scheme.

1.3.2.2. FS-MPCC operating principle

FS-MPC utilizes a control technique focused on a limited set of switching states produced by a converter and a system model which can be utilized to determine the system status for every switching state (Suman, Rishi, 2017). The resulting moving condition is selected based on the selection criteria. This selection criterion is a cost function that can be used to estimate future values of the variables to be monitored. For every switching condition, the estimation of future values of the variable

to be regulated shall be made. The state that reduces the cost function is implemented in the converter.

1.4. Categories of Cost Functions

Cost function classification is required to enable the description of a weighting factor adjustment process that can be implemented to related forms of the cost function. The cost function accepts any required term that may be used to forecast another system variable or system necessity.

This feature makes it possible for FS-MPC to accomplish the most control objectives that may result in higher system performance, power quality, efficiency, and other potential merits. A difference in physical characteristics between these terms may overestimate the power of respecting each term to the other in the cost function, rendering their existence unworthy and therefore uncontrollable (Rodriguez and Cortes, 2015), (Young *et al.*, 2020). This subject has frequently been clarified in MPC by including weighting factors for every cost function term. Some of the kinds of the cost function are addressed and the operation for each type is shown below.

1.4.1. Analysis of Cost Functions Excluding the Incorporation of Weighting Factors

No weighting factors are required in this type of cost function, as only one variable is monitored. Some examples of such cost functions include predictive current control of a VSC, predictive current control with the applied switching frequency, and more (Rodriguez and Cortes, 2015), (He *et al.*, 2016). All the cost function terms are made up of factors of similar character (same unit and order of magnitude). In addition, some of them are broken down into two components of a single variable. There is little or no need for weighting factors and their correlating tuning.

1.4.2. Analysis of Cost Functions Incorporating Weighting Factors.

A few other systems have a key target to reach to maintain adequate system behavior, and extra secondary constraints are to be attained to enhance system performance or efficiency as well. In this instance, the cost function introduces primary and secondary terms (Cortés *et al.*, 2009), (Dragičević and Novak, 2019). The second term can differ according to the application and its requirements, and some definitions of it include predictive current control with reduced switching frequency to increase efficiency; predictive current control with reduced reactive power to boost power quality; and others. The value of the second term (i.e. how much the reactive power or switching frequency is decreased) will rely on the particular needs of the system and will force a trade-off with the primary control goal, in this instance the current control(Cortés *et al.*, 2009), (Gao *et al.*, 2022). The weighting factor is included for each cost function with

the correlated secondary term. Thus, trade-off resolution can be viewed as the adjustment of the weighting factor in the cost function.

1.5. Research problem

The Model Predictive Current Control Scheme is often utilized primarily for calculations of stronger and faster microprocessors. The main research problems which need to be tackled are:

i. Selection of cost functions that enable the balance between reference tracking and control effort adjustments.

ii. How to reduce time delay by minimizing calculation effort for model predictive current control, which is required when the VSC is controlled without the use of a modulator.

The sub-problems of the study that emerged include the following:

iii. The load current of the 3-phase, 2-level VSC, and the reference current. The biggest obstacle is to always ensure that the load current closely follows the reference current throughout the operation, while also minimizing the Total Harmonic Distortion in the converter's output stage.

iv. Another challenge to address in both aforementioned cases is the minimization of total harmonic distortion and the reduction of switching states.

1.6. Research Objectives.

The first goal of the research was to address the delay caused by the extensive computational requirements associated with model predictive current control when regulating the VSC without utilizing a modulator.

The second objective of the research is to minimize errors between the load currents and reference values by using the proposed Finite-state model predictive current control to select the best switching state that reduces the cost function.

The following must be accomplished to reach the aforementioned objectives:

i. A comprehensive literature study of MPC methods based primarily on 3-phase 2-level VSCs.

ii. Propose a three-phase 2-level VSC Predictive Current Control Technique, FS-MPCC, which regulates the load current for VSCs, to be implemented.

iii. A novel control algorithm, designed to deliver exceptional dynamic performance for VSCs, will be introduced. This algorithm aims to minimize computational complexity and reduce the number of possible combinations for MPCC while extending the prediction horizon. The proposed algorithm will be specifically applied to three-phase, two-level VSCs, enhancing their overall performance.

iv. Considerations surrounding the design of a suitable cost function.

v. Extensive simulation results will be presented to demonstrate the performance and efficacy of the MPCC approach.

1.7. Contributions of research

This research is based on the use of FS-MPCC on MPC using cost function with/without weighting factors in the three-phase, two-level VSC. This research will provide a guide on how predictive control methods are implemented to improve the quality and dynamic response of VSC. Moreover, it will bring tremendous advantages to potential power conversion systems and will lead to improvements in system quality, reliability, and performance. The research contributions will formulate, model, and rephrase theoretical findings and methods to apply them to manage real-life problems.

FS-MPCC provides the following research contributions:

a. Suited for RES

b. No modulation whatsoever.

1.8. The structure of the thesis

This thesis is divided into Five primary chapters, which can be summarized as follows:

Chapter One presents the subject of study. It begins with a theoretical overview of MPCC for a three-phase, two-level VSC. The research problem and objectives are stated. Finally, the contribution of the research is provided.

Chapter Two of this thesis provides a thorough examination of VSC technology and its wide-ranging applications. The chapter commences with an overview of power electronic converters, followed by an extensive exploration of the fundamental aspects and structures of VSCs. Additionally, a comprehensive evaluation of the advantages and disadvantages of each type of converter is conducted. By considering the number of components required and isolated DC sources, a comparison of the most promising DC-to-AC converter topologies is presented. The chapter also encompasses the presentation and discussion of various predictive control techniques employed in different power converters. It focuses primarily on the practical implementation of VSCs in renewable energy systems, specifically in their integration with PV systems and wind turbines. While not exhaustive in covering all VSC power converter applications, the chapter delivers a meticulous and systematic overview of the underlying principles that govern diverse VSC technologies.

In Chapter Three of this study, the methodology is discussed in depth. The chapter begins with a general overview and then delves into the proposed control scheme for the voltage source inverter. The classifications of cost functions in terms of delay compensation procedures and reference frames were discussed. In addition, the chapter elaborated on the various compensating procedures that can be incorporated into cost function equations.

In Chapter Four of this study, the modeling and simulation of the utilized circuit are described in depth. Following a general introduction, the chapter discusses the employed load model. The chapter then examines the procedure for selecting the most optimal cost function to reduce computational needs. Furthermore, the integration of Matlab and Simulink software for the simulation is described. Finally, the chapter concludes with a presentation and analysis of the results and discussions.

In Chapter Five, a summary of the completed research is presented. This chapter describes the significant contributions made as a consequence of this research, emphasizing its significance and prospective impact. Furthermore, the chapter concludes by discussing potential future research projects, highlighting promising avenues for further exploration and development in the field.

CHAPTER TWO

LITERATURE REVIEW

2.1. Introduction

This chapter focuses on the integration of power converters, particularly voltage source converters with predictive current control to optimize efficiency, as well as other aspects in certain power converter categories, including power quality and dynamic responsiveness. In recent decades, power converters have become increasingly prevalent for applications such as motors, power conversion, and distributed generation. Extensive research has been conducted to investigate the control of power converters, leading to the continuous introduction of novel control approaches. Predictive control has emerged as one of the established control strategies for power converters and drives. Predictive control possesses several characteristics that make it well-suited for power converter control. Its concepts are straightforward to understand, making it accessible to a wide range of users. It can be applied to diverse systems, accommodating various limitations and nonlinearities. Moreover, predictive control enables the investigation of multivariable scenarios, and the resulting controller is relatively simple to implement. This chapter discusses the various types of power converters currently available and how they operate, as well as a comparative analysis of various topologies with respect to their component count and the presence of isolated DC sources, and a study of the most significant predictive control techniques employed in the realm of power electronics and drive systems.

2.2. Power converters Classification

The first studies about power electronics date to the late nineteenth century. The Mercury Arc Rectifier, which was invented by P.C. Hewitt in the United States in 1900, was the first Power Electronic Device (Guarnieri, 2018), (Hamid *et al.*, 2020). Subsequently, power devices including the metal tank rectifier, ignitron, grid-controlled vacuum tube rectifier, magnetic amplifier, and thyratron, were developed and progressively utilized for power control applications until 1950 (Guarnieri, 2018), (Hamid *et al.*, 2020). The second electronic revolution started in 1958 when the General Electric Company developed the commercial-grade Thyristor (Mohammed, A and Hasanin, 2013), (Fewson, 2015). Consequently, a new age of power electronics was created. Today, power electronics is a fast-increasing area of electrical engineering, and the technology encompasses a broad range of electronic power converters. The increasing prevalence of power converters across various applications can be primarily attributed to their improved performance and efficiency, resulting in heightened production rates. The purpose of a power converter is to manage and control the

transmission of electrical energy by providing the necessary voltages and currents in the desired format for the user loads (Bordry, 2004), (Bordry and Aguglia, 2018). In contrast to other kinds of electrical circuits, where the control components are operated in a linear or near-linear active area, power converter switches function in just one of two states: either "on" or "off."

Power converters are a crucial enabling technology for industrial applications due to their capacity to manage electrical energy appropriately. Transport, energy conversion, manufacturing, mining, and petrochemicals, to name a few, are among the many applications for which they are used (José *et al.*, 2009), (Blaabjerg and Round, 2021). There has recently been a sharp rise in the number of alternative energy sources in power system networks, particularly solar and wind facilities. Because of the expansion of distributed generation, it is vital to employ electric energy storage, and active power transfer from alternative sources and energy storage to the grid assured by regulators built on power electronic converters (Lepanov and Rozanov, 2013), (Das *et al.*, 2018), (Rajagopalan *et al.*, 2022). To achieve higher production rates, lower prices, and more efficiency, industrial processes have increased their power consumption. The research community and industry in power electronics have reacted to this demand in two ways. The first approach is to develop a semiconductor technology capable of producing potentially greater currents and voltages while preserving existing converter architectures, particularly two-level voltage, and current source converters (CSCs). The second option is to construct Multilevel Converters, which are innovative converter topologies, employing conventional semiconductor technology. Power converters are constructed using semiconductor switches and passive components. Electronic power converter systems are classed based on whether the input and output currents are alternating currents or direct currents. As indicated in Figure 1.1, power converters are classified into four types, which are explored more below: AC to DC, DC to DC, AC to AC, and DC to AC.

2.2.1. DC to DC converters

A dc-dc converter converts a dc input voltage into a dc output voltage. A dc converter is the dc version of an ac transformer with a continually turning ratio. It may be used similarly to a transformer to step down or step up a dc voltage source. In electronic autos and trolley cars, dc-dc converters are commonly utilized for traction motor control. They provide smooth acceleration control, great performance, and rapid dynamic response. DC-DC converters may be used in the regenerative braking of dc motors to return energy to the supply, resulting in energy savings for transportation

systems with frequent shutdowns. Buck, Boost, and Buck-Boost converters are examples of DC-to-DC converters.

2.2.2. AC to DC converters

An AC-DC converter, commonly referred to as a rectifier, is an electrical circuit that utilizes both half cycles of the supplied AC voltage to convert it into a pulsating DC voltage. (Rodriguez and Cortes, 2015). AC-to-DC converters utilize rectifiers to convert alternating current input into direct current output. They also incorporate regulators to modify the voltage level and reservoir capacitors to effectively stabilize the fluctuating DC signal. These converters are used in personal computers, TVs, mobile phone chargers, and other electrical consumer gadgets. The rectifier serves as an illustration of an AC-to-DC converter.

2.2.3. AC to AC converters

AC-AC converters modify AC voltage characterized by a consistent amplitude and frequency, transforming it into AC voltage with adjustable amplitude and frequency. AC-to-AC converters are used in drives that demand regenerative power capabilities, such as cranes, turbines, etc. Examples of A-AC converters are matrix converters and Cycloconverters.

2.2.4. DC to AC converters

DC-to-AC converters serve the purpose of transforming DC power into AC power, ensuring the desired output voltages, currents, and frequencies are achieved. The DC-AC power converter has a variety of uses, including lighting lights in our homes, driving motors in small and medium-sized businesses, and providing uninterruptible power in the telecommunications industry. Current source converters (CSCs) and VSCs are examples of DC-to-AC devices as shown in Figure 1.1. In the last decade, much research has been conducted on DC-to-AC converters in response to the growing requirement for power quality and efficiency, as well as the rising need for energy. Power converters play a pivotal role in various industries and find applications in diverse systems. The transformation and regulation of electrical energy through power electronics have become increasingly important due to the rising energy requirements and the necessity for enhanced power efficiency and quality. To meet these demands, ongoing research focuses on developing new semiconductor devices, topologies, and control strategies. DC/AC converters can be categorized into two main types: voltage source converters and current source converters. The following sections provide detailed explanations of each type.

2.2.4.1. Current Source Converter

A CSC is a form of converter circuit that converts the DC at its input to the corresponding AC. The input current is a constant independent of the load or the state of the inverter, but the output current, which may be either single- or three-phase, depends on the load. CSCs are less popular than VSCs because they employ massive inductors linked in series to the supply source, which maintains a constant current, and a capacitor across the output, as seen in Figure 2.1 (Vazquez *et al.*, 2010), (Danial W. Hart, 2011), (Sener and Ertasgin, 2022). The resistive-capacitive load is one of the reasons why CSC is not as often used as VSC, and it is suggested in situations where boosting capabilities are necessary (Buckner *et al.*, 2016). CSC may be classified into pulse-modulated (PWM) CSI and load-commutated inverters (LCIs) (Danial W. Hart, 2011).

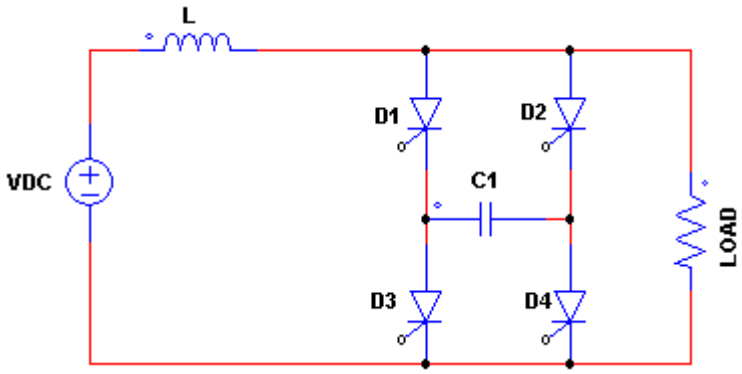

Figure 2. 1: Current source converter circuit diagram.

2.2.4.2. Voltage source converter

A voltage-source converter converts dc voltage to alternating current voltage (Hamid *et al.*, 2020). Its most common characteristic is a high-capacity capacitor connected in parallel to the power supply source, which maintains a steady voltage. The capacitor present on the DC side of the converter serves the purpose of maintaining voltage stability. It possesses a sufficient capacity to handle a continuous charge or discharge current that aligns with the converter valve switching sequence and fluctuations in the phase angle of the switching valves, all while avoiding significant fluctuations in the DC voltage. The VSC enables the control of output voltage parameters such as amplitude, phase angle, and frequency. These converters maintain a unipolar DC voltage on their DC side, allowing power reversal by reversing the polarity of the DC voltage (Navpreet *et al.*, 2012), (Raju *et al.*, 2019).

A VSC is an essential element in variable-speed ac motor drives, renewable energy production and microgrid systems, and high-voltage dc transmission systems

(Alsokhiry *et al.*, 2019), (Dahono and Dahono, 2021). According to recent research, voltage converters are now built utilizing a new basic cell known as a modified Cuk dc-dc power converter (Dahono and Dahono, 2021). These VSCs are typically seen in high-voltage microgrids. It is demonstrated that the developed voltage-source converters have low input and output ripples and do not require extra external filtration. There is no longer any need for a common-mode filter. Several voltage source converters are described further below.

2.2.4.2.1. Two-level voltage source converter

The least difficult multiple levels are two-level VSC three-phase power converters. It is referred to as 2-level because the AC sides of the converter operate at two voltage levels, VDC and -VDC (Lindblom and Lindblom, 2019). A two-level VSC employs two high-frequency switching devices, such as bipolar transistors (IGBTs) or Gate turn-off thyristors (GTOs), in each phase, and such a converter also functions as a rectifier in addition to power control. The two-level VSC enables the series connection of IGBTs based on the voltage rating of the device and the supply voltage required (Watson and Watson, 2020). A two-level VSC can operate in single or three phases. In single-phase converter circuits, two kinds of circuits are used: half-bridge and full-bridge.

i. Single-phase Half-Bridge Converter

As shown in Figure 2.2, a single-phase half-bridge inverter circuit comprises two power switches and two diodes coupled in parallel to the power switch to inhibit the reverse voltage (Hamid *et al.*, 2020). The switching process is performed in a back-and-forth motion, (ON/OFF) (Hsieh *et al.*, 2012).

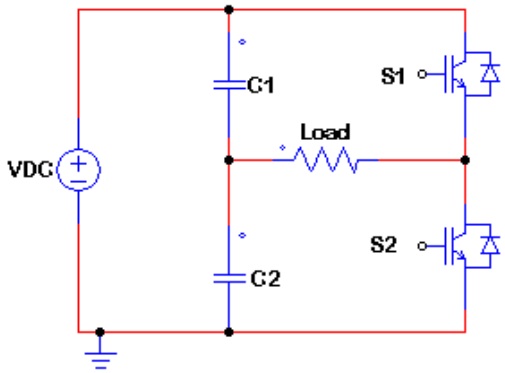

Figure 2. 2: Single-phase Half-Bridge Inverter Topology.

ii. Single-phase Full-Bridge Converter

As shown in Figure 2.3, a single-phase full-bridge converter features four power switches and is utilized in applications requiring a greater power rating. When two switches are switched ON, the other two must be OFF. For instance, when switches S2 and S3 are switched on, switches S1 and S4 are switched off (Hamid *et al.*, 2020).

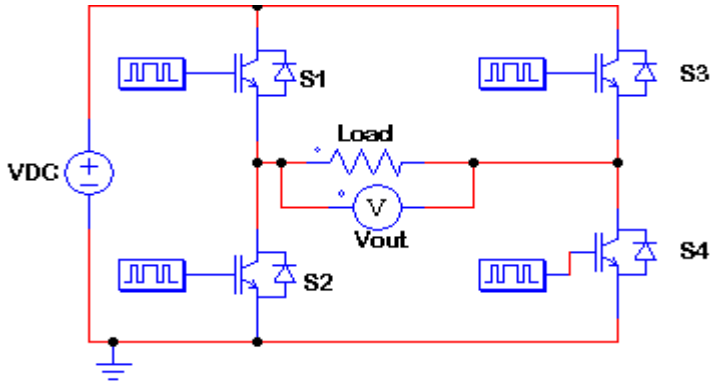

Figure 2. 3: Single-phase Full-Bridge Inverter Topology.

To build a three-phase converter, three single-phase, two-level voltage source converters can be coupled to the same capacitor (Wang *et al.*, 2009). As shown in Figure 2.4 below, a three-phase, two-level VSC is made up of six switches and two DC capacitors (C1 and C2). The circuit works by switching S1, S2, S3, S4, S5, and S6, and it employs a configuration with two sets of complementary controlled switches in each converter leg (S1, S2), (S3, S4), and (S5, S6) (S5, S6) (Almaktoof, Raji and Kahn, 2013), (Ashraf *et al.*, 2020). The converter can supply bidirectional power flow between the DC side and the three-phase AC system.

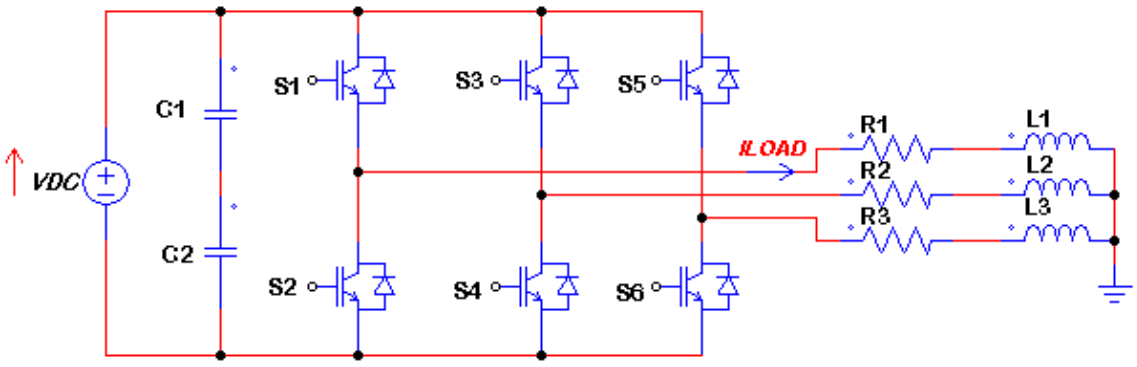

Figure 2. 4: Two-level Voltage Source Converter.

Two-level VSCs have dominated dc–ac and ac–dc power conversion applications such as aerospace, solid-state transformers, AC motor drives, battery energy storage

systems, and other renewable energy generation systems (Quan and Li, 2019), (Xu *et al.*, 2020), and (Zhang *et al.*, 2021). The high power density of two-level VSCs is a foremost need (Quan and Li, 2019). The application of these converters in High Voltage Direct Current (HVDC) power transmission fields has grown significantly. The two-level VSC-HVDC transmission systems are well-known for their simple power circuits, straightforward control systems, and small footprint (Adam *et al.*, 2017), (Alsokhiry *et al.*, 2019).

The key advantages of the two-level VSC are its simplicity, established technology, as well as the capacity to include redundancy into a chain of series-connected switching devices, which are typically insulated gate bipolar transistors (IGBTs) (Wang *et al.*, 2009), (Alhasheem, Abdelhakim, *et al.*, 2018). The main disadvantages of two-level VSC in HVDC transmission systems are that they suffer from significant semiconductor losses, particularly switching losses, and need large ac filters; and they raise dc fault levels because dc-link capacitors contribute huge discharge currents to dc fault (Alsokhiry *et al.*, 2019).

2.2.4.2.2. Multilevel Voltage Source Converter

NABE-EL pioneered the concept of multilevel converters in 1975. Multilevel approaches are employed to improve the power and voltage capabilities of voltage-source converters (Dahono and Dahono, 2021). In recent years, there has been a lot of interest in multilevel converters, and they have been researched for a variety of high-voltage and high-power applications. The term multilevel converter begins at three levels and progresses upward (Dahidah and Agelidis, 2008), (Salem *et al.*, 2022). The converter is built of converter cells or modules. Each module can be a half-bridge or full-bridge cell. Multilevel converters are now regarded as the most ideal power converters for high voltage capability and high power quality demanding applications, thanks to the introduction of high-power switching semiconductors such as IGBTs (Dahono and Dahono, 2021). One significant advantage of the multi-level arrangement is that harmonics in the converter output can be minimized without enhancing the switching frequency (Shanono, Abdullah and Muhammad, 2018)

Multi-level converters are categorized into three main topologies namely Flying Capacitors (FC), Neutral Point (NPC), or Diode Clamped and Cascaded H-bridge (CHB) as shown in Figure 2.5 (a, b, & c), and all these are derived from the two-level converter (Li and Quan, 2017), (Shanono, Abdullah and Muhammad, 2018). MLIs were created to increase converter output power while also solving the problem of normal conventional inverters being unable to endure high switching frequency, high voltage, and current stress, all of which result in decreased efficiency and significant

electromagnetic interference (EMI) in the system (Shanono, Abdullah and Muhammad, 2018), (Al-Shamma'a *et al.*, 2018).

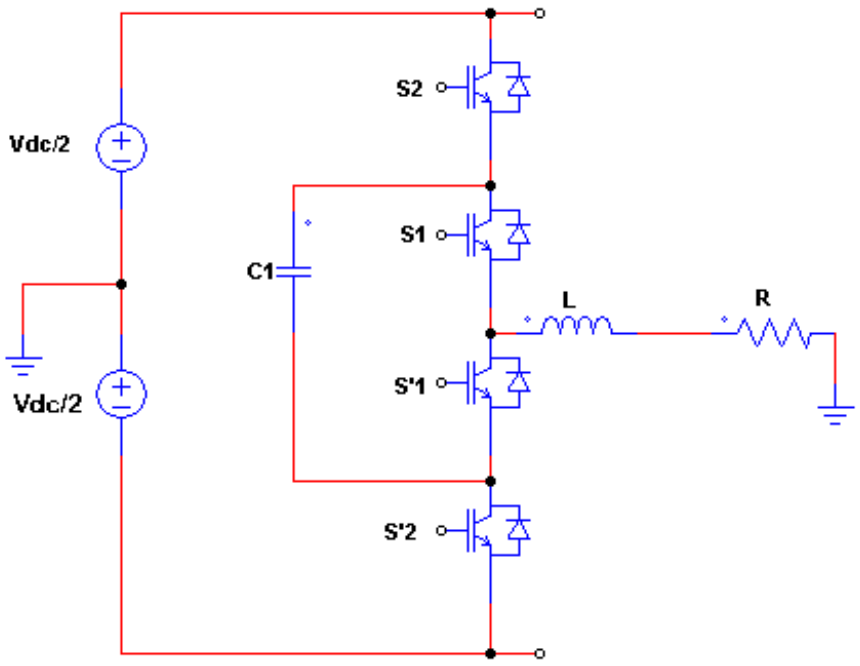

(a)

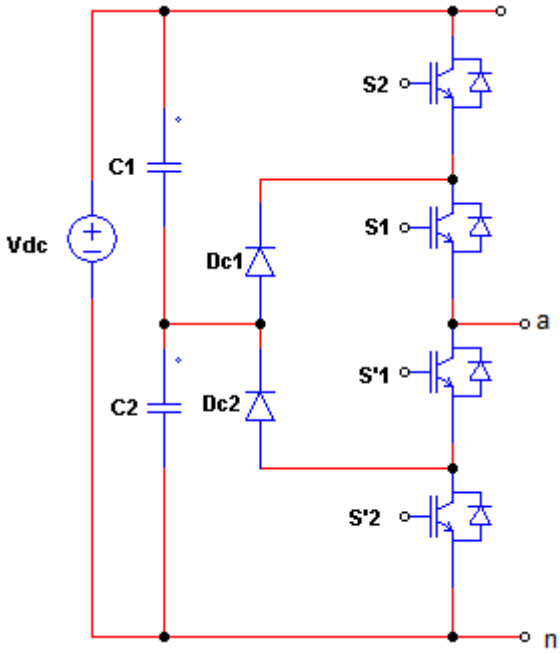

(b)

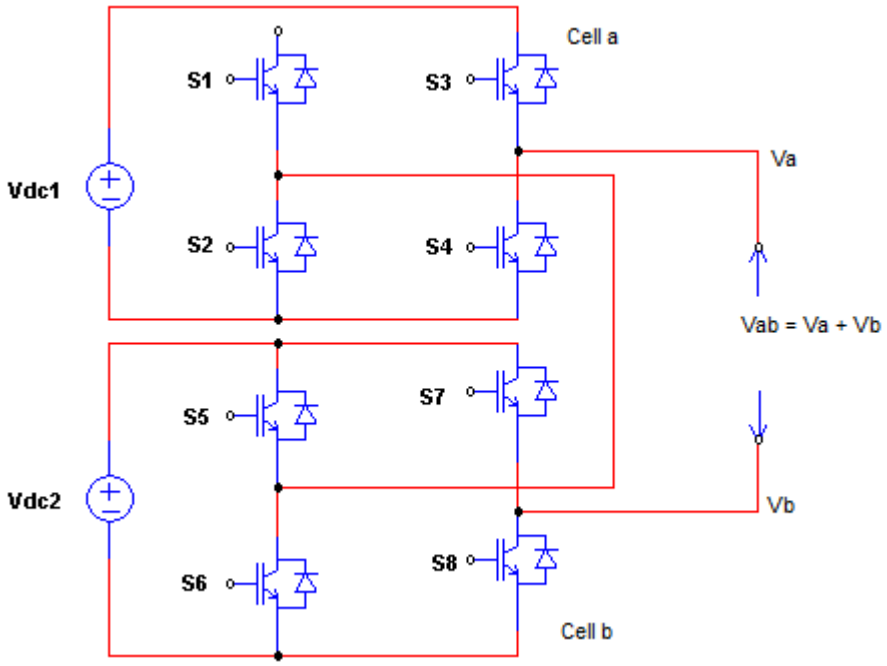

(c)

Figure 2. 5: (a): Three-level flying capacitor converter with one leg, Figure 11 (b): Three-level Diode Clamped converter, and (c): Single-phase 5-level Cascaded H-bridge Converter.

2.3. Applications of power converters

Even though fossil fuel is the primary source of energy for the global economy, scientists continue to explore other resources that can be used to generate electricity because of the damage that fossil fuel does to the environment (Buccella, Cecati and Latafat, 2012). The generation of electricity through the use of renewable energy sources is widely acknowledged to be environmentally friendly, socially advantageous, and economically competitive for a variety of different uses. Distributed generation systems rely mostly on solar systems, fuel cells, and wind turbines as their primary sources of energy (Buccella, Cecati and Latafat, 2012), (Zietsman *et al.*, 2022). There are now increased efforts to utilize renewable energy sources. The public is more aware than ever before that renewable energy is the answer to rising energy bills. Energy pricing, harmful contaminants, and the depletion of fossil fuels are all variables to consider. What the public is less aware of are the obstacles that must be solved before renewable energy technology can be extensively deployed. These challenges aim to reduce the cost and improve the controllability of renewable energy sources, allowing them to reach their full potential for broad deployment. Photovoltaic solar energy is a particularly promising choice among these sources (Buccella, Cecati and Latafat, 2012), (Buckner *et al.*, 2016), (Brahmi and Dhifaoui, 2021). It is undergoing

rapid expansion, aided by the growing awareness of governments and other groups committed to environmental preservation. For a long time, photovoltaic solar energy was primarily employed to power specific loads such as satellites and/or rural areas located distant from traditional electricity transmission lines (Brahmi and Dhifaoui, 2021). Modern society's concern for the environment, economic considerations, and technological advancements have led to an increased interest in solar energy and related conversion technologies as viable future options. In addition, several nations in Europe and Africa have the potential to generate vast amounts of solar power (Brahmi and Dhifaoui, 2021). As a result, solar photovoltaic energy to the power grid has grown rapidly in the last decade. At the moment, governments in many European nations, Japan, and the United States, among others, are advocating economic incentives for renewable energy to combat climate change (Brahmi and Dhifaoui, 2021). According to the IEA analysis, approximately 61% of worldwide energy output in 2050 will come from renewable sources, with solar PV and wind accounting for about 40% of the total (IEA, 2021). The report also predicts that global electricity consumption will rise from 26,800 TWh in 2020 to 37,300 TWh in 2030 (IEA, 2021). Figure 2.6 illustrates the share of solar PV and wind in the overall generation, as well as other sources.

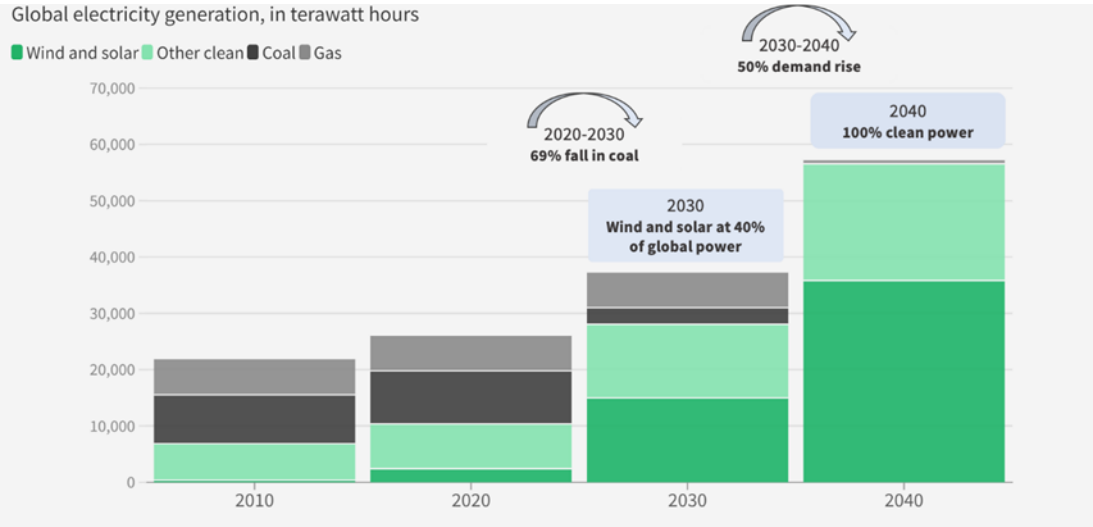

Figure 2. 6: The overall generation of wind and solar share (IEA, 2021).

The integration of renewable energy sources on a large scale has significantly enhanced the environmental sustainability of electricity production within the utility system. The utilization of integrated renewable energy sources reduces the power requirements from the grid in typical home applications. This is achieved through the implementation of a grid-connected voltage source converter, which acts as a power electronics interface for efficient power transmission (Dai, Lam and Zhang, 2014). The

subsequent sections delve into the appealing attributes of VSC applications within wind turbine and photovoltaic systems.

2.3.1. Photovoltaic systems

Due to the depletion of fossil fuels, as well as their high prices and negative environmental effects, the usage of renewable energy sources, particularly photovoltaic energy, has expanded in recent years (Brahmi and Dhifaoui, 2021). Despite all of the benefits of photovoltaic energy, it does have certain limits. These constraints include the expensive cost of PV modules and interference converter systems, as well as the variable power of PV cells. PV array output voltage fluctuates greatly with changing irradiance and temperature. Photovoltaic generation systems serve as a captivating illustration of power converter applications. This is due to the requirement of a converter to enable the transmission of electricity from the PV panel to the grid. Consequently, whether operating in stand-alone or grid-connected mode, the implementation of an intermediate DC/DC converter is imperative to supply a high DC voltage to the inverter DC-link. This, in turn, necessitates the utilization of a high-voltage DC-AC inverter, as depicted in Figure 2.7 (Rodriguez and Cortes, 2012). To convert sunlight into usable power, a photovoltaic generator that can provide the appropriate amount of direct current is required. After that, a DC/AC converter, such as a VSC, is employed to produce alternating current and to smooth the current that is provided by the high-voltage DC side of the DC/DC inverter as shown in Figure 2.8 (Bauer, 2010), (Brahmi and Dhifaoui, 2021), (Mantilla Arias *et al.*, 2021). A VSC is needed in photovoltaic systems to generate power for household appliances such as fans, blenders, and bulbs, among others; consequently, it is essential to control the output voltage of this converter to ensure suitable conditions at various loads or modifications in the battery bank (Mantilla Arias *et al.*, 2021). Figure 2.9 is a block schematic of the residential connection from the solar plant to the residence.

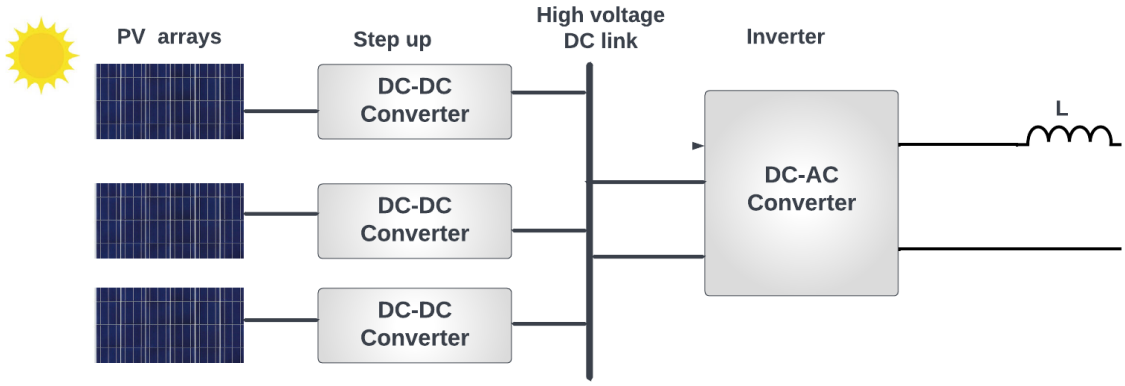

Figure 2. 7: Power conversion in a Photovoltaic system without a transformer.

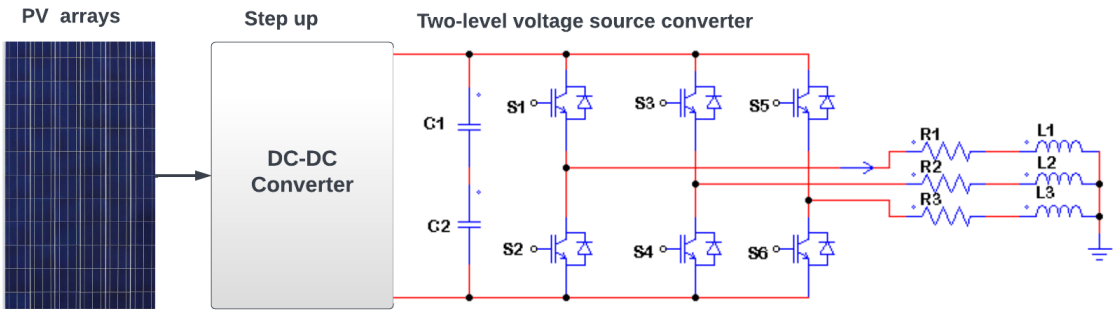

Figure 2. 8: Voltage Source Converter in a PV system without a transformer.

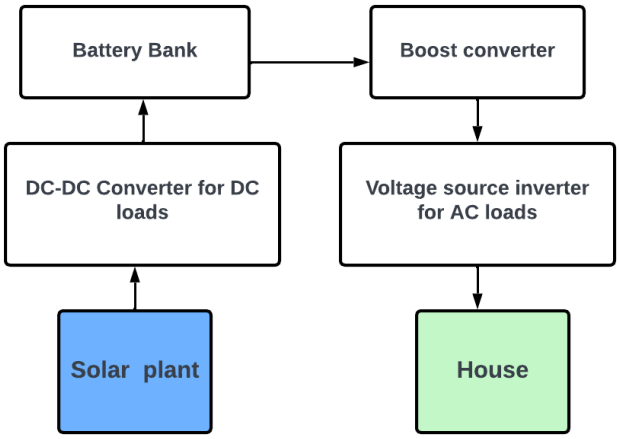

Figure 2. 9: Block diagram illustrating the connection between the solar plant and the residential building.

2.3.2. Wind turbine system

Compared to other forms of renewable energy, wind power is more cost-effective and ideal for some applications. Wind turbine system (WTS) technology continues to be the best renewable energy technology. It began in the 1980s with a per-unit power output of a few tens of kW (Blaabjerg, Liserre and Ma, 2012). Today, wind turbines with a capacity of multiple megawatts are being constructed; they are highly advanced power producers. Power electronics have been introduced during the last decade as an intelligent link between wind turbines and the grid (Christensen, 2009), (Mantilla Arias *et al.*, 2021). It is transforming the fundamental feature of wind turbines from an energy source to a grid-active power source. Variable-speed wind energy systems are favored in wind turbine systems over fixed-speed systems owing to their capacity to produce more output power, enhance efficiency, create less mechanical stress, and provide higher power quality (El-Saady, Ibrahim and Gelany, 2017). Utilizing power converters

and drives within wind generation systems enables the optimization of energy extraction from wind resources. This approach ensures alignment with contemporary grid regulations, which impose constraints on both power quality and overall system performance (Rodriguez and Cortes, 2012). Utilizing power converters may assist in enhancing the quality and reliability of the grid. Using two two-level VSCs in a back-to-back arrangement is the most popular approach for wind turbine power converters in the best-selling 1.5–3 MW range (Blaabjerg, Liserre and Ma, 2012).

The pulse width modulation-voltage source converter (2L-PWM-VSC) with two levels of output voltage has emerged as the prevailing choice for three-phase power converter topology in variable speed wind turbine systems up to the present time (P. Tenca, A. A. Rockhill, T. A. Lipo, 2008), (Blaabjerg, Liserre and Ma, 2012). This technology has garnered extensive knowledge and holds a firmly established position. In wind turbines, a common arrangement involves two 2L-PWM-VSCs configured in a back-to-back (2L-BTB) setup, utilizing a transformer on the grid side as the intermediary between the generator and the grid. This configuration is depicted in Figure 2.10. The comparatively basic construction and few components of the 2L-BTB system contribute to its well-proven durable and dependable performance. The variable speed architecture employs a diode rectifier with a boost chopper converter coupled to two-level PWM-VSCs connected back-to-back as shown in Figure 2.10. The objective of AC/DC/AC technology is to rectify the fluctuating voltage from the generator to DC before converting it to AC and feeding it to the grid or load (Bharanikumar, Senthilkumar and Kumar, 2008), (Buckner *et al.*, 2016). There are various kinds of generators utilized in Wind Turbine Systems, including doubly-fed induction generators (DFIG), permanent magnet synchronous generators (PMSG), and self-excited induction generators (SEIG). PMSGs are favored over induction generators due to their simplicity and great dependability. The permanent magnet eliminates the synchronous machine's excitation winding and delivers price reduction and enhanced magnetic material properties (Buckner *et al.*, 2016). The structure of wind turbine conversion systems is shown in Figure 2.11.

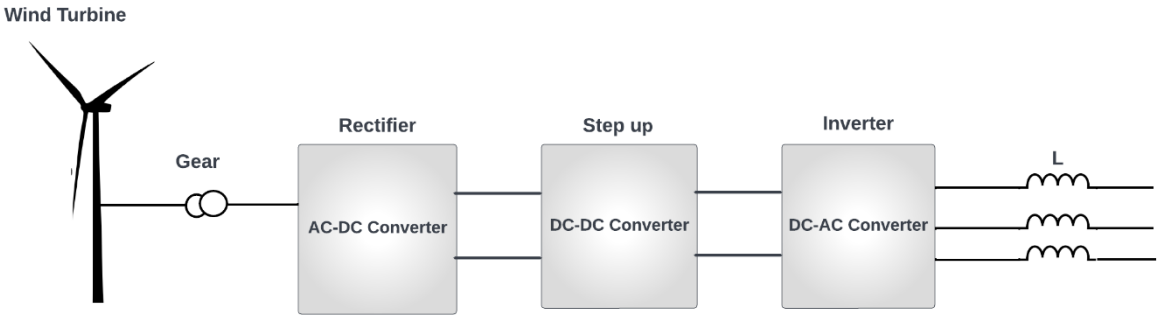

Figure 2. 10: The structure of wind turbine conversion systems.

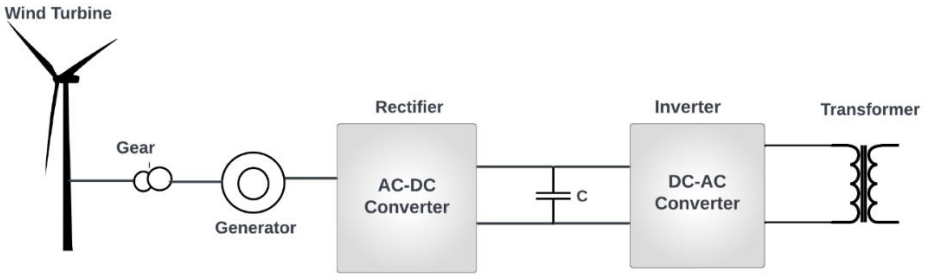

Figure 2. 11: Power Conversion Employing Back-to-Back Configuration in Wind Turbine Systems.

2.4. Predictive control Techniques

Predictive control encompasses a range of controllers that have recently gained relevance in the realm of power converters. What sets predictive control apart from alternative control methodologies is its capacity to employ the system model for anticipating the forthcoming dynamics of controlled variables. This predictive data is subsequently harnessed by the controller to compute optimal actuation determined by a predefined optimization criterion. The classification of predictive control methodologies is visually depicted in Figure 2.12 and thoroughly examined in the subsequent sections.

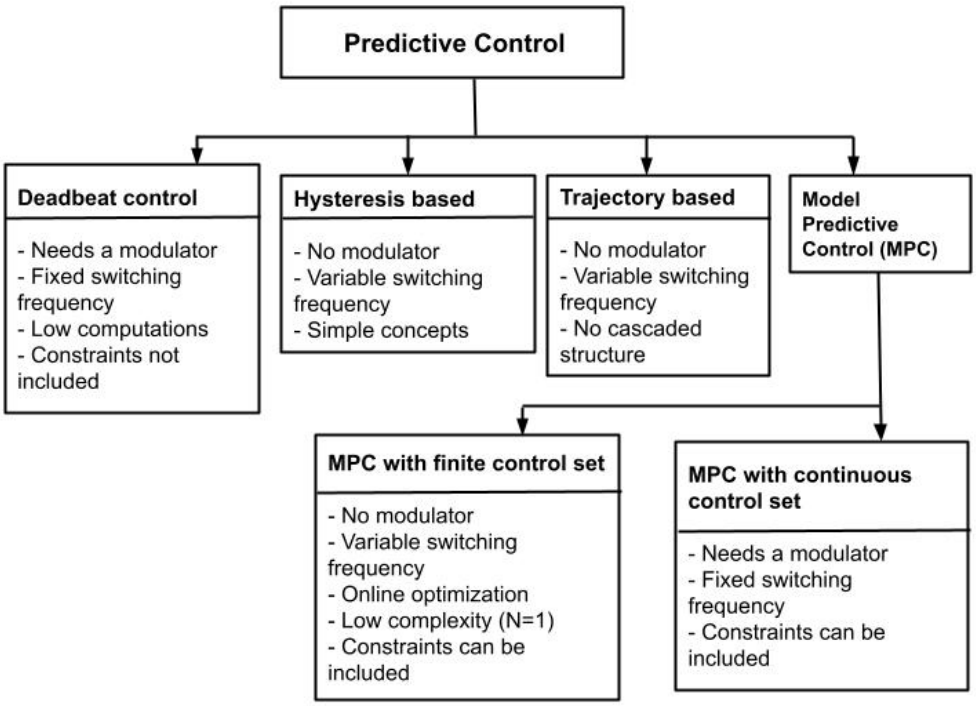

Figure 2. 12: Categorization of predictive control techniques employed in power electronics.

2.4.1. Hysteresis-based predictive control

In hysteresis-based predictive control, the optimization criterion is utilized to keep the controlled variables inside the bounds (Holtz and Stadtfeld, 1983), (Cortés, Kazmierkowski, *et al.*, 2008), (Walz and Liserre, 2020). The hysteresis-based MPC predicts the present trajectories of future switching states using motor equations. The present trajectory is defined by the boundaries, and the cost function chooses the voltage vector that assures the current will remain inside the bounds for the longest amount of time while reducing switching occurrences. By adjusting the bound size, the current's THD may be altered. The long prediction horizon is among the primary benefits of employing hysteresis-based MPC (Scoltock, Geyer and Madawala, 2013). Furthermore, parameter mismatches caused by converter non-linearities, deadtimes, or saturation must be considered. As an example, Figure 2.13 depicts a circular boundary, the placement of which is determined by the current reference vector i^*_s. When the current vector i_s makes contact with the boundary line, the prediction and optimization processes are used to choose the next switching state vector. After computing the trajectories of the current vector for each potential switching state, predictions are given for the corresponding time intervals necessary to approach the error boundary once again. These occurrences also rely on the position of the error boundary, which is regarded to be shifting in the complex plane in accordance with the

current reference prediction. The movement is shown by the circle with dots in Figure 2.13. The switching instants are predicted by machine equations. Finally, the state vector with the most on-time is chosen. This reduces switching frequency. Whereas in trajectory-based predictive control, the variables follow a predetermined trajectory (Nascimento, Dórea and Gonçalves, 2018).

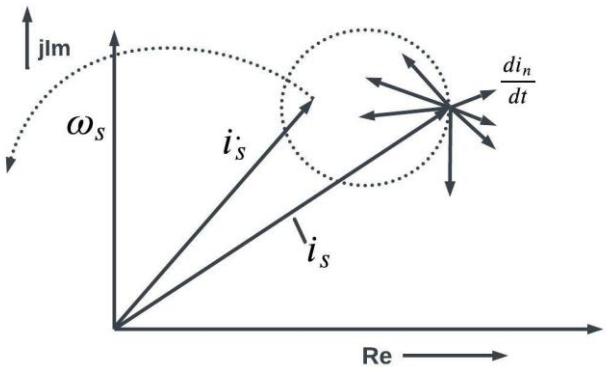

Figure 2. 13: Hysteresis-based predictive control.

2.4.2. Deadbeat predictive control

The deadbeat controller is a popular predictive control strategy that involves computing the reference voltage required to attain the desired reference value at the next sampling time, based on the system model. This method calculates the reference voltage only once per sampling interval. A modulator is then used to apply this voltage. It's used in three-phase inverters (Kukrer, 1996), (Slimani and Viarouge, 1994), (Moon, Kim and Youn, 2003), (Bode *et al.*, 2005), (Zeng and Chang, 2008), (Hamid *et al.*, 2020), rectifiers (Hamid *et al.*, 2020), power factor correctors (Zhang *et al.*, 2003), DC-DC converters (Stefanutti *et al.*, 2006), and induction machine torque control among others (Correa, Pacas and Rodríguez, 2007). When fast dynamic response is required, the deadbeat-based technique can become fragile. Model parameter inaccuracies, unmodeled delays, and other model defects may reduce system performance and induce instability. Furthermore, it can be challenging to incorporate nonlinearities and system constraints into deadbeat control methods. Figure 2.14 depicts a common deadbeat current control method. When compared to a traditional current control system, the PI controller has been substituted with the deadbeat controller. A modulator is used to apply the reference voltage. Figure 2.15 depicts the fundamental operation of deadbeat current control. In this case, the load current i at time K varies from the reference current i^*. This inaccuracy is used to calculate the reference voltage V that is supplied to the load at time K. Ideally, the load current will be equal to the reference current at time $K + 1$.

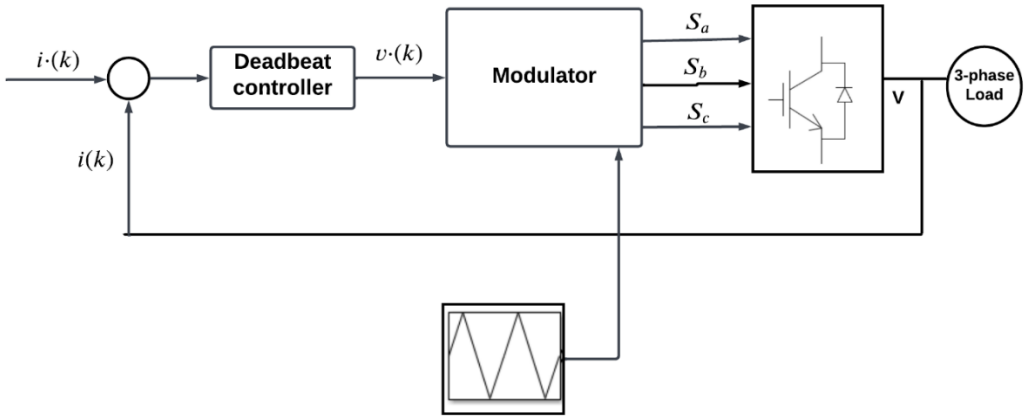

Figure 2. 14: Deadbeat current control.

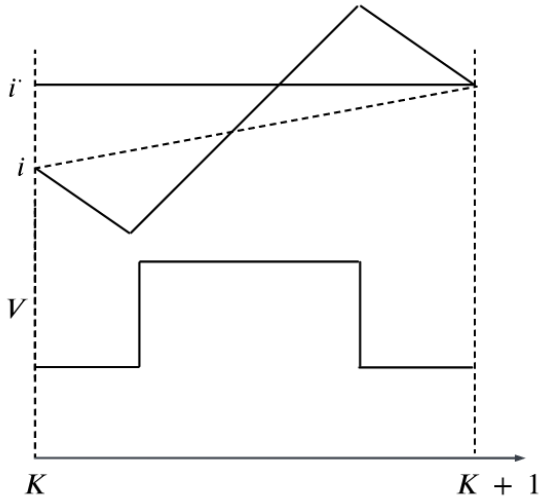

Figure 2. 15: Illustration of deadbeat current controller operation.

2.4.3. Model-based predictive control

MPC, sometimes termed receding horizon control, is the only so-called advanced control approach (more advanced than PID control) that has been effective in actual applications in recent decades, influencing industrial control system research and development. One appealing characteristic of MPC is its ability to handle broad constrained nonlinear systems with various inputs and outputs in a unified and straightforward way. According to several researchers' criteria, the most often utilized predictive control techniques in power converters are continuous-control set MPC and finite control set MPC. A summary of recent implementations of MPC in different power converter topologies is presented in the following section.

2.5. Applications of MPC in Various power converters

The application of MPC has been widely studied and implemented in various power converters.

MPC is an advanced control methodology that employs a mathematical model of the system to anticipate its future dynamics and optimize control inputs within a defined time horizon. This predictive control strategy has demonstrated its efficacy in enhancing the dynamic performance and efficiency of power converters, particularly in scenarios that necessitate rapid switching and simultaneous control of multiple variables. In Figure 2.16, a summary of the latest applications of MPC in various power converter configurations is provided.

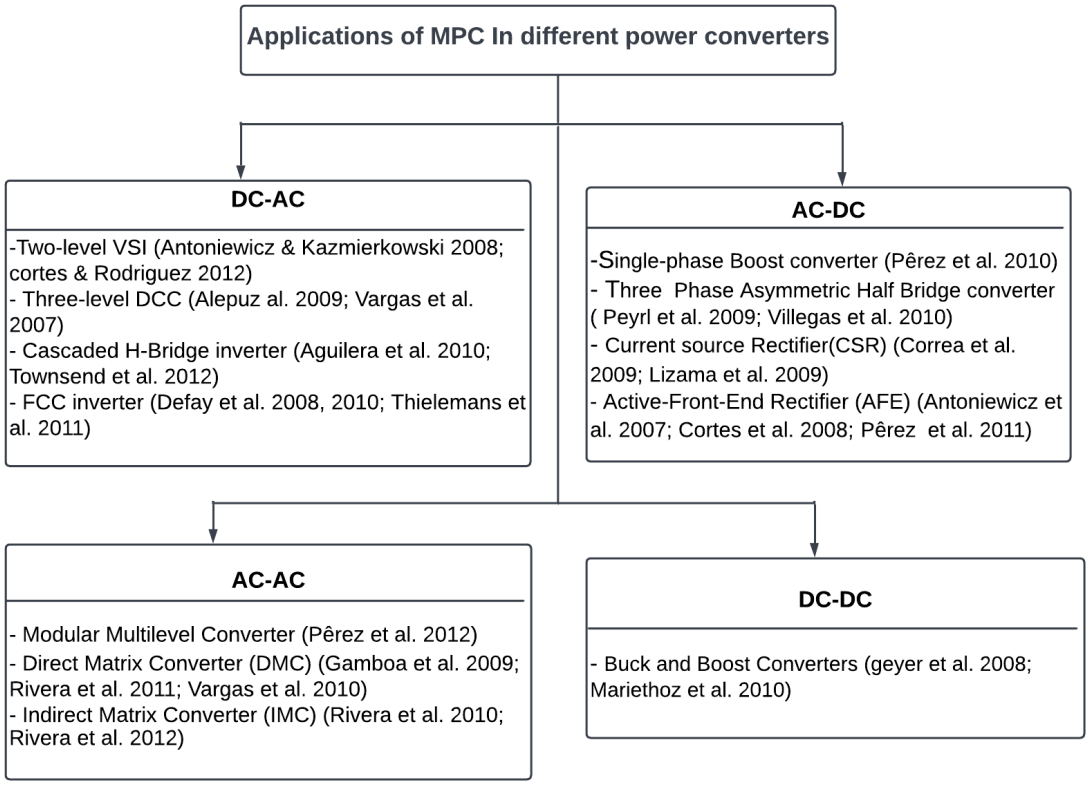

Figure 2. 16: Applications of MPC in various power converters.

In a CCS-MPC strategy, the MPC controller generates an appropriate reference signal, which is utilized in SPWM or SVM modulators. This control technique assumes that the converter operates continuously, and therefore, does not consider the specific states of semiconductor commutation. This results in the production of a continuous control signal, which is then fed into a modulator to produce the switching states, resulting in a fixed-frequency output (Vazquez *et al.*, 2014). This control technique gets its name from the continuous nature of the modulation method it employs. Nevertheless, one of

the primary obstacles that can impact the effectiveness of any MPC model is the rise in harmonic distortion (Rivera *et al.*, 2017). In contrast to alternative control techniques, CCS-MPC offers several benefits attributed to its implementation of a fixed-frequency modulator. These advantages include a swifter dynamic response and reduced harmonic distortion. Furthermore, larger prediction horizons can be employed without a significant escalation in computing costs.

The utilization of a linear model limits its suitability to particular operating points, necessitating the creation of distinct linear models at different operating points when non-linear modeling is necessary. Additionally, due to the complexity of model formulation, a modulator is required. To address these challenges, Finite Control Set Model Predictive Control techniques are designed.

FCS-MPC was devised as a solution to address the complexities associated with the model and the utilization of modulators. In contrast to the need for modulation, FCS-MPC takes into consideration the discrete characteristics of converters and employs a more straightforward algorithm. By doing so, FCS-MPC addresses the aforementioned drawbacks and selects the state that minimizes the cost function (Kouro *et al.*, 2009), (Bakeer, Alhasheem and Peyghami, 2022). The FCS-MPC method is characterized by a limited number of potential states and control actions, which makes it a type of finite state MPC. Despite this limitation, FCS-MPC is an attractive alternative due to its quick dynamic response, ability to include non-linearities and constraints in the prediction model, simplicity, and lack of modulators. However, the significant computing cost required by this model has hindered its progress. To mitigate the overall harmonic distortion, even modest electrical systems necessitate frequent calculations at a high rate. The advent of programmable devices like Field-Programmable Gate Arrays, incorporating more advanced CPUs, has played a significant role in tackling these limitations.

The difference between these control schemes is that in Power converters, Hysteresis-based control and trajectory-based control generate the switching signals for the converter without the need for a modulator, and this results in having a variable switching frequency. While deadbeat control and model predictive control with a continuous set, generates voltage with the help of a modulator, resulting in a fixed switching frequency. The implementation of MPC and dead-beat control especially in two-level converters, and when FS-MPC is considered, is simple. However, the implementation can be more complex if CS-MPC is considered, and to make basic deadbeat control more robust, its modifications can become quite complicated to

comprehend. One of the speed control methods for obtaining quick transient responses without the use of a cascaded structure is trajectory-based predictive control.

MPC offers a distinct advantage compared to deadbeat control by allowing the integration of nonlinearities within the model. This eliminates the need for linearizing the model at specific operating points, thereby improving system performance across all conditions. It is also feasible to include constraints on specific variables while constructing the controller. The primary focus of this study revolves around the implementation of MPC in power converters, specifically VSCs. The research specifically takes into account the utilization of a finite control set and a finite prediction horizon. Among the advanced control techniques available, MPC stands out as the sole control strategy that has achieved successful implementation in industrial applications (Maciejowski, 2002), (Goodwin, Seron and Dona, 2005), (Khan *et al.*, 2021).

2.6. Fundamental Principles of Model Predictive Control

The concepts of MPC as an application of optimal control theory were established in the 1960s, and industry interest began in the late 1970s (Morari, Garcia and Prett, 1988), (Lee, 2011), (Parihar *et al.*, 2022). Ever since, MPC has found utility in the chemical process sectors, particularly in situations where there's ample time available to perform all requisite computations. MPC was first used in power electronics in the 1980s, specifically for high-power devices with low switching frequency (Holtz and Stadtfeld, 1983), (Bacheti *et al.*, 2022). MPC is not feasible for devices that operate at high switching frequencies because the required computation time for the control technique is considerable. There has been a substantial increase in recent years in the interest in utilizing MPC in power electronics, driven by the advancements in fast and robust microprocessors. In various power converter topologies, Figure 2.16 offers an overview of recent applications involving MPC. MPC refers to a broad family of controllers rather than a single control approach. The basic aspects of this type of controller are that it utilizes a system model to forecast the future behavior of the variables until a predetermined time horizon, and it chooses the best actions by reducing a cost function MPC can be categorized into two subsets: continuous MPC and finite set MPC. Figure 2.12 displays the classification of MPC methods. The MPC structure provides several significant benefits:

i. The ideas are highly intuitive and simple to comprehend.
ii. It applies to a wide range of systems.
iii. The multivariable example is simple to consider.
iv. Non-linearities can be easily incorporated into the model.
v. Compensation for dead times is possible.

vi. Simple management of constraints and easy incorporation of non-linearities in the model
vii. The resultant controller is simple to use.
viii. Depending on the application, this technique is useful for incorporating modifications and additions.

One of the drawbacks of MPC is that it requires a substantial amount of computation compared to conventional controllers. The efficiency of the controller is influenced by the quality of the model, and any change in the system's parameters over time will necessitate the consideration of certain adaptations or estimation algorithms. The following are the fundamental principles underlying MPC:

i. The application of a model to anticipate the future trajectory of variables up to a specified time limit.
ii. A cost function that captures the intended system behavior.
iii. The optimal control input is achieved by reducing the cost function.

Figure 2.17 summarizes the operating concept of MPC (Jalili, 2018). Using the system model and existing measurements up to time K, the future values of the system's states are forecasted until a predetermined horizon of K+N. The series of optimal actuation is determined by minimizing the cost function, and the initial element of this series is selected. This entire procedure is then repeated for each sampling instant, taking into account the newly measured data.

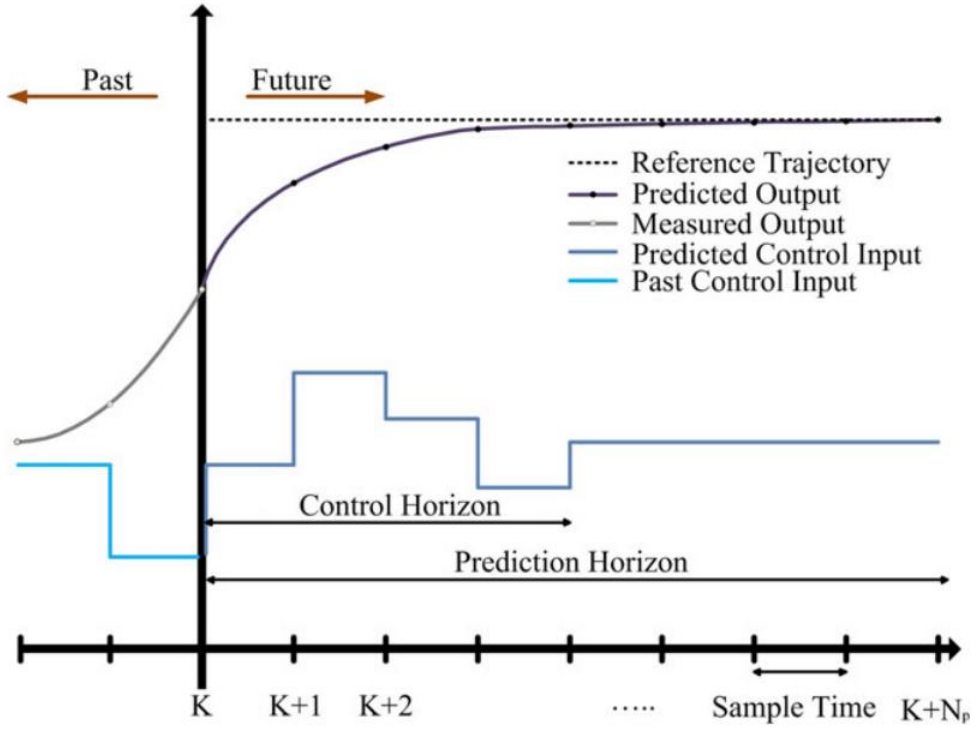

Figure 2. 17: Working principle of MPC.

2.7. Advancements in Model Predictive Control for Power Electronics and Drives

Due to the rapid sampling time required in power electronics systems, the implementation of MPC has been a recent development. The advancement of swift microprocessors over the last decade has catalyzed extensive exploration into the utilization of MPC for power electronics and drive applications. Generalized Predictive Control (GPC) is a promising alternative within the wide spectrum of MPC controllers. It presents an analytical solution to the optimization problem for linear systems without constraints, thereby offering numerous implementation possibilities. An explicit control rule arises from this, which can be easily put into practice. By employing GPC, MPC can improve the control of power electronic systems by reducing the effects of disturbances, uncertainties, and non-linearities (Clarke, Mohtadi and Tuffs, 1987), (Bordons and Camacho, 1998), (Kouro *et al.*, 2015). This control technique has been employed in many power converters (El-Kholy, 2005) (Effler *et al.*, 2008) (Low, 1998) and drives applications (Alkorta Egiguren *et al.*, 2008) (Kennel, Linder and Linke, 2001) (Hassaine *et al.*, 2007). In addition to GPC, another attractive option for implementing MPC in power electronic systems is Explicit MPC. Explicit MPC allows for the transfer of most of the optimization calculations offline, enabling real-time implementation despite the limited computation time available due to rapid sampling. By pre-computing the control actions over a large set of possible system states, Explicit MPC generates

a lookup table that provides the optimal control action for any given state. This eliminates the need for online optimization calculations, thereby reducing computational complexity and enabling fast response times. Explicit MPC has demonstrated successful implementation in controlling a range of power converters, including DC-DC converters, permanent magnet synchronous motors, and three-phase inverters (Beccuti *et al.*, 2009), (Mariéthoz and Morari, 2009), (Chen *et al.*, 2020).

Most GPC and explicit MPC techniques employ a modulator to mimic the power converter model as a linear system. This similarity simplifies the optimization procedure and facilitates the derivation of a straightforward control rule, eliminating the necessity for online optimization. Nevertheless, this simplification overlooks the discrete characteristics inherent in power converters. Incorporating the discrete character of power converters in the optimization process can simplify the control issue and enable online implementation. With the current powerful microprocessors and a limited number of switching states, computing the optimal actuation by evaluating each switching state online is a viable option. This approach can lead to a more flexible and simpler control scheme. Certain publications refer to the operational states of power converters, limited to a finite number of feasible actions, as Finite Set MPC. The upcoming chapters of this paper will focus on the Finite Set MPC approach.

2.8. Categorization of Cost Functions.

In Model Predictive Control, the cost function has the flexibility to incorporate multiple system variables, limitations, or needs beyond just a single variable. This feature enables the inclusion of physical variables such as current, voltage, and flux, which typically have different units and magnitudes. To address this challenge, MPC often employs weighting factors, denoted by λ, for each term in the cost function. These factors help to balance the contribution of each variable to the overall control objective.

$$g = \lambda_x \left| |x^{ref} - x^p| \right| + \lambda_y \left| |y^{ref} - y^p| \right| + \cdots + \lambda_z \left| |z^{ref} - z^p| \right| \qquad (2.1)$$

The various terms utilized in the formulation of the cost function can be categorized into distinct categories based on their nature. This categorization is required to assist the construction of a weighting factor modification technique that can be used to comparable kinds of cost functions. Discussed below are some of the types of cost functions.

2.8.1. Analysis of Cost Functions Excluding Weighting Factors

This is the easiest cost function because only one kind of variable is controlled and no weighting factors are required. Predictive current control of a voltage source inverter (Rodríguez *et al.*, 2007), predictive voltage control of an uninterruptible power supply

(UPS) system (P. Cortés, Ortiz, *et al.*, 2009), predictive current control with imposed switching frequency (Cortes *et al.*, 2008), predictive power control of an active front-end (AFE) rectifier (Cortés, Rodríguez, *et al.*, 2008), and predictive current control in multi-phase inverters (Barrero *et al.*, 2009) (P. Cortés, Vattuone, *et al.*, 2009) (Duran *et al.*, 2011), are a few representative instances of this sort of cost function. Table 2.1 summarizes the corresponding cost functions.

All of the terms in this form of the cost function are composed of the same type of variable (same unit and order of magnitude). Furthermore, some of them are the result of the breakdown of a single vector into two or more elements. As a result, no weighting factors or equivalent tuning procedures are required.

Table 2. 1: Cost functions without weighting factors

Application	Cost function
Controlling the current of a VSC	$\left\|i_{\alpha}^{ref} - i_{\alpha}^{p}\right\| + \left\|i_{\beta}^{ref} - i_{\beta}^{p}\right\|$ (2.2)
Controlling the voltage of a VSC	$\left(v_{c\alpha}^{ref} - v_{c\alpha}^{p}\right)^2 + \left(v_{c\beta}^{ref} - v_{c\beta}^{p}\right)^2$ (2.3)
Controlling the current of a VSC with multiple phases	$\left\|i_{\alpha}^{ref} - i_{\alpha}^{p}\right\| + \left\|i_{\beta}^{ref} - i_{\beta}^{p}\right\| + \left\|i_{y}^{ref} - i_{y}^{p}\right\|$ (2.4)

2.8.2. Analysis of Cost Functions Incorporating Secondary Terms

Many systems have a primary control goal that must be met to ensure correct system behavior, as well as secondary limitations or criteria that must be met to increase system performance or efficiency. This kind of cost function has primary and secondary terms, with the relevance of the secondary terms varying significantly depending on the application and its specific requirements predictive current control with reduction of common-mode voltage to avoid motor damage (Vargas *et al.*, 2008); predictive current control with reduction of the switching frequency to enhance efficiency (Vargas *et al.*, 2007); and predictive current control with reactive power reduction to enhance power quality (Müller, Ammann and Rees, 2005) (Vargas *et al.*, 2010), are few examples of this kind of cost function. Table 2.2 shows the corresponding cost functions.

Table 2. 2: Cost Functions Incorporating Secondary Terms.

Application	Cost function
Switching frequency reduction	$\left\|i_{\alpha}^{ref} - i_{\alpha}^{p}\right\| + \left\|i_{\beta}^{ref} - i_{\beta}^{p}\right\| + \lambda_{SW} n_{SW}^{p}$ (2.5)
Common-mode voltage reduction	$\left\|i_{\alpha}^{ref} - i_{\alpha}^{p}\right\| + \left\|i_{\beta}^{ref} - i_{\beta}^{p}\right\| + \lambda_{cm}\left\|V_{cm}^{p}\right\|$ (2.6)
Reactive power reduction	$\left\|i_{\alpha}^{ref} - i_{\alpha}^{p}\right\| + \left\|i_{\beta}^{ref} - i_{\beta}^{p}\right\| + \lambda_{Q}\left\|Q^{p}\right\|$ (2.7)

The significance of the secondary element in the cost function, which dictates the extent to which the common-mode voltage, switching frequency, or reactive power ought to be diminished, relies upon the distinct requirements of the application. Striking a balance to attain this reduction might entail compromising the primary control objective, such as current regulation in the context of the MPCC of a VSC. To balance these conflicting objectives, a weighting factor is typically assigned to the secondary term in the cost function. Adjusting this factor can help to fine-tune the trade-off between primary and secondary objectives, making it a crucial aspect of the control design process.

2.9. Summary

This chapter provides a comprehensive overview of a broad spectrum of power converters and their diverse applications in various systems. It focuses specifically on the present-day and practical industrial uses of VSCs in RES, with a particular emphasis on their use for interfacing with PV and wind turbine resources. It is crucial to acknowledge that although this chapter does not encompass all VSC power converter applications, it offers a systematic discussion focusing on the fundamental principles of various VSCs.

Furthermore, the chapter explores various predictive control methods that have gained significant recognition for regulating power electronic converters and motor drives. It offers an in-depth examination of the terminology utilized for predictive control through a comprehensive examination. Additionally, it offers an array of cost functions, considering both the inclusion and exclusion of weight factors. Additionally, the chapter provides insights into various kinds of terms that can be incorporated into a broad range of cost functions. To ensure a comprehensive understanding of the subject matter, the chapter includes examples of the discussed procedures presented in a tabular format. These examples serve to highlight the extensive array of cost function options for implementation in predictive control applications.

CHAPTER THREE

FS-MPCC APPROACH FOR A THREE-PHASE, TWO-LEVEL VSC

3.1. Introduction

MPC necessitates a large number of computations, leading to significant delays in actuation. In addition, the cost function used in MPC relies on future reference variable values, which further contributes to the delay in control systems. This chapter focuses on analyzing the impact of delay caused by measurement time and future reference values in MPC applied to a three-phase, two-level VSC. The delay between monitored and reference variables in the cost function of the voltage source inverter is also investigated. To address the delay caused by the predictive control algorithm's computational time, a simple compensation method is proposed. This method incorporates the delay into the prediction model without creating substantial variations in the monitored variable. Accurately assessing future reference variables is crucial to account for the delay that occurs in the cost function between the monitored and reference variables.

3.2. The proposed three-phase two-level voltage source converter model

The power circuit of the three-phase two-level VSC employs the electrical configuration shown in Figure 3.1 to convert DC electrical power into AC form. To ensure the prevention of potential short-circuits from the DC source, the switching state of the power switches can be represented by the switching signals S_a , S_b, and S_c. This is achieved by operating the two switches within each converter leg in a complementary mode.

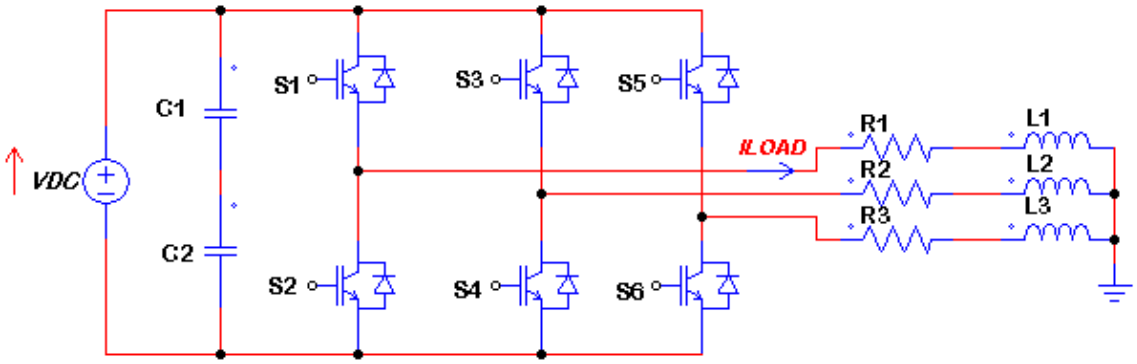

Figure 3. 1: The power circuit of the three-phase, two-level VSC

The switching signals are defined as follows:

$$S_a = \begin{cases} 1 \text{ if } S_1 \text{ on and } S_4 \text{ off} \\ 0 \text{ if } S_1 \text{ off and } S_4 \text{ on} \end{cases} \quad (3.1)$$

$$S_b = \begin{cases} 1 \text{ if } S_2 \text{ on and } S_5 \text{ off} \\ 0 \text{ if } S_2 \text{ off and } S_5 \text{on} \end{cases} \quad (3.2)$$

$$S_c = \begin{cases} 1 \text{ if } S_3 \text{ on and } S_6 \text{off} \\ 0 \text{ if } S_3 \text{ off and } S_6 \text{on} \end{cases} \quad (3.3)$$

The magnitude of the output voltage can be defined by these switching signals as follows:

$$V_{aN} = S_a V_{dc} \quad (3.4)$$

$$V_{bN} = S_b V_{dc} \quad (3.5)$$

$$V_{cN} = S_c V_{dc} \quad (3.6)$$

Where V_{dc} is the source DC voltage. The output voltage vector can be calculated by taking into account the unitary vector $\boldsymbol{a} = \boldsymbol{e^{2\pi j/3}} = -\frac{\mathbf{1}}{\mathbf{2}} + \frac{\sqrt{\mathbf{3}}}{\mathbf{2}}\boldsymbol{j}$, which symbolizes the 120° phase shift between the phases as follows:

$$\boldsymbol{v} = \frac{2}{3}\left(V_{aN} + \boldsymbol{a}V_{bN} + \boldsymbol{a^2}V_{cN}\right) \quad (3.7)$$

The phase-to-neutral voltages of the converter are denoted by V_{aN}, V_{bN}, and V_{cN}. As depicted in Figure 3.2, the three-phase two-level converter produces different switching states that lead to diverse arrangements of the three-phase load connected to the DC source.

The switching state $(S_a, S_b, S_c) = (0,0,0)$ produces voltage vector V_0 calculated using equation (3.7) as:

$$V_0 = \frac{2}{3}\left(0 + \boldsymbol{a}0 + \boldsymbol{a^2}\mathbf{0}\right) = 0 \quad (3.8)$$

This is equivalent to the circuit seen in Figure 3.2(a). Produced by switching state (1,0,0) as shown in Figure 3.2(b), the voltage vector V_1 is calculated as:

$$V_1 = \frac{2}{3}\left(V_{dc} + \boldsymbol{a}0 + \boldsymbol{a^2}\mathbf{0}\right) = \frac{2}{3}V_{dc} \quad (3.9)$$

Produced by switching state (1,1,0) as shown in Figure 3.2(c), the voltage vector V_2 is calculated as:

$$V_2 = \frac{2}{3}\left(V_{dc} + \boldsymbol{a}V_{dc} + \boldsymbol{a^2}\mathbf{0}\right)$$

$$V_2 = \frac{2}{3}\left(V_{dc} + (-\frac{\mathbf{1}}{\mathbf{2}} + \boldsymbol{j}\frac{\sqrt{\mathbf{3}}}{\mathbf{2}})V_{dc}\right) = \frac{V_{dc}}{3} + \boldsymbol{j}\frac{\sqrt{\mathbf{3}}}{\mathbf{2}}V_{dc} \quad (3.10)$$

Produced by switching state (1,1,1) as shown in Figure 3.2(d), the voltage vector V_7 is calculated as:

$$V_7 = \frac{2}{3}\left(V_{dc} + \boldsymbol{a}V_{dc} + \boldsymbol{a^2}V_{dc}\right)$$

$$V_7 = \frac{2}{3}\left(V_{dc} + \left(-\frac{\mathbf{1}}{\mathbf{2}} + \boldsymbol{j}\frac{\sqrt{\mathbf{3}}}{\mathbf{2}}\right)V_{dc} + \left(-\frac{\mathbf{1}}{\mathbf{2}} + \boldsymbol{j}\frac{\sqrt{\mathbf{3}}}{\mathbf{2}}\right)^2 V_{dc}\right) = 0 \quad (3.11)$$

When all possible gating signal combinations are considered, there are eight possible switching states and hence eight possible voltage vectors. However, since V_0 is equivalent to V_7, only seven distinct voltage vectors are considered. This is illustrated in Table 3.1.

Table 3. 1: Switching states and voltage vectors.

S_a	S_b	S_c	Voltage vector $\mathbf{V}$
0	0	0	$\mathbf{V}_0 = 0$
1	0	0	$\mathbf{V}_1 = \frac{2}{3}V_{dc}$
1	1	0	$\mathbf{V}_2 = \frac{1}{3}V_{dc} + j\frac{\sqrt{3}}{3}V_{dc}$
0	1	0	$\mathbf{V}_3 = -\frac{1}{3}V_{dc} + j\frac{\sqrt{3}}{3}V_{dc}$
0	1	1	$\mathbf{V}_4 = -\frac{2}{3}V_{dc}$
0	0	1	$\mathbf{V}_5 = -\frac{1}{3}V_{dc} - j\frac{\sqrt{3}}{3}V_{dc}$
1	0	1	$\mathbf{V}_6 = \frac{1}{3}V_{dc} - j\frac{\sqrt{3}}{3}V_{dc}$
1	1	1	$\mathbf{V}_7 = 0$

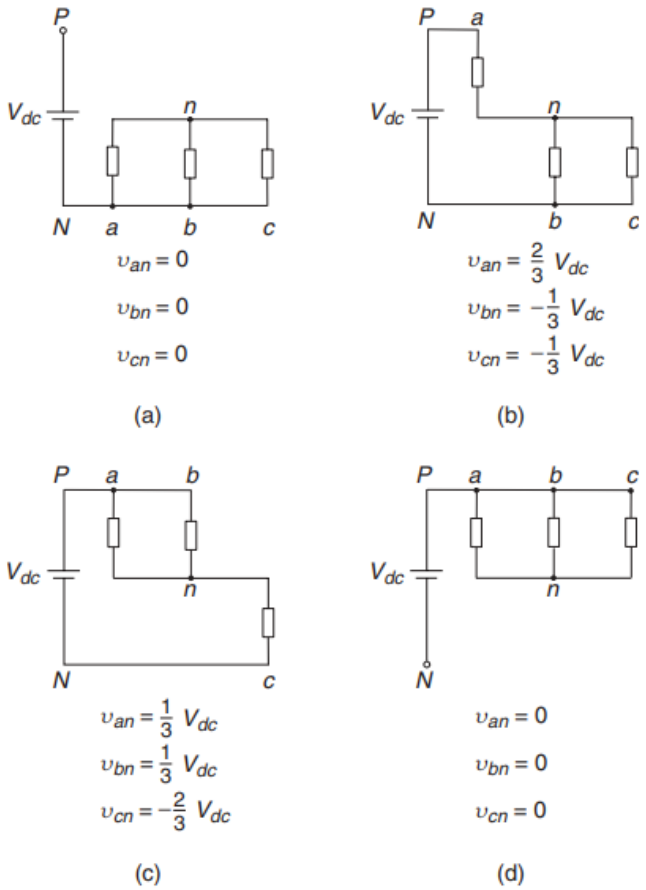

Figure 3. 2: Different Load Arrangements under Different Switching Conditions: (a) Represented as V_0 for switching state (0, 0, 0), (b) Represented as V_1 for switching state (1, 0, 0), (c) Represented as V_2 for switching state (1, 1, 0), and (d) Represented as V_7 for switching state (1, 1, 1).

3.3. Predictive Control of a Three-Phase Converter

As a first step, it is vital to study the usage of MPC in a current control scheme, as current control is one of the most investigated issues in power electronics (Holtz, 1994) (Kazmierkowski, Krishnan and Blaabjerg, 2002) (Mohan, Undeland and Robbins, 2003), (Schwenzer *et al.*, 2021). Furthermore, the three-phase, two-level inverter is a well-known architecture that may be found in most drive applications.

3.3.1. Predictive Current Control

The proposed predictive control scheme, illustrated in Figure 3.3, is implemented on a three-phase voltage source converter. The scheme is designed based on the principle that a static power converter has a limited range of switching states. It relies on system models to anticipate the behavior of variables associated with each switching state. A selection criterion is established, which includes a cost function to evaluate the anticipated values of the variables intended for regulation, before implementing the suitable switching state. The future values of the variables are predicted for each potential switching state, and the choice is made based on the prediction that minimizes the cost function. The control strategy can be outlined in the following sequence of actions:

i. defining a cost function g,
ii. constructing a model of the converter and its available switching states, and
iii. creating a model of the load to facilitate prediction.

The employed model for prediction is a discrete-time one, and it can be depicted as a state-space model in the subsequent manner:

$$\boldsymbol{x}(k+1) = A\boldsymbol{x}(k) + B\boldsymbol{u}(k) \tag{3.12}$$

$$\boldsymbol{y}(k) = C\boldsymbol{x}(k) + D\boldsymbol{u}(k) \tag{3.13}$$

At a given time, denoted as k, $\boldsymbol{x}(k)$ represents the current state values and $\boldsymbol{u}(k)$ represents the control input values, while $\boldsymbol{x}(k+1)$ represents the predicted state. To achieve the desired system behavior, it is necessary to define a cost function g. This function takes into account future states, references, and future control actions in its evaluation.

$$g = f(\boldsymbol{x}(k), \boldsymbol{u}(k), \ldots., \boldsymbol{u}(k+N)) \tag{3.14}$$

The MPC approach involves an optimization problem where the objective is to minimize the cost function g over a predetermined time horizon N, taking into consideration the system's model and constraints. As a result, a series of N optimal actuations are produced. Once the optimization problem is solved at each sampling instance by

considering updated measured values and a newly generated sequence of optimal control actions, the controller selectively employs only the initial element from the sequence. This is known as a receding horizon strategy.

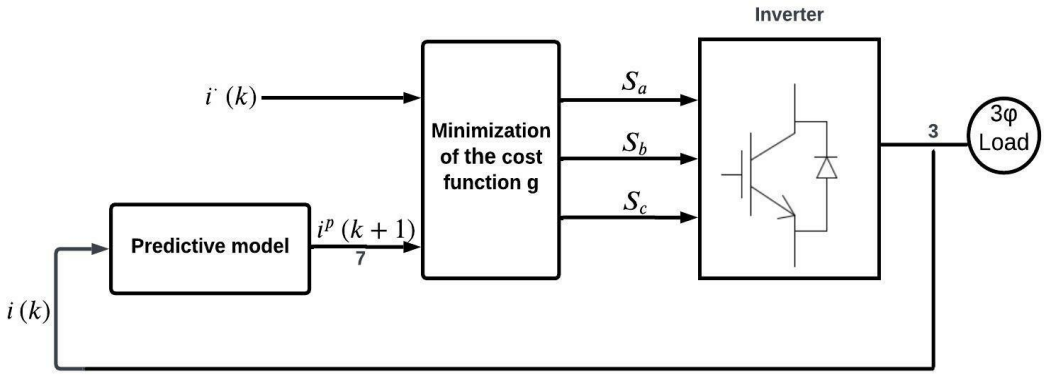

Figure 3. 3: Predictive current control block diagram.

3.3.2. Control design of a power converter employing finite set model predictive current control

The design phase of the Finite control set MPC of a power converter consists of the following steps:

i. Power converter modeling that identifies all possible switching states and their relationships to input or output currents and voltages
ii. Determining a cost function that describes the intended system behavior.
iii. Developing discrete-time models that enable one to forecast the future behavior of the variables to be controlled.

When modeling a converter, the fundamental element under consideration is the power switch. It could be an IGBT, a GTO, or other similar components. The representation of this power switch assumes an ideal nature with two states: ON and OFF. Therefore, the complete array of switching states in a power converter corresponds to the unique combinations of these two states for each switch. However, certain combinations that could lead to a short circuit in the DC connection are not practically achievable. The number of feasible switching states, denoted as N, can be determined as follows:

$$N = X^Y \tag{3.15}$$

X denotes the number of potential switching states for each converter leg, while Y represents converter phases. Therefore, for a three-phase, two-level converter, the total number of feasible switching states N can be calculated as $N = 2^3 = 8$ possible

switching states. In multilevel converters, like nine-level cascaded H-bridge converters, the switching states of the converter are usually high equalling more than 16 million switching states. The converter model is characterized not only by the power switch but also by the relationship between switching states and voltage or current vectors. While voltage vectors are relevant for some types of converters, such as single-phase converters, current vectors are more applicable to current converters. However, it is important to note that multiple switching states can generate the same voltage or current vector. For instance, in a three-phase, two-level converter, eight switching states can result, with two of the switching states producing a zero vector, in eight unique voltage vectors. The three-phase, three-level converter exhibits significant redundancy, as 27 switching states can generate only 19 distinct voltage vectors. A visualization of voltage vectors produced by a three-phase, two-level converter can be found in Figure 3.4, represented in the complex plane.

A critical consideration when modeling converter topologies is the method used to calculate switching states. The method employed may differ depending on the application's control requirements, including power, current, torque control, or low switching frequency. The control criteria can be represented by a cost function that requires minimization. The cost function measures the discrepancy between a reference and a predicted variable, such as power error, and load current error, among others. Predictive control approaches offer the advantage of regulating various kinds of variables and incorporating constraints into the cost function. The cost function incorporates weighting factors for each term to accommodate varying units and magnitudes of the controllable variables. These factors can be adjusted to alter the significance of each term within the cost function. When constructing a prediction model, it is important to consider the controlled variables and develop discrete-time models to forecast these variables accurately. Additionally, it is crucial to identify which variables are measured and which are not since there may be situations requiring an estimation where critical variables for the prediction model are not measured.

To acquire a discrete-time model, discretization techniques are utilized. Because it is easy, it is advantageous to estimate the derivatives of first-order systems utilizing the Euler forward approach, which can be expressed as follows:

$$\frac{dx}{dt} = \frac{x(k+1)-x(k)}{T_S} \qquad (3.16)$$

Where T_S is the sampling time. Nonetheless, as the system order rises, the precision of the discrete-time model derived through the Euler method declines due to the significant error introduced by this technique for systems with elevated orders. To

address this issue, an exact discretization technique is necessary when dealing with higher-order systems.

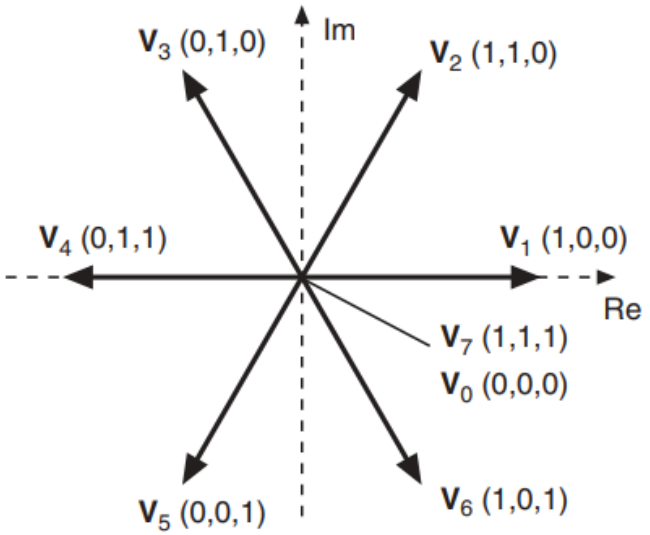

Figure 3. 4: Voltage vectors produced by a three-phase, two-level VSC in the complex plane.

3.3.3. Implementations of Model Predictive Current Control

The controller must take into account the following tasks when it is implemented:

i. Predict how the controlled variables will behave in all switching states.
ii. For each forecast, determine the cost function.
iii. Choose the switching state that has the lowest cost function.

The implementation of predictive models and control algorithms can present varying challenges contingent upon the type of platform employed. For instance, when utilizing fixed-point processors, programming must be done with utmost care to achieve excellent precision in the fixed-point depiction of variables, especially when dealing with small signals. In contrast, floating-point processors offer greater precision and can handle more complex calculations, enabling the use of programming similar to that used in simulations.

The number of computations needed can be influenced by the complexity of the controlled system, and this can impact the minimum sampling time. While predictive current control requires short calculation times, other schemes like torque and flux control rely on calculation time to determine the permissible sampling duration. As such, careful consideration is necessary when selecting the platform and designing the control algorithm to ensure optimal performance.

To select the switching state that minimizes the cost function, an evaluation is conducted for all feasible states, and the most favorable value is retained for subsequent utilization. The quantity of calculations required is directly proportional to the number of switching states. While calculating predictions for the eight possible switching states poses no issue for a three-phase, two-level inverter, alternative optimization strategies need to be explored for multi-level and multi-phase systems to reduce the computational burden.

3.4. Design and Implementation Challenges of Model Predictive Current Control

MPC is a popular control strategy that utilizes a mathematical model of the system to optimize control inputs over a finite time horizon. Despite the successful application of MPC in various industrial settings, several design and implementation issues must be addressed for its effective use. Among the critical issues are:

3.4.1. Cost Function selection

This chapter explores a wide variety of terms that can be incorporated into a cost function and illustrates their relationship with different control criteria for system operation. The cost function can accommodate any pertinent term representing a prediction for another system variable, limitation, or requirement. These terms include reference tracking, actuation limitations, stringent restrictions, and spectral properties.

3.4.1.1. Reference following

Terms like current control, power control, and torque control are the most common terms in a cost function that represent a variable following a reference. These terms can be expressed in a general way as the error between the predicted variable and its reference:

$$g = ||\left|x^{ref} - x^{P}\right|| \quad (3.17)$$

Where x^{ref} denotes the reference and x^{P} denotes the forecasted value of the controlled variable, for a certain switching state of the power converter. The norm, denoted as $|| \cdot ||$, quantifies the discrepancy between the reference and predicted values, and its implementation typically involves options such as squared value, absolute value, or integral value of the error over a single sampling period.

$$g = \left|x^{ref} - x^{P}\right| \quad (3.18)$$

$$g = \left(x^{ref} - x^{P}\right)^{2} \quad (3.19)$$

$$g = |\int_{k}^{k+1} \left(x^{ref}(t) - x^{P}(t)\right) dt| \quad (3.20)$$

When the cost function includes only one error component, absolute error, and squared error provide identical results. Nevertheless, in scenarios where the cost function

comprises multiple distinct terms, the outcomes can potentially vary. When extra terms are incorporated in the cost function, squared error offers an excellent reference following, as demonstrated in the next section. The cost function (3.20) examines the variable's trajectory between time t_k and t_{k+1}, rather than only the final value at the instant t_{k+1}, resulting in the mean value of the error being reduced. This leads to more precise reference tracking. This simple type of cost function may be used to regulate a variety of systems, including those described in this paper.

The cost function utilized in three converters, an active front-end rectifier and a matrix converter that can provide current control for three-phase systems is defined in orthogonal coordinates below:

$$g = \left|i_{\propto}^{ref} - i_{\propto}^{p}\right| + \left|i_{\beta}^{ref} - i_{\beta}^{p}\right| \quad (3.21)$$

The following cost function is utilized to accomplish direct power control:

$$g = \left|P^{ref} - P^{P}\right| + \left|Q^{ref} - Q^{P}\right| \quad (3.22)$$

3.4.1.2. Actuation Constraints

In a control system, it is critical to strike a balance between reference following and control effort. The use of model predictive control allows for the consideration of any measure of control effort in the cost function to decrease it. The control effort in power converters and drives is proportional to the switching frequency or losses, as well as fluctuations in current or voltage. The control effort in the three-phase converter is represented by the change in the voltage vector applied to the load.

3.4.1.3. Hard Constraints

One advantage of predictive control is the ability to provide direct control of output variables without the necessity of inner control loops. However, it has been discovered in various circumstances that when internal variables are not controlled, they can reach values that are outside their allowable range. In predictive control, this kind of internal variable constraint is handled by incorporating it as an additional term in the cost functions. These constraints can be addressed in traditional control methods by incorporating saturation values for these variables' references.

3.4.1.4. Spectral Content

It is feasible to specify requirements for the spectral content of the variables in the cost function in addition to controlling the instantaneous values of the variables. The basic predictive control system given in this thesis does not enforce any pattern on the switching signals. The sampling frequency limits the maximum switching frequency; however, the optimal switching state can be maintained throughout numerous sampling

periods. As a result, the controlled variables have a spread spectrum and a variable switching frequency.

3.4.2. Delay Compensation

When implementing MPC in experimental systems, a significant number of computations may be required, leading to a delay in actuation that can potentially degrade system performance. To address this, several compensation approaches have been developed to account for this delay in MPC design. These compensation techniques have been applied in various predictive control systems, including deadbeat control.

Delays in these control systems are often caused by the need to incorporate future reference variable values in the cost function. It is often assumed that future reference values represent the real reference if the sampling frequency significantly exceeds the reference variable frequency or the reference is constant. Nonetheless, delays could arise in cases of transients or when dealing with sinusoidal references, necessitating the computation of upcoming reference variables for delay mitigation.

To overcome this issue, basic extrapolation techniques can be used to compute future reference variables in advance. By leveraging past measurements and predictions, these techniques can help estimate future reference values and update the control inputs accordingly, reducing the delay in actuation and improving system performance. This chapter provides an overview of these basic extrapolation techniques for computing future reference variables.

3.4.2.1. The impact of delays caused by calculation time.

The control of a three-phase VSC with a passive load serves as an illustrative example to showcase the impact of calculation time delay and compensation techniques. The concepts discussed in this context apply to various predictive control methods. Figure 3.3 presents the algorithm for the MPC system, comprising the following stages:

Step 1: Measure the current of the load.

Step 2: Predict the load current for the upcoming sampling moment, considering all potential switching states.

Step 3: Assess the cost function for each prediction.

Step 4: Choose the switching state that minimizes the cost function.

Step 5: Implement the new switching state.

A flowchart in Figure 3.5 illustrates the predictive control method. This method involves repeating the calculation of the forecast current and cost function for each possible switching state, resulting in a large number of computations performed by the CPU, as

shown in the diagram. When focusing on current control, the cost function is determined by the disparity between the reference current and the anticipated currents corresponding to a specific switching state. It can be mathematically represented as:

$$g = \left|i_{\alpha}^{ref}(k+1) - i_{\alpha}^{p}(k+1)\right| + \left|i_{\beta}^{ref}(k+1) - i_{\beta}^{p}(k+1)\right| \qquad (3.23)$$

Where i_{α}^{ref} and i_{β}^{ref} represent the actual and imaginary components, respectively, of the reference current vector, and i_{β}^{ref} and i_{β}^{p} denote the real and imaginary components, respectively, of the predicted load current vector $i^{P}(k+1)$. By utilizing a discrete-time model of the load, the predicted load current vector is formulated. It is a function of the measured currents $i(k)$ and the inverter voltage (the actuation) $v(k)$, Mathematically, it can be expressed as follows:

$$i^{p}(k+1) = (1 - \frac{RT_S}{L})ik) + \frac{T_S}{L}v(k) \qquad (3.24)$$

Where R is the load resistance, L is the inductance and T_S is the sampling time. The functioning of model predictive control with and without time delay is shown in Figures 3.6 and 3.7, respectively. Figure 3.6 displays the operation of MPC without any time delay, showcasing the steps involved in the algorithm. In the given scenario, the dotted line represents the predictions for i_{β}, which are derived using equation (3.24). On the other hand, the solid line represents the actual trajectory attained by implementing the optimal voltages obtained through the minimization of the cost function as defined in equation (3.23). At time t_k, the currents are assessed, and the optimal switching state is promptly computed. The switching state that minimizes the error at the time t_{k+1} is chosen and executed at the time t_k. As a result, the predicted value guides the convergence of the load current at the time t_{k+1}.

The three-phase two-level converter encompasses a set of eight switching states, resulting in the generation of seven distinct voltage vectors. The sequential calculation of the predicted current and cost function is carried out in this system. The illustration in Figure 3.6 highlights the optimal performance attained by MPC when the computational time is negligible. However, in situations where the sampling frequency and microprocessor speed utilized for control yield a computation time that exceeds the sampling period, a delay arises between the measurement of load currents and the application of new switching states, as depicted in Figure 3.7. This delay introduces a notable drawback, as the previous switching state persists, leading to a degradation in overall system performance. The voltage vector selected based on measurements at a time t_k continues to be applied beyond the subsequent time instant, t_{k+1}, resulting in a deviation of the load current from the reference value. The subsequent actuation will be determined using measurements at a time t_{k+1} and implemented close to the time

t_{k+2}. As a consequence of this delay, the load current experiences fluctuations around its reference, leading to an amplified current ripple.

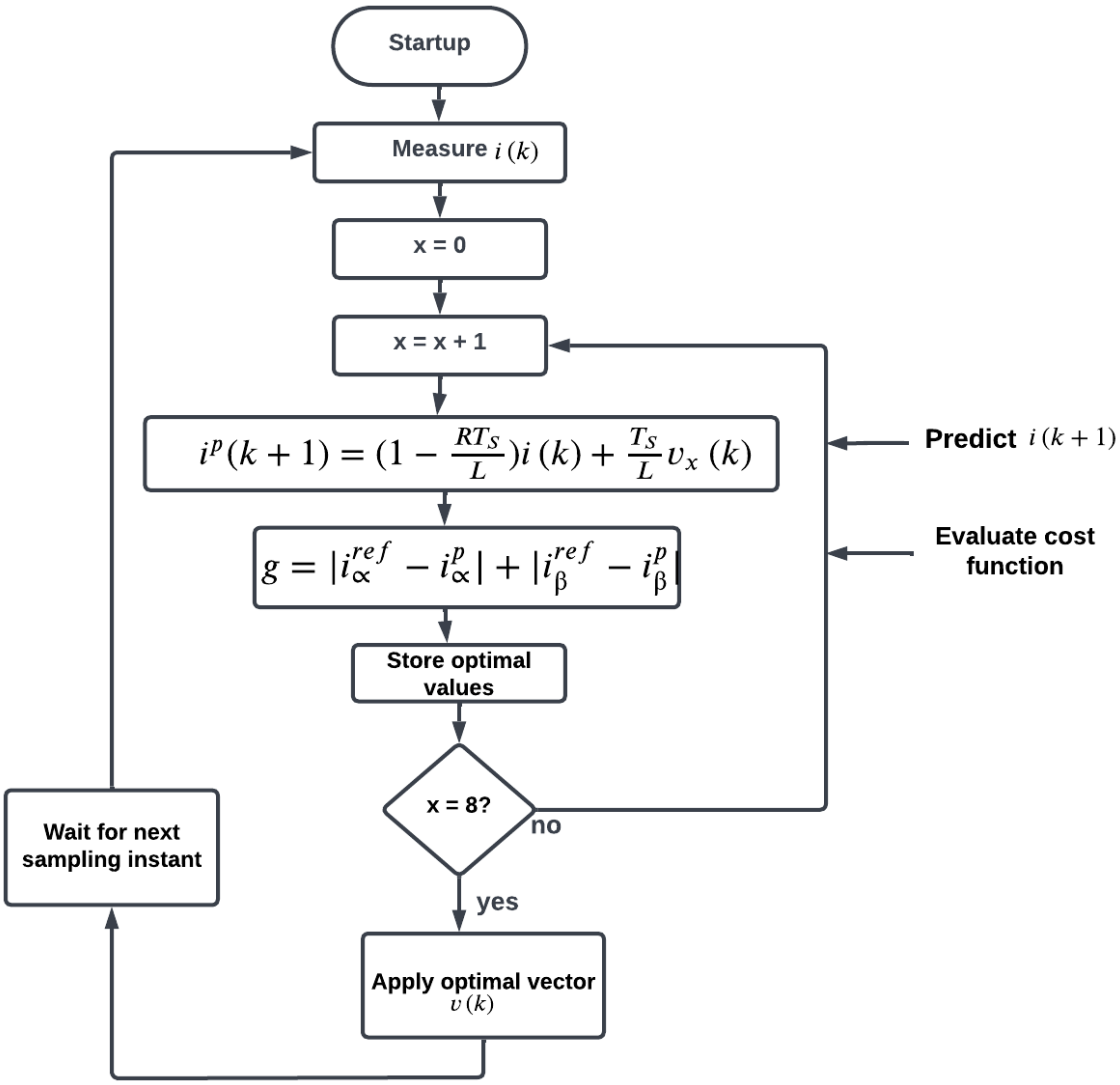

Figure 3. 5: Flowchart of the predictive current control.

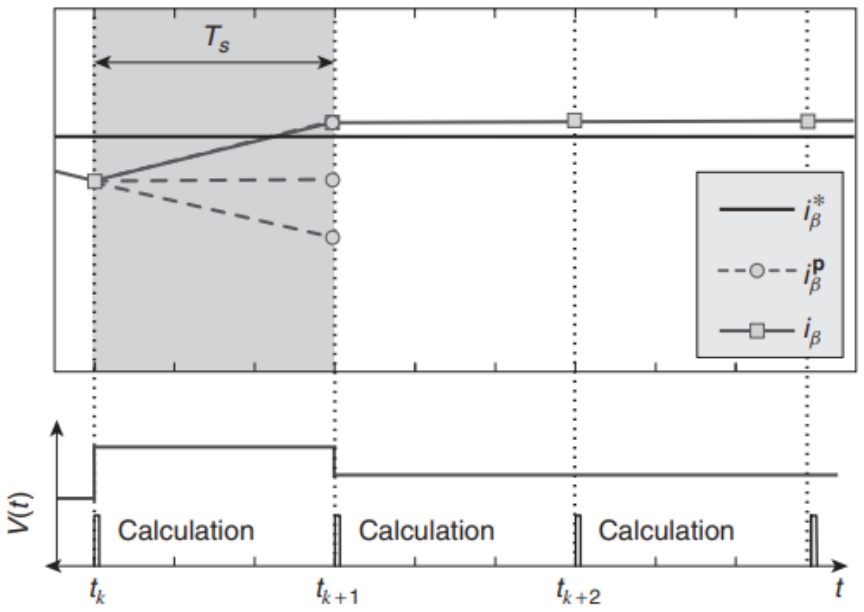

Figure 3. 6: MPCC Operation with Zero Calculation Time Delay.

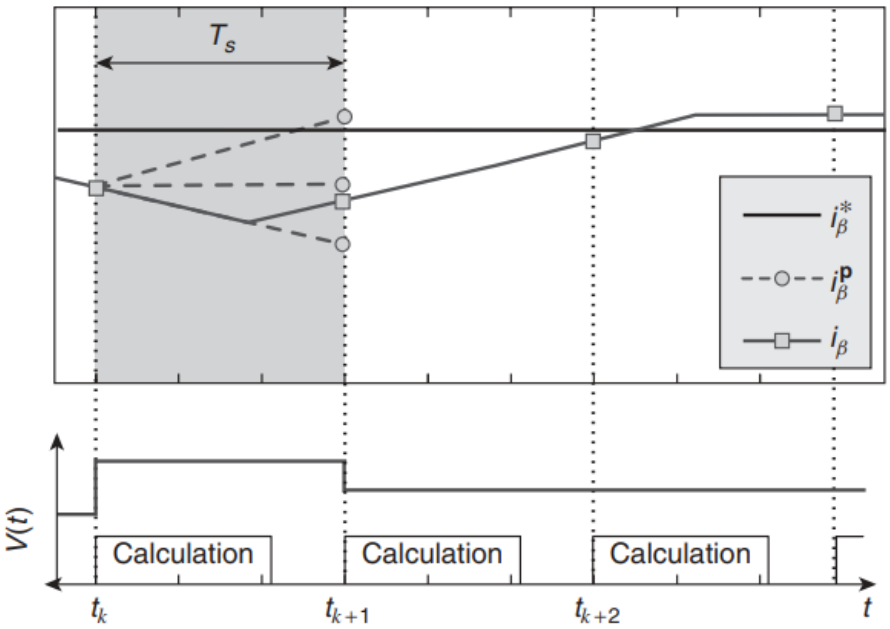

Figure 3. 7: Performance of MPCC under time delay with significant calculation time.

3.4.2.2. Procedures for Delay Compensation

To compensate for the delay caused by computation time, the control algorithm can be adjusted as follows:

i. Perform measurements of the load currents.
ii. Apply the switching state determined in the preceding interval.
iii. Estimate the currents at the time t_{k+1}, considering the selected switching state.
iv. Forecast the load currents for time t_{k+2} considering all viable switching states.
v. Assess the cost function for each prediction.
vi. Choose the switching state that minimizes the cost function.

The predictive control method with delay compensation may also be shown as a flowchart, as shown in Figure 3.8. Compared to Figure 3.5, the new voltage vector is applied first, and currents are estimated at t_{k+1}. Figure 3.9 shows predictive control with delay compensation. The currents measured at the time t_k along with the switching state, are employed in equation (3.24) to forecast the load currents at the time t_{k+1}). This forecasted current serves as the initial point for all subsequent switching state predictions. These predictions are generated by utilizing the load model advanced by a one-time step:

$$i^p(k+2) = \left(1 - \frac{RT_S}{L}\right) ik+1) + \frac{T_S}{L} v(k+1) \qquad (3.25)$$

Where t_{k+1}, the predicted current is the vector, and $v(k+1)$ is the actuation. The cost function for $i^p(k+2)$ is adjusted, resulting in:

$$g = \left|i_\alpha^{ref}(k+2) - i_\alpha^p(k+2)\right| + \left|i_\beta^{ref}(k+2) - i_\beta^p(k+2)\right| \qquad (3.26)$$

The switching state that reduces this cost function is chosen and saved for use at the subsequent sampling time.

3.4.3. Future Reference Predictions

The predictive control strategies rely on a cost function that takes into account the future error, i.e., the difference between the predicted variable and the reference at the next sampling instant. However, since future references are often unknown, they must be approximated. One basic method for approximation assumes that the future value of the reference signal is roughly equal to its current value, given that the sampling frequency is much higher than the reference signal frequency. This approach is straightforward but may not be sufficient in cases where the reference signal changes rapidly or unpredictably. In the case of predictive current control, the cost function can be simplified by assuming that $i^{ref}(k) = i^{ref}(k+1)$

$$g = \left|i_\alpha^{ref}(k) - i_\alpha^p(k+1)\right| + \left|i_\beta^{ref}(k) - i_\beta^p(k+1)\right| \qquad (3.27)$$

This approximation will delay current tracking by one sample. If the preceding section's computation time delay is included, $i^{ref}(k+2)$ is needed. Using the same logic, the future reference can be simplified by assuming that $i^{ref}(k+1) = i^{ref}(k+2)$, yielding the cost function:

$$g = \left|i_{\alpha}^{ref}(k+1) - i_{\alpha}^{p}(k+2)\right| + \left|i_{\beta}^{ref}(k+1) - i_{\beta}^{p}(k+2)\right| \qquad (3.28)$$

And the reference track will have a two-sample delay. This strategy is suitable in predictive control systems that employ smaller sample durations. When the references are constant, this strategy has no detrimental impacts, and the two-sample delay can only be detected during transients.

3.4.4. Model Parameter Errors

MPC is a control method that uses system models to determine the best actuations, making it unique among other control strategies. However, variations in system parameter values can negatively impact the performance of MPC in terms of the root-mean-square (RMS) error of load currents. Despite this, the dynamic performance of MPC remains unaffected. Given that parameter values may fluctuate in certain systems and may be impossible to obtain in others, it is crucial to investigate how MPC methods perform when model parameter inaccuracies are present. It should be noted that while variations in system parameter values can impair the RMS error of load currents, the dynamic performance of MPC remains robust.

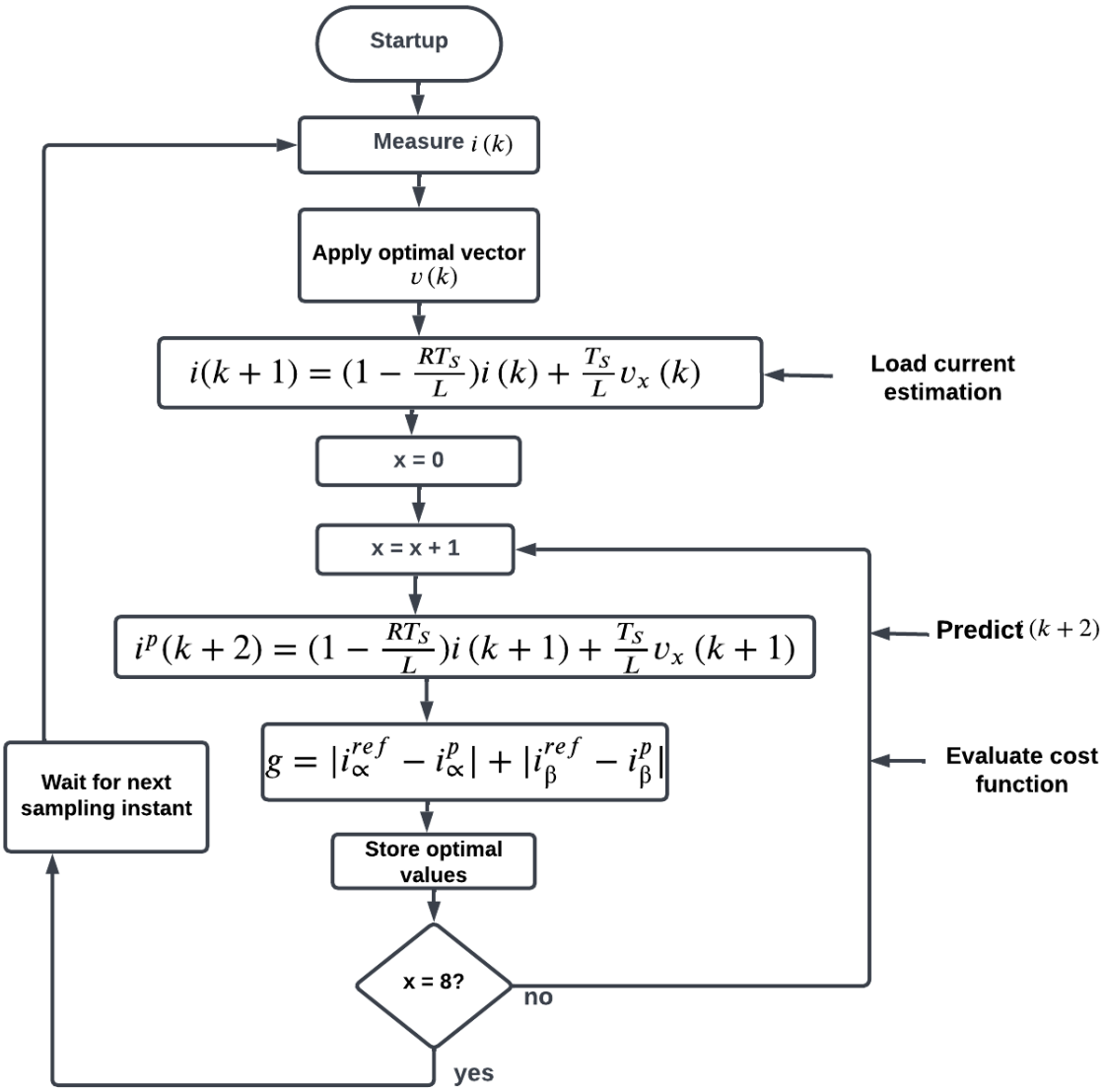

Figure 3. 8: Flowchart of the MPC method with delay compensation.

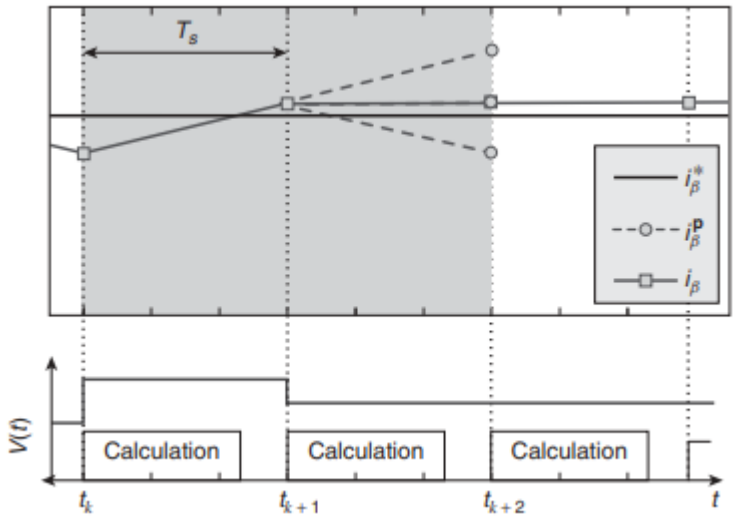

Figure 3. 9: MPCC Delay Compensation: Addressing Lengthy Calculation Time

3.5. Summary

This chapter begins with a comprehensive overview of the proposed model for a three-phase two-level VSC. The structure and characteristics of the model are discussed in detail, providing valuable insight into its design and operation. Next, the chapter addresses predictive control techniques applied specifically to three-phase converters. The concept of predictive current control, which plays a critical role in the effective control of the converter, is introduced and its importance is highlighted. The chapter focuses on the approximations employed for the derivatives of the differential equations within the MPC framework. The purpose is to clarify the fundamental concepts of predictive control and to describe the system modeling procedure, including approximations for differential equation derivatives. Additionally, the chapter delves into the classification of cost functions with regard to delay compensation methods and reference frames. It explains the various compensation procedures that can be incorporated into the equations of the cost functions. Several examples of these procedures are provided, illustrating different types of cost functions.

Overall, this chapter aims to provide a comprehensive understanding of the proposed model, predictive control techniques, and key considerations such as system modeling, derivative approximations, cost function classifications, and compensating procedures.

CHAPTER FOUR

MODELLING AND SIMULATION

4.1. Introduction

This chapter is divided into two sections: The first section describes the modeling approach, while the second section discusses the simulation results and proposed solutions for delay compensation in MPC applied to a three-phase, two-level VSC. The simulation segment results are based on a balanced DC link and evaluate the efficacy of the proposed delay compensation methods.

4.2. Modeling of three-phase two-level VS inverter with MPC controller

The topology and control of the three-phase two-level VSC were presented in the previous chapters. Figure 4.1 depicts the topology of the three-phase two-level with the MPC controller which consists of 6 switches, 2 capacitors (C1 and C2), a DC source, and a load.

Different switching configurations led to unique arrangements of the three-phase load linked with the DC source, as depicted in Figure 3.1. By examining all potential permutations of the gating signals (Sa, Sb, Sc), a total of 8 switch states were derived, resulting in 8 associated voltage vectors. However, since voltage vectors 0 and 1 are equal, only 7 finite sets of voltage vectors were considered in this paper as shown in Figure 3.4.

In the operation of MPC for a two-level VSC with an RL load in a three-phase system, the following typical steps are carried out:

i. Step of Estimation
ii. Step of Prediction
iii. Step of Optimization

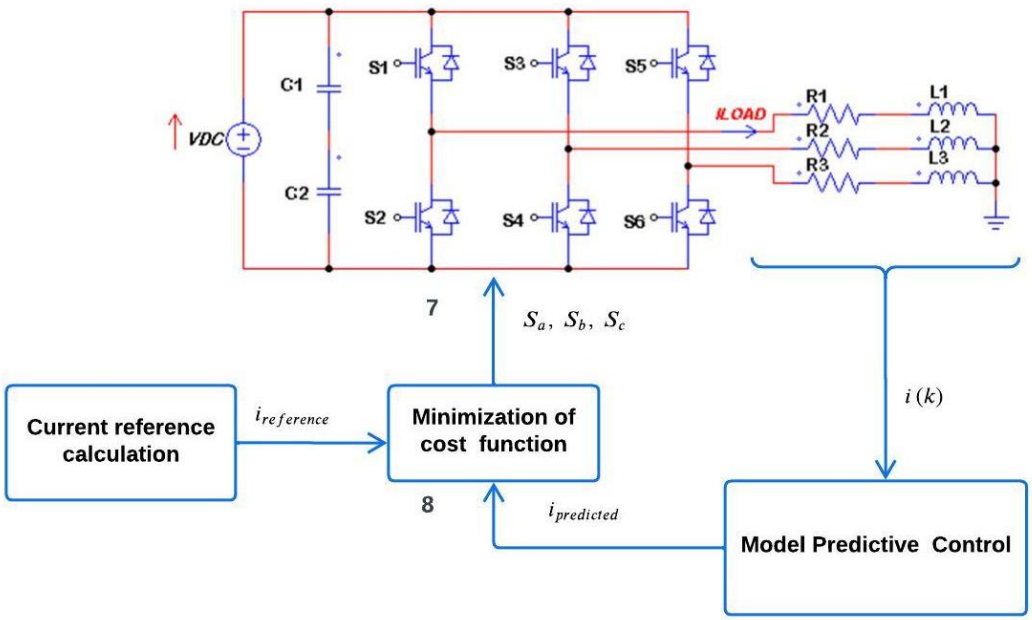

Figure 4. 1: Two level three phase VSC with RL load and MPC controller.

4.2.1. Load model

The equations of the load for each phase in continuous-time state-space are derived by utilizing the following differential equation representing the load currents:

$$V_{DC}(t) = R.i(t) + L\frac{di}{dt} \quad (4.1)$$

The load model can be represented in a coordinate system with two linearly independent axes, α *and* β, by employing the Clarke transformation to the voltages and currents. This results in the following simplified expression:

$$\alpha = \frac{2}{3}(a - 0.5b - 0.5c) \quad (4.2)$$

$$\beta = \frac{2}{3}(0 + 0.5\sqrt{3}b + 0.5\sqrt{3}c \quad (4.3)$$

Consequently, the equation of the load in continuous-time state-space is obtained as follows:

$$\begin{bmatrix} i_\alpha \\ i_\beta \end{bmatrix} = \begin{bmatrix} -\frac{R}{L} & 0 \\ 0 & -\frac{R}{L} \end{bmatrix} \begin{bmatrix} i_\alpha \\ i_\beta \end{bmatrix} + \begin{bmatrix} \frac{1}{L} & 0 \\ 0 & \frac{1}{L} \end{bmatrix} \begin{bmatrix} v_\alpha \\ v_\beta \end{bmatrix} \quad (4.4)$$

4.2.2. Discrete-Time Load model

Using a discrete-time description established through the Euler-forward approximation, an equation for the future load current is constructed. The approximation thus achieved is written as:

$$\dot{x} \approx \frac{x(k+)-x(k)}{T_s} \quad (4.5)$$

In this equation, x indicates the state variable, k indicates the current sampling instant, and T_S indicates the sampling period. The discrete-time load model, as a result, is as follows:

$$\begin{bmatrix} i_\alpha(k+1) \\ i_\beta(k+1) \end{bmatrix} = \begin{bmatrix} 1 - T_s\frac{R}{L} & 0 \\ 0 & 1 - T_s\frac{R}{L} \end{bmatrix} \begin{bmatrix} i_\alpha(k) \\ i_\beta(k) \end{bmatrix} + \begin{bmatrix} \frac{T_s}{L} & 0 \\ 0 & \frac{T_s}{L} \end{bmatrix} \begin{bmatrix} v_\alpha(k) \\ v_\beta(k) \end{bmatrix} \qquad (4.6)$$

To forecast the load current for every potential switching state, Equation 4.6 is employed.

4.2.3. Cost function and computation reduction

The cost function, indicated as g, is selected as follows:

$$g = \left|i_\alpha^{ref}(k+1) - i_\alpha^p(k+1)\right| + \left|i_\beta^{ref}(k+1) - i_\beta^p(k+1)\right| \qquad (4.7)$$

To determine the future value of the load current, the cost function was assessed for each of the 8 voltage vectors that the inverter can provide. However, since voltage vectors 0 and 1 are equivalent and yield the same result, only 7 vectors are considered. This eliminates one switching state, reducing the computation time required by the equation. At the next sampling instance, the voltage vector that minimizes the cost function is chosen and applied.

4.3. Software simulation using MATLAB/Simulink

MATLAB is one of the different types of software packages available for the simulation of power electronics and drives. MATLAB/Simulink is a widely used software platform for modeling, simulation, and implementation of control systems, including MPCC for a three-phase two-level VSC.

One of the objectives of this study is to show how to integrate MATLAB with Simulink for a three-phase VSC using a model predictive strategy with an RL load. In this study, the theoretical approach of the system model is explained, and subsequently, the simulation results are presented to show the effectiveness of the system.

To validate the feasibility of the proposed control algorithm, MATLAB/Simulink modeling work was carried out for different conditions of the current references and loads implemented for a three-phase, two-level VS with an RL load. MATLAB provides an environment for algorithm development and data analysis, while Simulink allows for the creation of block diagrams and models of systems, as well as the simulation and testing of those models.

To integrate MATLAB with Simulink for a three-phase, two-level voltage source converter with an MPC controller, the following steps were followed:

i. A MATLAB script was created to define the control algorithm for the MPC controller and any necessary functions or parameters.
ii. A Simulink model was created, and necessary blocks for the three-phase, two-level voltage source converter were added.
iii. An MPC Controller block was added to the Simulink model.
iv. The MPC Controller block was set up as an S-Function and incorporated the provided code to execute the control algorithm defined in the MATLAB script. Here is the code snippet:

```
% Back-EMF estimate
e = v(x_old) - L/Ts*ik - (R - L/Ts)*i_old;
% Store the measured current for the next iteration
i_old = ik;
for i = 1:8
    % i-th voltage vector for current prediction
    v_o1 = v(i);
    % Current prediction at instant k+1
    ik1 = (1 - R*Ts/L)*ik + Ts/L*(v_o1 - e);
    % Cost function
    g(i) = abs(real(ik_ref - ik1)) + abs(imag(ik_ref - ik1));
end
% Optimization
[~,x_opt] = min(g);
% Store the present value of x_opt
x_old = x_opt;
% Output switching states
Sa = states(x_opt,1);
Sb = states(x_opt,2);
Sc = states(x_opt,3);
```

v. Relevant inputs and outputs were connected to the MPC Controller block.

By following these steps, the MATLAB script was successfully integrated with the Simulink model for the three-phase, two-level VSC with an MPC controller.

Figure 4.2 depicts the MATLAB/Simulink model utilized to simulate the FS-MPCC for a VSC, as detailed in Chapter 3. The simulation diagram comprises five major components: input references, coordinate transformations, the predictive control algorithm, the inverter, and load modeling. Sine wave sources are employed to generate the three-phase current references, allowing customization of parameters such as peak amplitude, frequency, and phase angle according to specific requirements. The implementation of the predictive control algorithm is feasible for three-phase currents. Nevertheless, to minimize the number of predictions required, the control can be carried out using two-phase complex coordinates ($\alpha\beta$ coordinates). As the reference current and load current measurements are expressed as three-phase variables, it is necessary to apply coordinate transformation to each signal. However,

in certain applications where the reference current is already represented in $\alpha\beta$ coordinates, this step can be omitted.

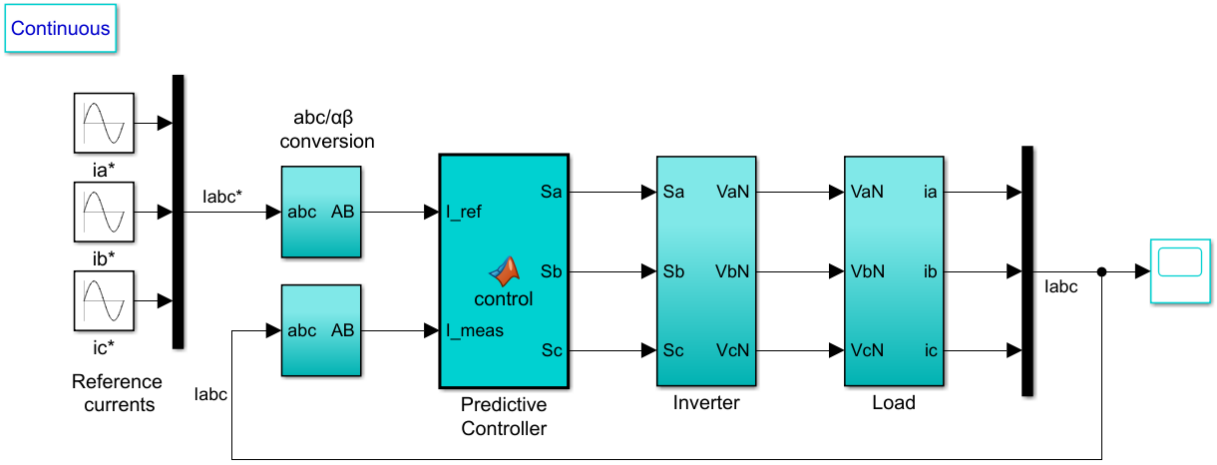

Figure 4. 2: Simulink-based modeling and simulation of predictive current control for a VSC.

4.4. Effect of a powerful microprocessor

Since the simulation involves complex mathematical calculations and requires a large amount of data processing, this necessitates The requirement for highly capable computers equipped with fast microprocessors and sufficient RAM capacity. A powerful microprocessor can handle the calculations more quickly and efficiently. This can result in faster simulation times and more accurate results, especially when running the simulation for longer periods or when dealing with complex systems. The specifications of the computer used in this study are presented in Table 4.1.

Table 4. 1: The following are the characteristics of the computer hardware components utilized in the simulation:

Computer hardware components	**Specifications**
CPU	Overclocked to 4.5GHz per core, the Intel Core i7-3930K boasts 12 cores, each operating at 3.2GHz with a cache of 12M.
Memory	Quad Channel 32 GB DDR3 RAM operating at 1600MHz, configured as 8 modules of 4GB each.
Two Storage Drives	The SSD has a capacity of 128GB and boasts a read speed of 560MB/s, coupled with a write speed reaching 430MB/s.
	A 4-terabyte hard drive boasting a 6.0 gigabits-per-second data transfer rate.

4.5. Simulation Results and Analysis

To assess the performance and validate the effectiveness and robustness of the proposed FS-MPC scheme for a three-phase two-level VSC, simulations were conducted using MATLAB/Simulink. The simulations aimed to evaluate the proposed control algorithm and its applicability in a VSC system. The simulation was analyzed under four distinct scenarios. First, the simulation was set up with a sinusoidal reference current, having an amplitude of 10 A and a frequency of 50 Hz per phase. Second, the control algorithm's effectiveness was assessed by employing varying sampling intervals and employing a two-step prediction approach. Third, under variable DC-Link voltage and load inductance, the control strategy was examined to assess its impact in terms of THD. Finally, the control algorithm was evaluated for its dynamic response by testing it with various current waveforms, including square waveforms, constant reference steps, and sawtooth waveforms. The VSC output was connected to a resistive-inductive load. The simulation parameters used are presented in Table 4.2.

Table 4. 2: Simulation Parameters

Parameter	Value
Load resistance, R	10 Ω
Load inductance, L	10 mH
DC link voltage, V_{dc}	520 V
Reference amplitude current, i_{ref}	4 A, 10 A
Sampling time, Ts	25 μs, 75 μs, 150 μs

4.5.1. Delay compensation

The measured currents and the switching state at the time $(k)$are utilized to calculate the load currents at the time $(k+1)$. This current is then employed as a starting point for all switching state predictions, bringing the regulated currents considerably closer to their reference. The load model pushed two steps ahead in time, is used to produce these predictions:

$$i^p(k+2) = \left(1 - \frac{RT_S}{L}\right) i(k+1) + \frac{T_S}{L} v(k+1) \quad (4.8)$$

The cost function for $i^p(k+2)$ is adjusted, resulting in:

$$g = \left|i_\alpha^{ref}(k+2) - i_\alpha^p(k+2)\right| + \left|i_\beta^{ref}(k+2) - i_\beta^p(k+2)\right| \quad (4.9)$$

The switching state with the least cost function is chosen and preserved for use at the subsequent sampling point. Figure 4.3 displays the FS-MPCC in operation, with a large delay resulting from computations. It can be seen in Figure 4.3 (a) that the load current ripple becomes observable with a total harmonic distortion of 7.11% when delay compensation is ignored. Nevertheless, when delay compensation is considered, the

load current ripple is reduced, and the output is near the ideal case with a total harmonic distortion of 2.44 as seen in Figure 4.3 (b). The future values of the reference currents $i^{ref}(k+1)$ and $i^{ref}(k+2)$, are necessary for the cost functions in Equations 3.24 and 4.8 respectively. The following section discusses the calculation of these values.

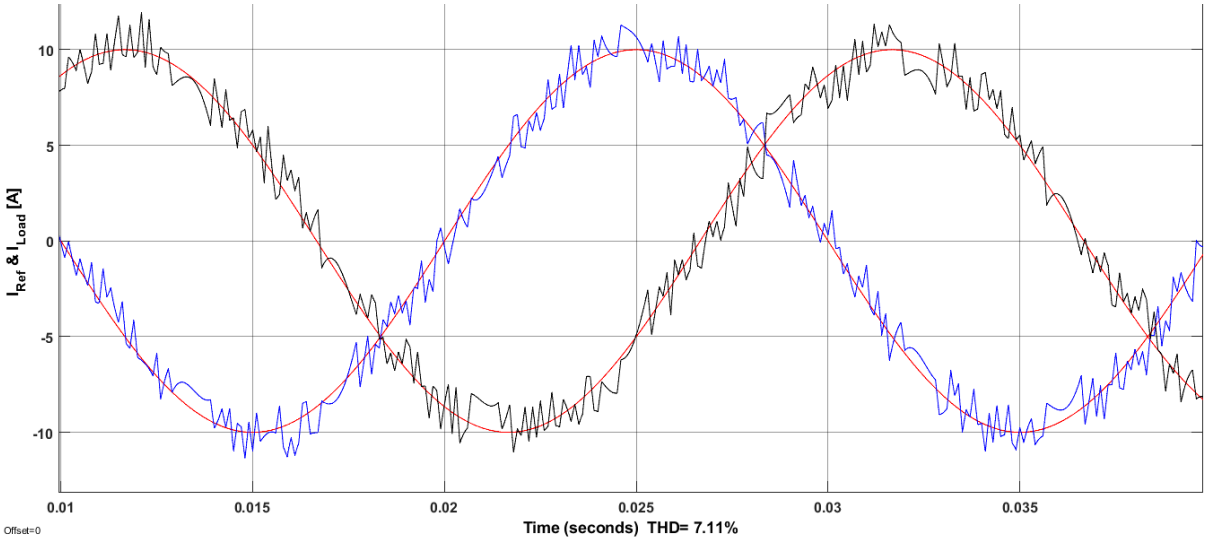

(a)

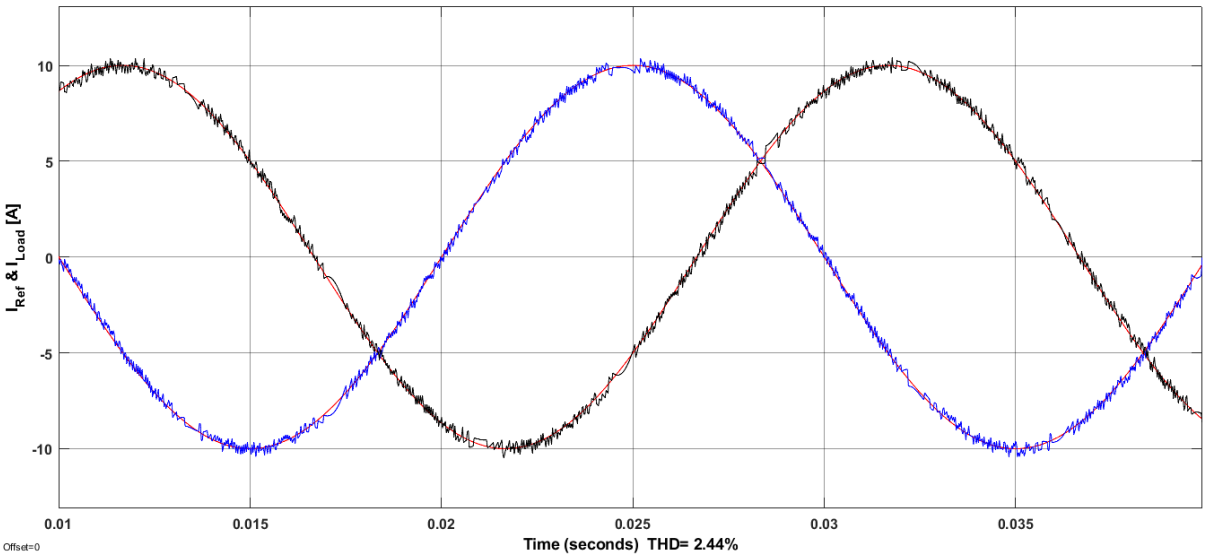

(b)

Figure 4. 3: FS-MPC operation (a) without and (b) with delay compensation.

4.5.2. Prediction of future references and switching states

The cost function in the application of the predictive control approaches described in this dissertation is dependent on future errors. This necessitates the knowledge of future references to compute the error between the reference and the predicted

variable at the next sampling interval. Future references must, however, be approximated since they are unknown. Based on the premise that the sampling frequency is significantly greater than the frequency of the reference signal, one easy method to do this is to assume the future value of the reference to be nearly equal to the current value of the reference. It may be inferred from the predictive current control example that, $i^{ref}(k) = i^{ref}(k+1)$, this implies that the cost function may be expressed as:

$$g = \left|i_{\alpha}^{ref}(k+1) - i_{\alpha}^{p}(k+1)\right| + \left|i_{\beta}^{ref}(k+1) - i_{\beta}^{p}(k+1)\right| \quad (4.10)$$

The monitoring of the reference currents will be delayed by one sample frame because of this approximation. When accounting for the compensation of the computation-time delay, the reference $i^{ref}(k+2)$ is needed. Applying the same logic, the future reference can be simplified by assuming that $i^{ref}(k+1) = i^{ref}(k+2)$, yielding the cost function:

$$g = \left|i_{\alpha}^{ref}(k+2) - i_{\alpha}^{p}(k+2)\right| + \left|i_{\beta}^{ref}(k+2) - i_{\beta}^{p}(k+2)\right| \quad (4.11)$$

and the reference track will be delayed by two samples. Figure 4.4 (a) illustrates the impact of the delay imposed by this future reference approximation. This delay is observable for larger sample durations, such as Ts = 75 μs. There is no steady-state inaccuracy in the current, but there is a noticeable ripple and a decrease in switching frequency, as depicted in Figure 4.4 (b). This current ripple is significantly reduced when a smaller sampling time is utilized, as illustrated in Figure 4.5 (a) for a sampling time Ts = 25 μs. However, by decreasing the sampling time, the switching frequency is increased, as shown in Figure 4.5 (b). In predictive control strategies, it is typical to employ reduced sampling intervals, which makes this method suitable for such situations. When setpoints remain constant in a steady-state process, there are no negative effects associated with this method, and the latency between two samples can only be observed during transient periods.

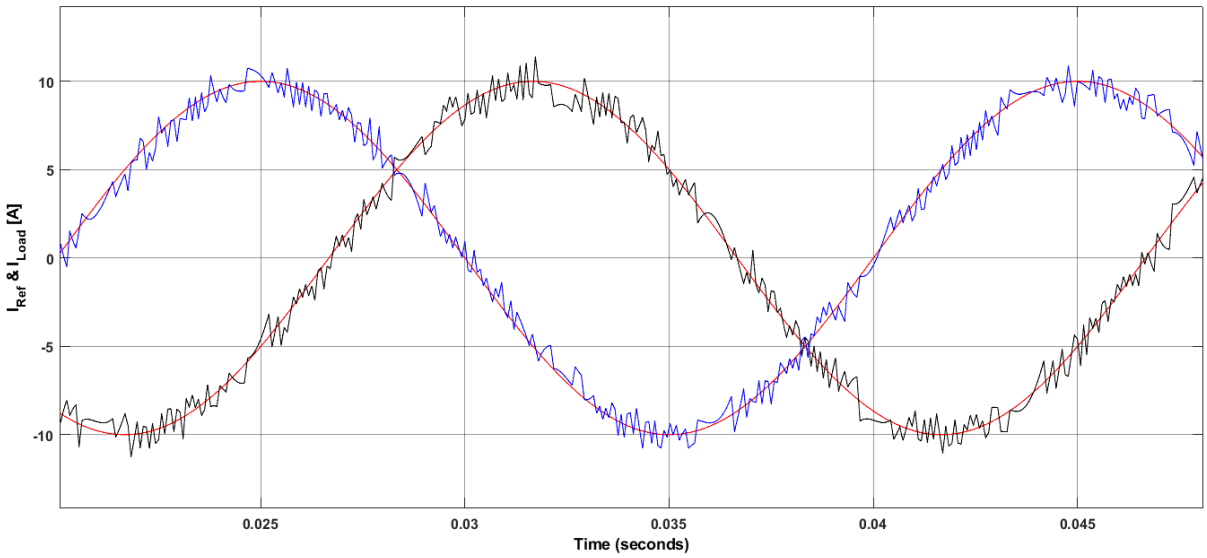

(a)

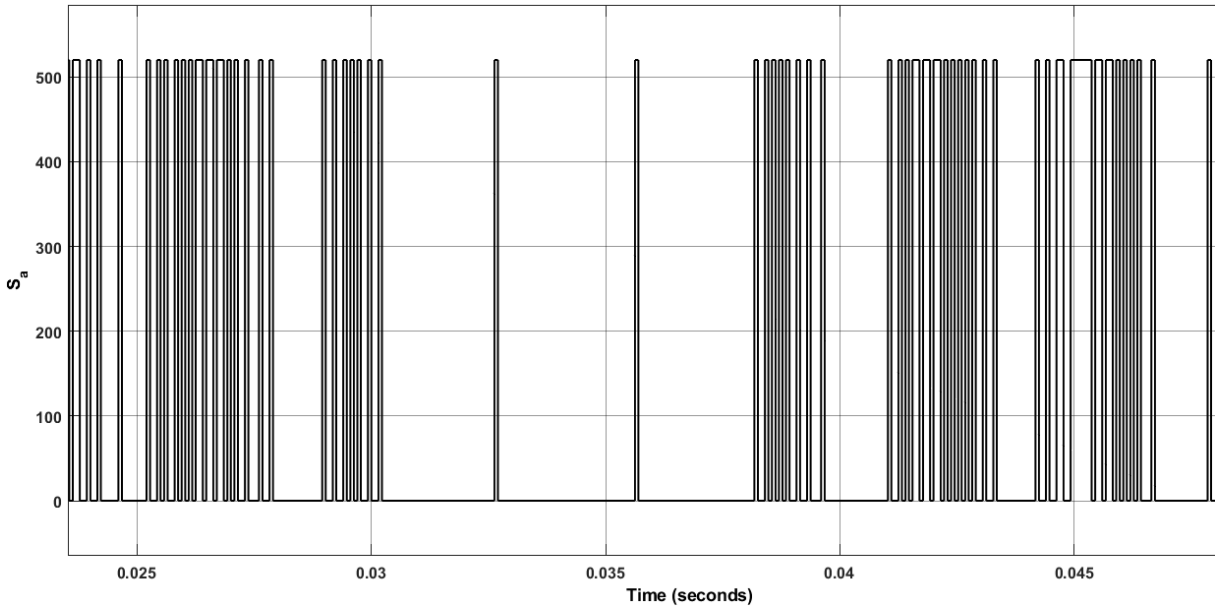

(b)

Figure 4. 4: (a) The load and reference currents and (b) switching states for FS-MPCC utilizing $i^{ref}(k) = i^{ref}(k+2)$, for a sampling time of 75 μs

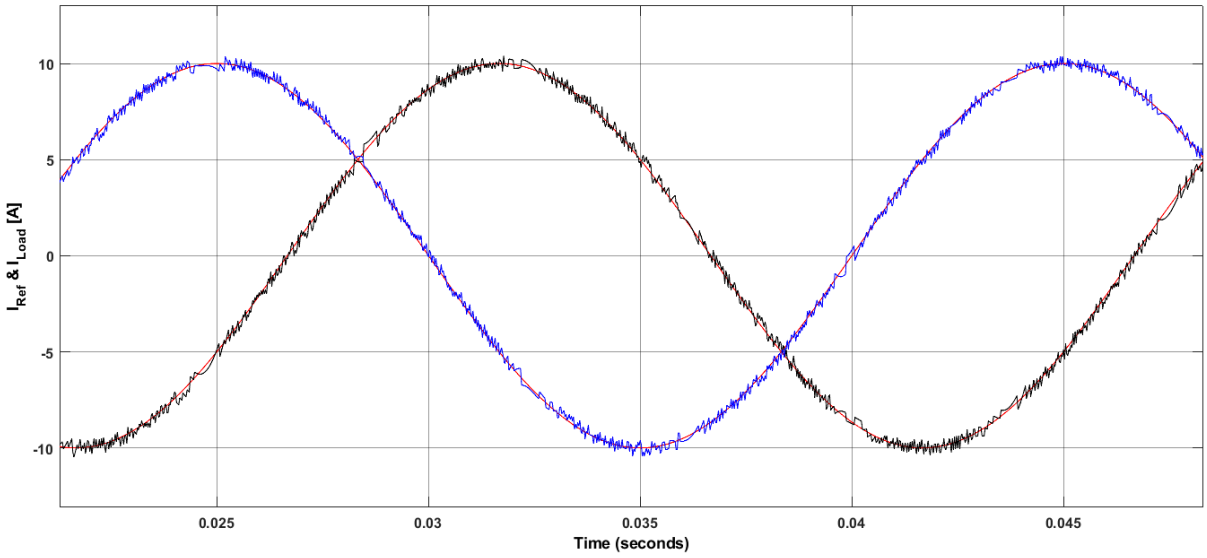

(a)

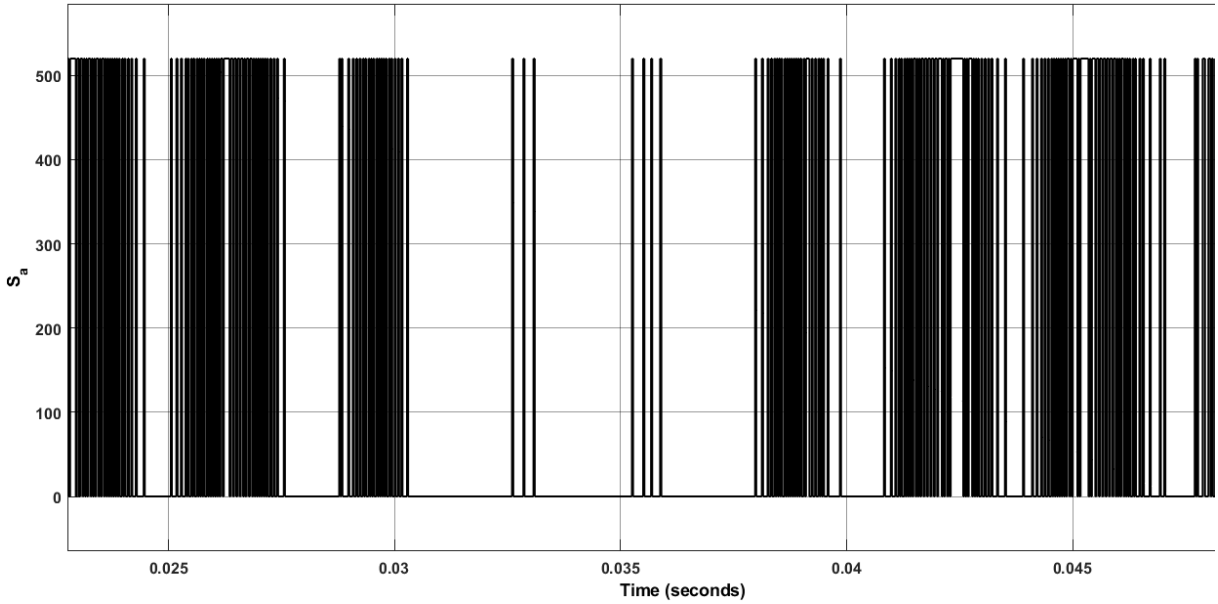

(b)

Figure 4. 5: (a) The reference and load currents and (b) switching states for FS-MPCC utilizing $i^{ref}(k) = i^{ref}(k+2)$, for a sampling time of $25\ \mu s$.

4.5.3. Stability Analysis

4.5.3.1. System Response to Variable DC-link Voltages

In this section, the robustness of the suggested control technique of a Voltage Source Inverter employing the delay compensation method was tested; more particularly, when the DC-link voltage was adjusted from 420 to 580 V for sampling time $T_S = 25\ \mu s$. Figure 4.6 depicts the output currents for different DC-link voltage levels. It is important to note that the suggested control algorithm can monitor sinusoidal reference currents

regardless of DC link voltage changes around the desired voltage. Table 4.3 contains a summary of the data presented in Figure 4.6. In Figure 4.6 (a), the DC-link was adjusted to 380 V, and the THD was at 1.84%; however, in Figure 4.6 (b), the DC-link was adjusted to 420 V, and the THD was raised to 1.89%. In Figure 4.6 (c), the DC-link was set to 540 V, and the THD was raised to 2.48%. In Figure 4.6 (d), on the other hand, the DC-link was set to 580 V, and the THD was raised to 2.87%. It was observed that voltages below the specified DC-link voltage value of 520 V resulted in a decreased THD which tracked the reference current with a very tiny error. DC-link values larger than the specified value, on the other hand, resulted in a significant THD but a very minor amplitude error. This simulation verifies that the predictive control approach can track sinusoidal reference currents while exhibiting good tracking behavior with all DC-link voltage values, even when DC-link voltage values vary by just a small amount.

Table 4. 3: THD and Fundamental output current for variable DC-link voltages using delay compensation.

Value of the DC-Link voltage [V]	Output current fundamental at 50 Hz, measured in amperes [A].	Percentage of Total Harmonic Distortion [%].
380	9.996	1.84%
420	9.997	1.89%
500	9.993	2.41%
540	9.986	2.48%
580	9.965	2.87%

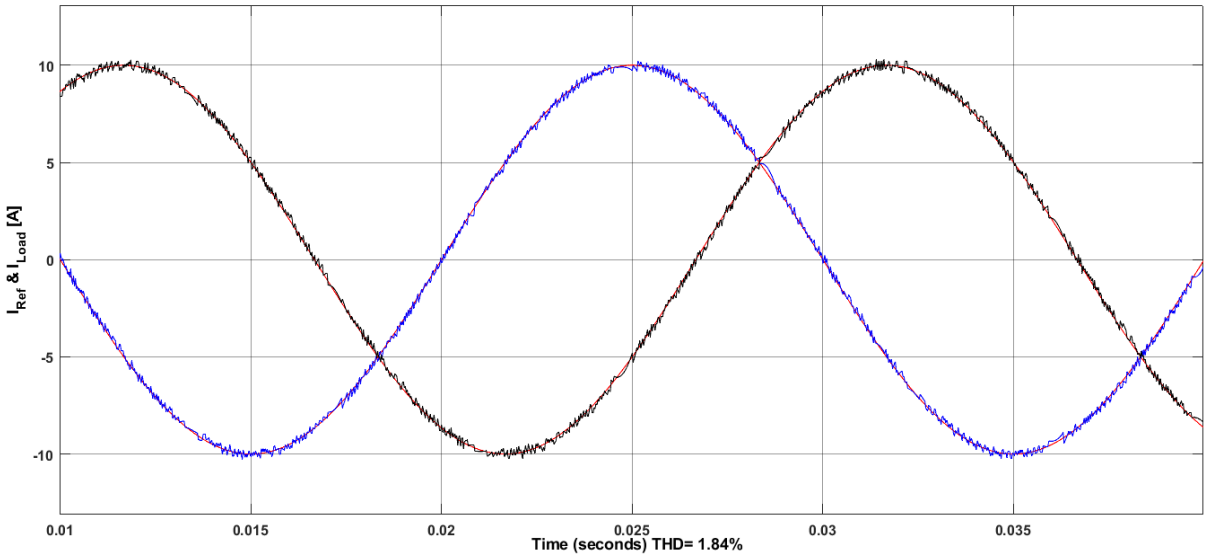

(a)

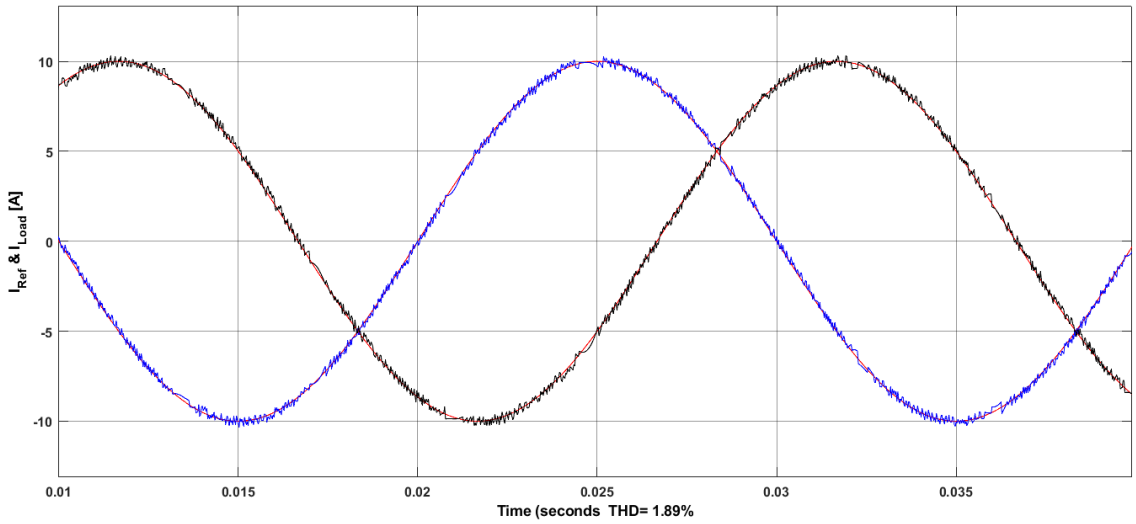

(b)

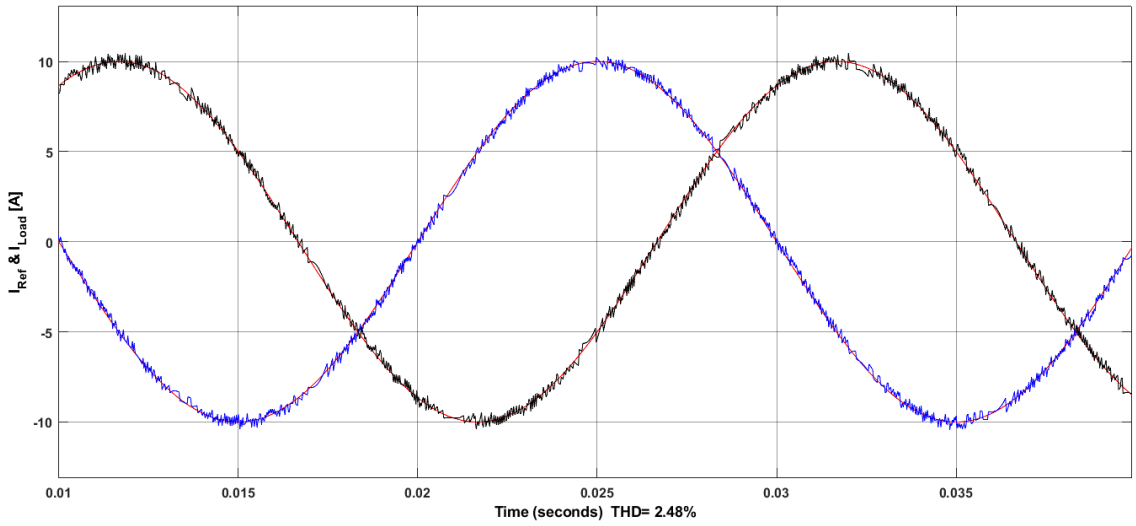

(c)

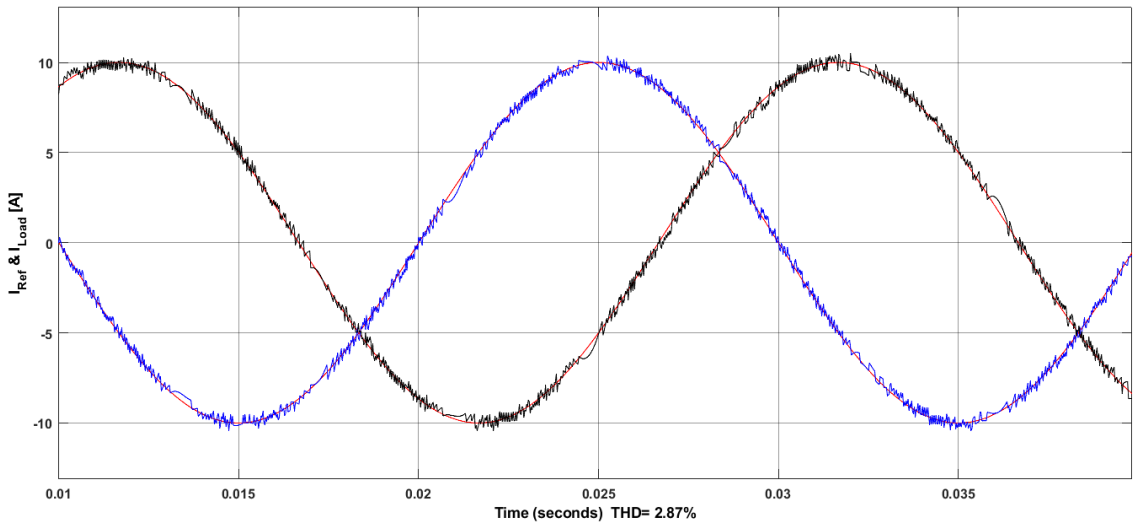

(d)

Figure 4. 6: Stability Analysis of FS-MPCC Scheme for a three-phase, two-level VSC with delay compensation under DC-Link voltage variation ($380 - 580\ V$) and $T_S = 25\ \mu s$.

4.5.3.2. System Response to Variable Load Inductance

This section evaluates the robustness of the proposed control technique for a Voltage Source Converter using delay compensation. Specifically, the performance was assessed as the Load Inductance was adjusted within the range of 20 to 60 mH, with a sampling time of $T_S = 25\ \mu s$. Figure 4.7 illustrates the output currents corresponding to different load inductance levels, while Table 4.4 summarizes the data from Figure 4.7. In Figure 4.7 (a), with a Load Inductance of 20 mH, the THD stood at 3.02%. Increasing the Load Inductance to 30 mH (Figure 4.7 (b)) led to a lowered THD of 2.08%. A Load Inductance of 40 mH (Figure 4.7 (c)) resulted in an even further reduction to 1.58%. Notably, a Load Inductance of 60 mH (Figure 4.7 (d)) achieved the lowest THD of 1.02%. Observations revealed that as Load Inductance increased, THD decreased while maintaining excellent tracking of the reference current with minimal error. This simulation provides strong evidence that the predictive control approach effectively tracks sinusoidal reference currents, maintaining consistent performance across varying load inductance levels.

Table 4. 4: THD and Fundamental output current for variable load inductance using delay compensation.

Value of the Load Inductance [mH]	Output current fundamental at 50 Hz, measured in amperes [A].	Percentage of Total Harmonic Distortion [%].
20	3.997	3.02%
30	4.001	2.08%
40	4	1.58%
60	4.003	1.02%

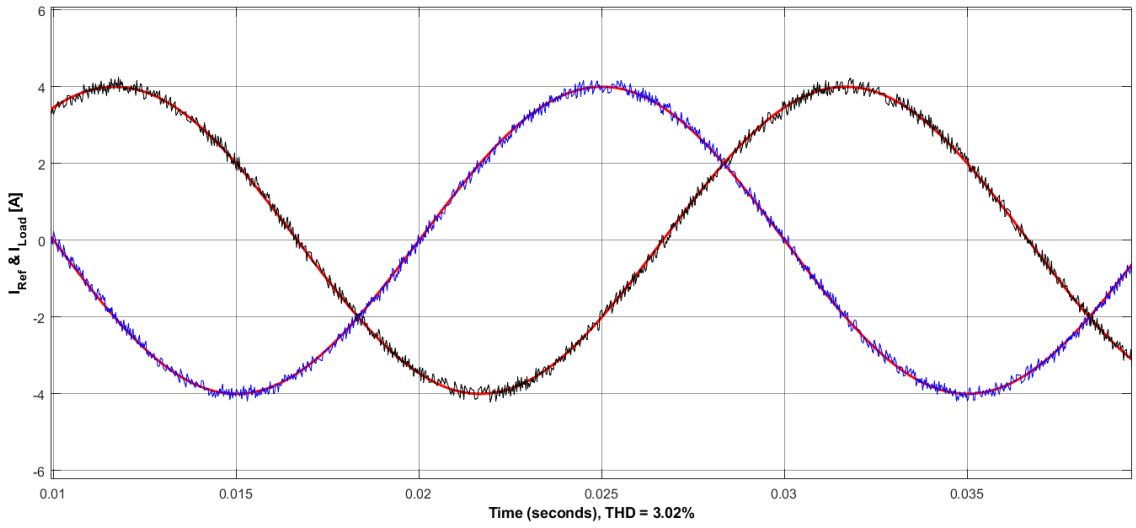

(a)

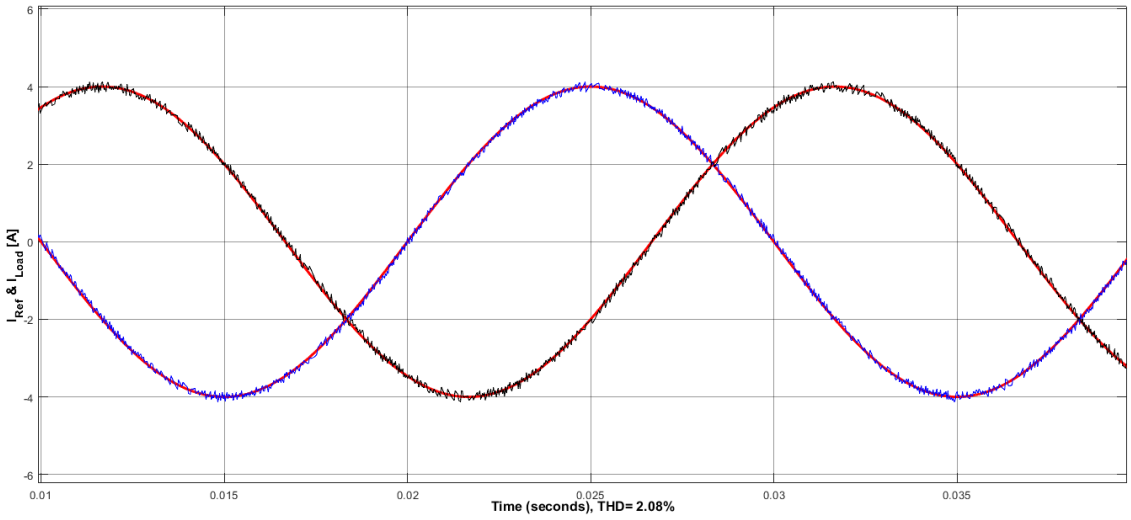

(b)

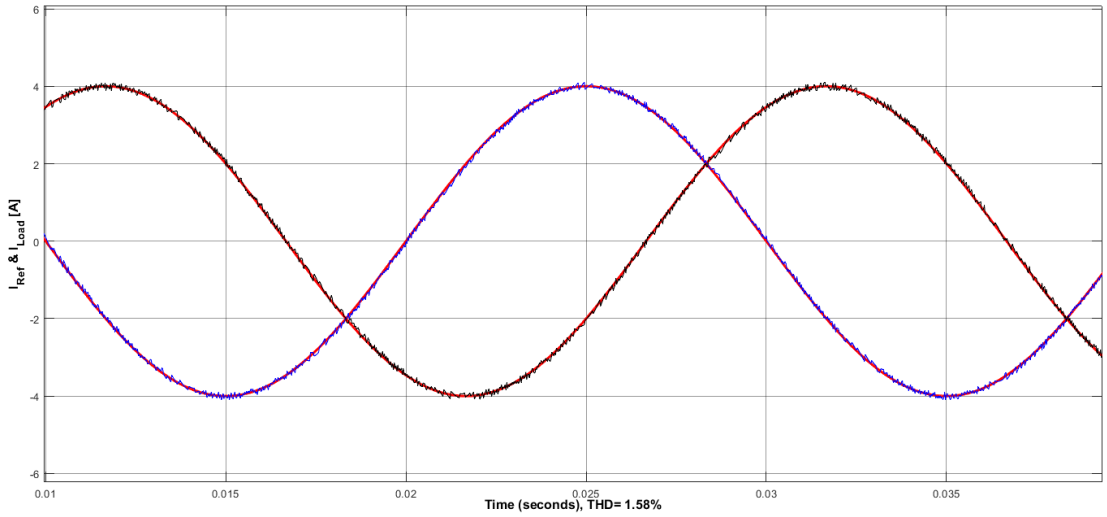

(c)

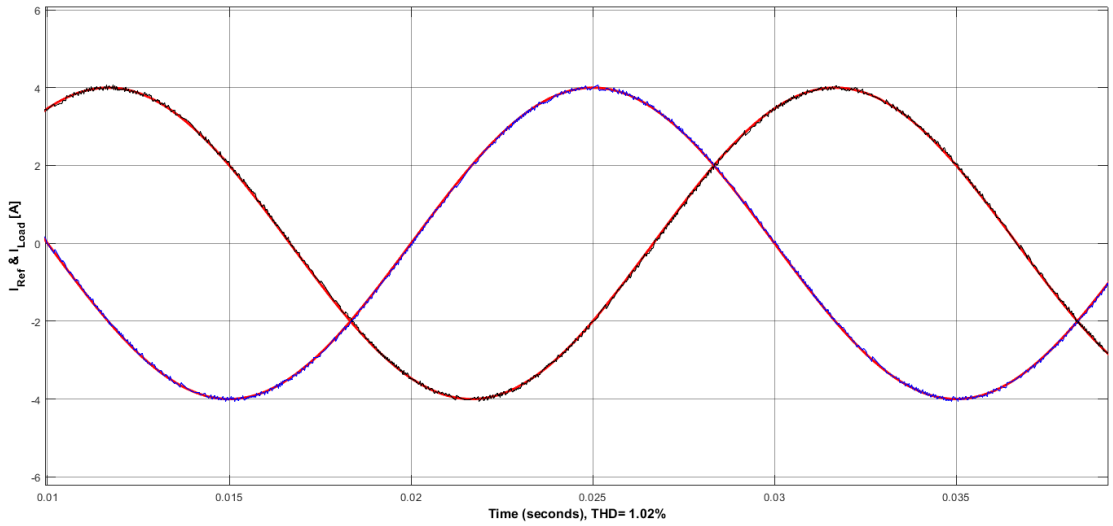

(d)

Figure 4. 7: Stability Analysis of FS-MPCC Scheme for a three-phase, two-level VSC with delay compensation under Load Inductance Variation (20 to 60 mH) and $T_S = 25\ \mu s$.

4.5.4. Reference Tracking using Constant Reference Steps

The control algorithm was evaluated utilizing constant reference steps to evaluate dynamic response, stability, settling time, robustness, performance optimization, and fault handling capabilities. The simulation depicted the response to a step change in the amplitude of the references i_α and i_β, presenting the control outcomes for constant reference step values, specifically. This step change occurred at 0.02 seconds, with the references increasing from $0\ A$ to $4\ A$. The response of the load currents to this step change is shown in Figure 4.8.

The control algorithm effectively tracked the new references and adjusted the control actions accordingly. In the steady state, there was an observable current ripple, resulting from the finite switching frequency and control algorithm operation. This ripple is a characteristic of the control system but can be minimized through proper design. As long as the ripple remains within acceptable limits and does not affect system performance and stability, it is considered acceptable. The simulation results confirmed the control algorithm's effectiveness in achieving accurate and fast-tracking of the reference currents during the step change. The presence of a current ripple in the steady state is a normal characteristic that can be managed through appropriate design considerations.

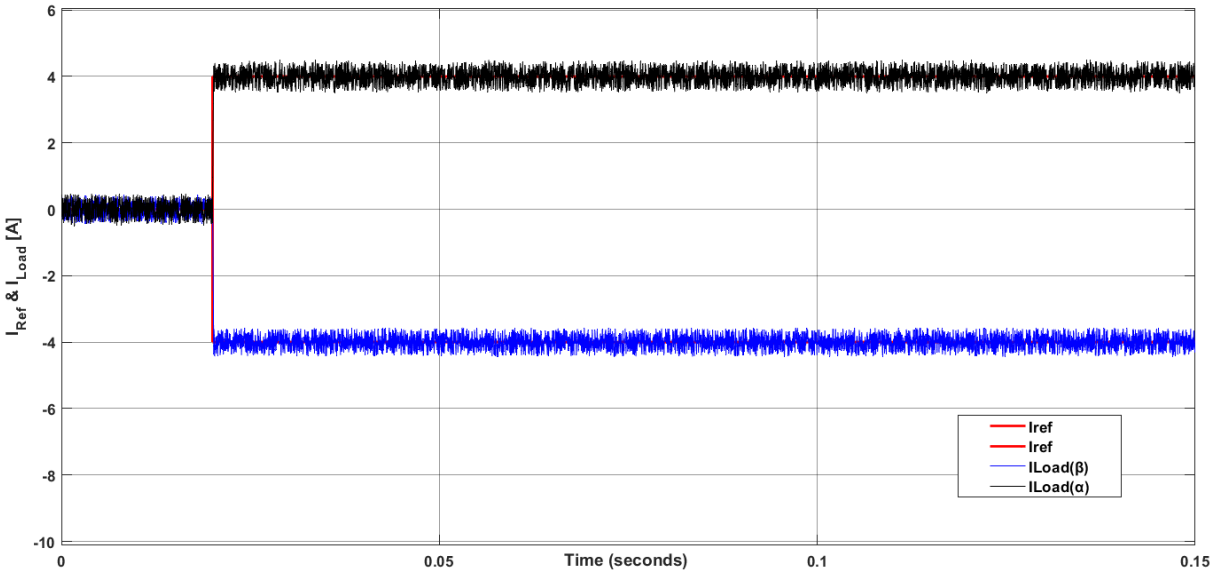

Figure 4. 8: Response of Load Current to Constant Reference Steps with Amplitude Change to $4\ A$.

4.5.5. Reference Tracking using Sawtooth waveform.

The control algorithm utilized a sawtooth waveform as the reference current and was evaluated in orthogonal coordinates. The simulation showed that the load current accurately tracked the reference waveform with an amplitude of $4\,A$ and a sampling time of $25\,\mu s$, as depicted in Figure 4.9. However, despite the precise tracking, a steady-state current ripple was present in the system. This ripple was caused by the finite switching frequency of the power electronic device and the controller frequency. The finite switching time introduced distortions in the current waveform, while any mismatch between the controller and switching frequencies contributed to the presence of the ripple. Despite the presence of this ripple, the control algorithm successfully achieved the desired tracking of the reference waveform by the load currents.

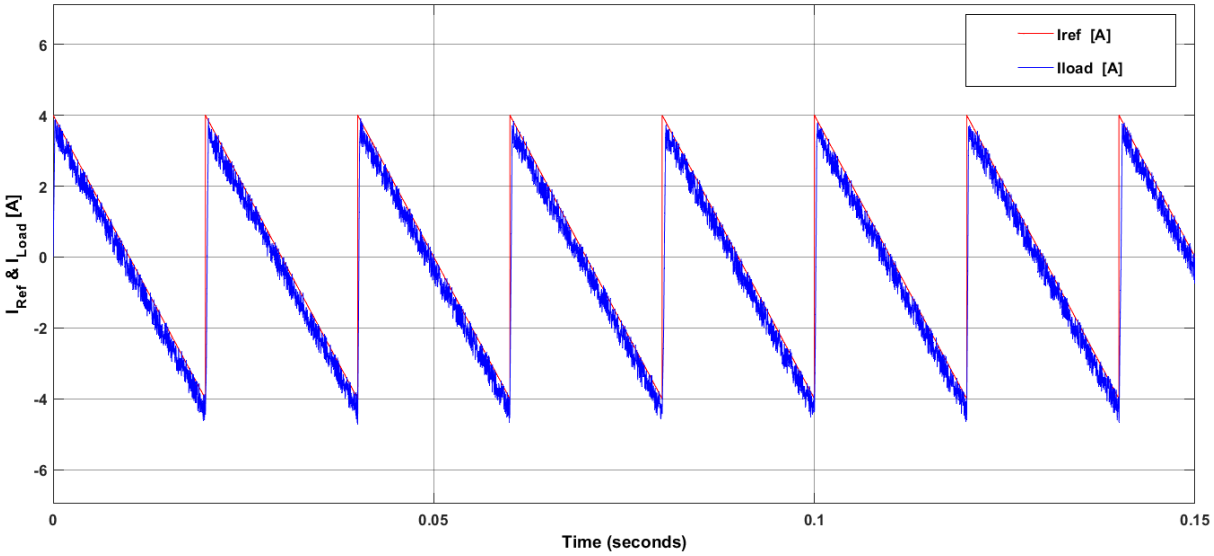

Figure 4. 9: Evaluating Load Current Tracking with a Sawtooth Waveform Reference at $Ts = 25\ \mu s$.

4.5.6. Reference Tracking using Square Waveform

The control algorithm was evaluated using a square waveform in orthogonal coordinates as the reference current. The reference waveform had amplitudes of i_α and i_β set to $4\,A$, and two different sampling times were considered: $25\,\mu s$ and $150\,\mu s$. The simulation results, depicted in Figure 4.10, showed that the currents i_α and i_β accurately tracked the reference waveform at both sampling times.

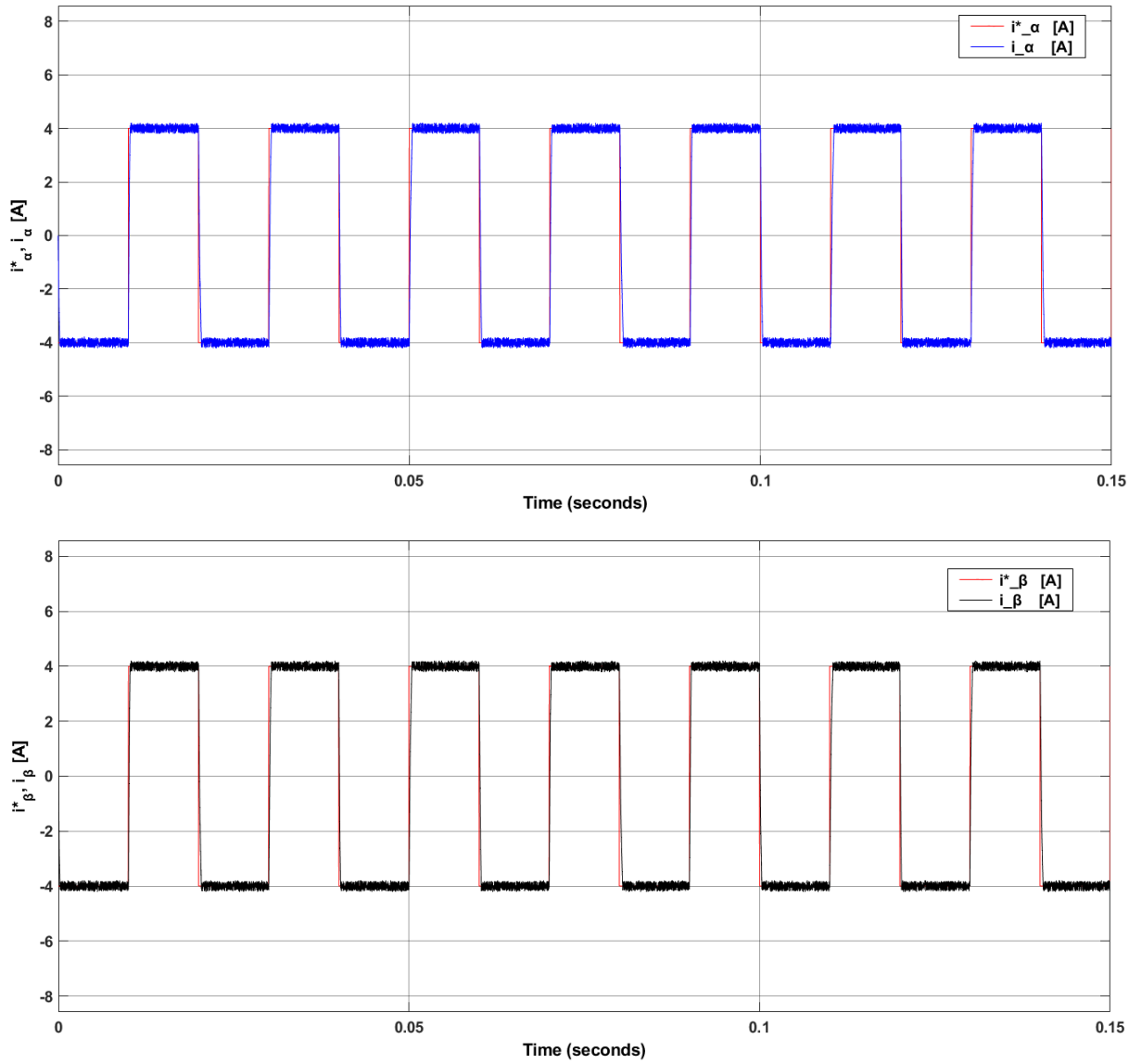

Figure 4. 10: Evaluating Load Current Tracking with a Square Waveform Reference at $Ts = 25\ \mu s$.

However, when the control algorithm was tested at a sampling time of $150\ \mu s$, it was observed that a noticeable steady-state current ripple was present compared to the case with a sampling time of $25\ \mu s$ as shown in Figure 4.11. Nevertheless, despite the presence of the ripple, the control algorithm maintained its effectiveness in accurately tracking the desired reference waveform using the currents i_α and i_β. The algorithm's robust performance was demonstrated, despite the increased prominence of the ripple at longer sampling times.

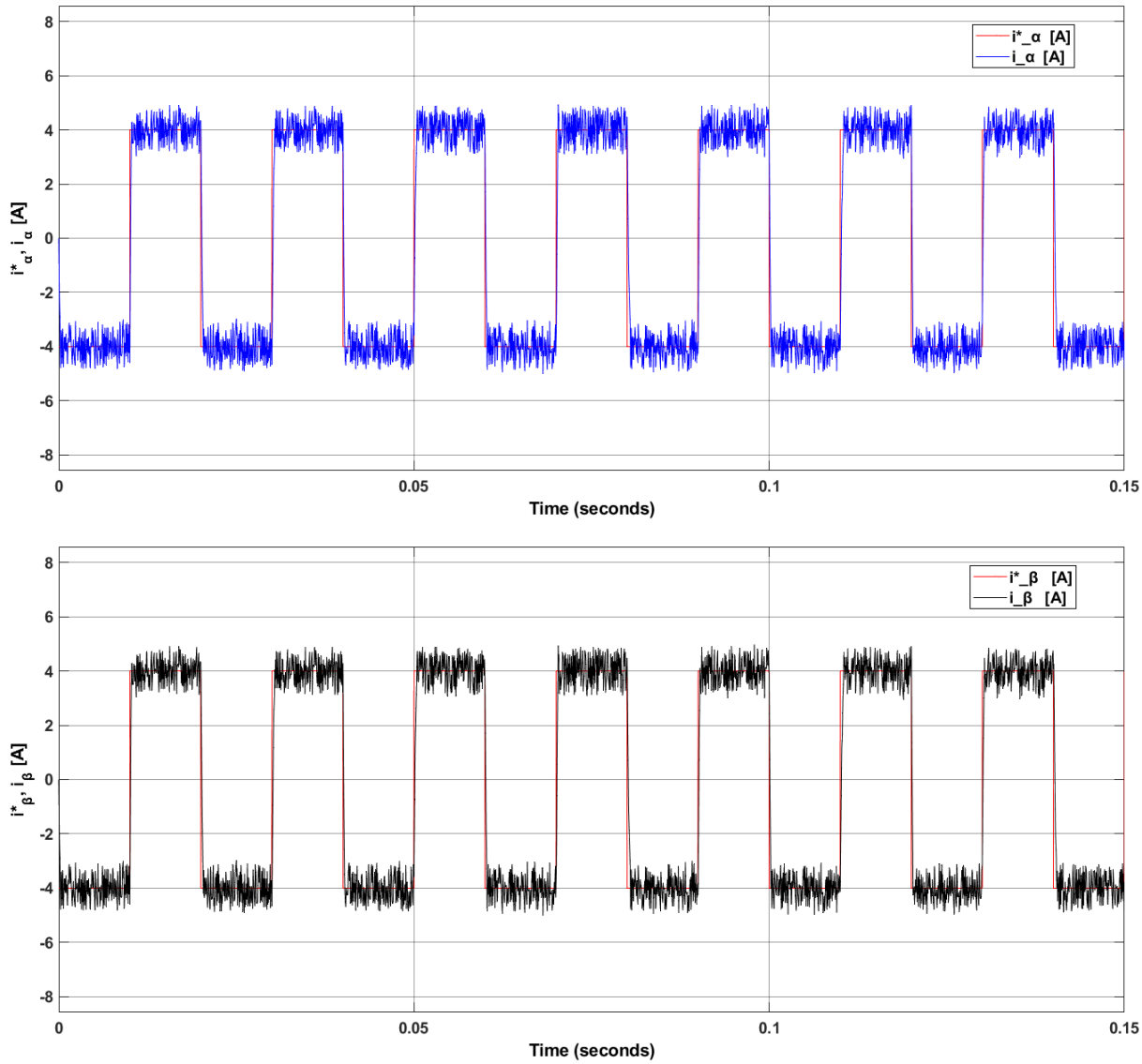

Figure 4. 11: Evaluating Load Current Tracking with a Square Waveform Reference at $Ts = 150\,\mu s$

4.6. Summary

The FS-MPCC approach was introduced in this chapter to control the three-phase, two-level VSC. In this analysis, The investigation employed the model to analyze the device output under the application of power to an RL load. The three-phase, two-level VSC, in turn, generates a total of 8 potential switching states, only 7 voltage vectors were chosen and applied to the converter since $V_0 = V_7$.

The project was simulated utilizing MATLAB/Simulink software. The use of MATLAB for the modeling and design of MPCC for a three-phase two-level VSC is highly useful for achieving accurate modeling, optimization, efficient implementation, and integration with other tools. It can significantly improve the performance and reliability of the VSC in grid-connected applications.

Minimizing current and voltage errors within the cost function yields a quick and responsive load current control. The two primary benefits of MPC are that it does not need any kind of modulation and a linear controller. This option enables the opportunity to change the connection between terms allocated to reference tracking.

In this study, an FS-MPC approach for a three-phase VSC is presented and implemented. The modulator is not required for the proposed control. Analytically, the computational effort required to generate multiple possibilities with a long prediction horizon has been decreased. The control method has been tested with four distinct instances using simulation results. In the first case, the control approach was tested using a sinusoidal waveform reference current. The results demonstrated that the MPC approach provided excellent output performance within the parameters set. Notably, using a two-time-step delay compensation strategy, as shown in Figure 3.8, resulted in better THD results, demonstrating effective delay compensation by monitoring the link between the inputs and outputs. Overall, the findings suggest that the MPC approach may be highly advantageous in terms of achieving greater control performance. Second, the resilience of the proposed control approach with two prediction stages and variable sampling times has been evaluated; the evaluation was carried out by comparing the load current and voltage between the reference and actual loads. The control method has been shown to produce extremely excellent current tracking behavior. Thirdly, the stability of the control technique was assessed by analyzing its robustness and adaptability across various DC-Link voltages and load inductance. This evaluation is based on the measurement of Total Harmonic Distortion. Furthermore, a control algorithm was tested utilizing a variety of current waveforms to assess its dynamic responsiveness. The waveforms included constant reference steps, square waveforms, and sawtooth waveforms. The algorithm demonstrated excellent tracking behavior, accurately following the desired current profiles without significant deviations. It also exhibited a fast dynamic response, quickly adapting to changes in the reference signals. Notably, the algorithm showed inherent decoupling between the i_α and i_β components during step changes, allowing independent control without interference.

The simulation results suggest that the FS-MPC method for two-level VSC for resistive-inductive loads is effective in achieving accurate tracking even under different conditions.

CHAPTER FIVE

CONCLUSION AND RECOMMENDATIONS

5.1. Conclusion

The objective of the research was to propose delay compensation approaches for a two-level three-phase VSC utilizing the MPCC strategy. The proposed control technique aims to decrease computing effort and forecast future load current values for all 8 switching states generated by the converter. The delay compensation techniques were used to decrease the number of calculations required and to avoid time delays in actuation or deteriorated performance. To validate the effectiveness of the proposed methodologies, the performance of the system with delay compensation was compared to that without delay compensation. The entire system was modeled and simulated in MATLAB/Simulink.

In the second Chapter of this thesis, a comprehensive review of VSC technology and its numerous applications is provided. The chapter began with an overview of power electronic converters and proceeded with an in-depth discussion of the basic principles and ideas of VSC structures, as well as a comprehensive analysis of the benefits and drawbacks of each converter type. According to the number of necessary elements and independent DC sources, a comparison of the most promising DC-to-AC converter topologies was presented. In addition, various predictive control techniques and their applications in various power converters were presented and discussed. This chapter focused on the practical industrial applications of VSCs in RES installations, particularly interfacing with PV systems and wind turbines. Not all VSC power converter-related applications were addressed, but the chapter provided a systematic and meticulous overview of the fundamental principles underlying various VSCs.

In Chapter 3, a thorough overview of numerous predictive control techniques is provided. Based on existing literature, the utilization of predictive control in power electronic converters and motor drives was addressed. The purpose of this chapter was to clarify the fundamental concepts of predictive control and to describe the system modeling procedure, including approximations for differential equation derivatives. The classifications of cost functions with regard to delay compensation procedures and reference frames were discussed. In addition, the chapter elaborated on the various compensating procedures that can be incorporated into cost function equations. Several examples of these procedures were provided for various cost function types.

Chapter 4 of the thesis focused on modeling and simulation of the system using MATLAB/Simulink to validate the proposed methodologies. The simulation results of a three-phase Voltage Source converter were analyzed using Finite Set-Model Predictive

Current Control to investigate the impact of different system parameters on load current and load voltage.

The control approach was tested in four different scenarios using simulation results. Firstly, a sinusoidal waveform reference current was used to test the control approach, and the results demonstrated excellent output performance within the defined parameters. Notably, employing a two-time-step delay compensation strategy, as shown in Figure 3.8, resulted in improved Total Harmonic Distortion results, indicating effective delay compensation by monitoring the input-output relationship.

Secondly, the robustness of the proposed control approach with two prediction steps and variable sampling times was evaluated by comparing the load current and voltage between the reference and actual loads. The control method exhibited highly accurate current tracking behavior.

Thirdly, the robustness and variability of the control strategy under variable DC-Link voltages and load inductance were assessed in terms of THD. The simulation results indicated that the predictive control method effectively tracked sinusoidal reference currents and exhibited excellent tracking behavior with varying DC-Link voltage and load inductance values. Overall, the simulation results suggest that the Finite Set-Model Predictive Control approach for a two-level VSC, designed for resistive-inductive loads, performed exceptionally well under the given circumstances.

Finally, the control algorithm underwent testing with different current waveforms to assess its dynamic response. It performed exceptionally well, displaying accurate tracking behavior and fast dynamic response across the square, constant, and sawtooth waveforms. Moreover, the algorithm exhibited inherent decoupling between the i_α and i_β components during step changes, enabling independent control without interference. Overall, the algorithm proved to be effective in achieving precise tracking, swift response, and decoupling capabilities.

5.2. Further work and recommendations

MPCC is a relatively new control strategy that has demonstrated promising results in the control of power electronics systems, particularly three-phase converters. However, there is still space for additional research and development in this field. Here are a few recommendations for further study and development on MPCC:

5.2.1. Explore various optimization techniques:

MPCC is based on optimizing current error over a finite horizon. Various optimization techniques, including linear programming, quadratic programming, and mixed-integer programming, can be utilized to address this optimization problem. Exploring various

optimization techniques will assist in identifying the most appropriate optimization method for application.

5.2.2. Expanding the prediction horizon:

It is widely acknowledged that selecting longer prediction horizons improves the closed-loop efficacy of control systems, such as Finite Set Model Predictive Current Control. To discover the optimal input sequence for FS-MPCC with longer horizons in practice, it is necessary to tackle a complex optimization problem. This constraint prompted the quest for suboptimal solutions based on the stability results presented in this thesis. To facilitate the practical application of longer horizons in FS-MPCC, more efficient algorithms that can solve the optimization problem in a reasonable period must be developed.

5.2.3. Compare with other state-of-the-art techniques:

FS-MPCC is a relatively new control technique, and alternative state-of-the-art approaches are continuously being developed. Comparing FS-MPCC performance to other cutting-edge methodologies may help find areas for development and further evaluate the MPCC algorithm's effectiveness.

5.2.4. Extension of MPCC to other power electronics systems:

While most FS-MPCC research has concentrated on three-phase inverters, there is potential for its application to other power electronics systems such as single-phase inverters and rectifiers. Investigating the applicability of FS-MPCC to various systems can widen its range of applications.

5.2.5. MPCC performance under diverse operating situations:

FS-MPCC has demonstrated promising results under steady-state settings, but its performance under dynamic conditions, such as during transients or in the presence of disturbances, is yet unknown. More study is needed to examine the performance of MPCC under varied operating conditions.

REFERENCES

Abbaszadeh, A. *et al.* (2017) 'Simplified model predictive control with variable weighting factor for current ripple reduction', *IET Power Electronics*, 10(10), pp. 1165–1174. doi: 10.1049/iet-pel.2016.0483.

Adam, G. P. *et al.* (2017) 'Improved Two-Level Voltage Source Converter for High-Voltage Direct Current Transmission Systems', *IEEE Journal of Emerging and Selected Topics in Power Electronics*, 5(4), pp. 1670–1686. doi: 10.1109/JESTPE.2017.2723839.

Al-Shamma'a, A. A. *et al.* (2018) 'Multilevel converter by cascading two-level three-phase voltage source converter', *Energies*, 11(4), pp. 1–15. doi: 10.3390/en11040843.

Al-Shetwi, A. Q. (2022) 'Sustainable development of renewable energy integrated power sector: Trends, environmental impacts, and recent challenges', *Science of the Total Environment*, 822. doi: 10.1016/j.scitotenv.2022.153645.

Alhasheem, M., Dragicevic, T., *et al.* (2018) 'Evaluation of multi predictive controllers for a two-level three-phase stand-alone voltage source converter', *Proceedings - 2017 IEEE Southern Power Electronics Conference, SPEC 2017*, 2018-Janua(1), pp. 1–6. doi: 10.1109/SPEC.2017.8333633.

Alhasheem, M., Abdelhakim, A., *et al.* (2018) 'Performance assessment of the VSC using two model predictive control schemes', *Conference Proceedings - IEEE Applied Power Electronics Conference and Exposition - APEC*, 2018-March, pp. 450–457. doi: 10.1109/APEC.2018.8341050.

Alkorta Egiguren, P. *et al.* (2008) 'SVPWM linear Generalized Predictive Control of induction motor drives', *IEEE International Symposium on Industrial Electronics*, pp. 588–593. doi: 10.1109/ISIE.2008.4677102.

Allerhand, A. (2021) 'A Contrarian History of Early Electric Power Distribution [History]', *IEEE Industry Applications Magazine*, 27(1), pp. 9–19. doi: 10.1109/MIAS.2020.3028630.

Almaktoof, A. *et al.* (2017) 'Predictive current-controlled converters for RE optimisation', (January).

Almaktoof, A. M. *et al.* (2014) 'Modeling and Simulation of Three-Phase Voltage Source Inverter Using a Model Predictive Current Control', 5(1), pp. 9–13. doi: 10.7763/IJIMT.2014.V5.477.

Almaktoof, A., Raji, A. and Kahn, M. (2013) 'Finite Set-Model Predictive Current control of three-phase voltage source inverter for Renewable Energy Systems (RES) applications', *The 12 International Conference on Sustainable Energy Technologies (SET 2013 …*, (August).

Alsokhiry, F. *et al.* (2019) 'Modular two-level voltage source converter for direct current transmission systems', *Proceedings of the 2018 5th International Symposium on Environment-Friendly Energies and Applications, EFEA 2018*. doi: 10.1109/EFEA.2018.8617108.

Ashraf, N. *et al.* (2020) 'A new single-phase direct frequency controller having reduced switching count without zero-crossing detector for induction heating system', *Electronics (Switzerland)*, 9(3). doi: 10.3390/electronics9030430.

Bacheti, G. G. *et al.* (2022) 'Model-Based Predictive Control with Graph Theory Approach Applied to Multilevel Back-to-Back Cascaded H-Bridge Converters', *Electronics (Switzerland)*, 11(11). doi: 10.3390/electronics11111711.

Bakeer, A., Alhasheem, M. and Peyghami, S. (2022) 'Efficient Fixed-Switching Modulated Finite Control Set-Model Predictive Control Based on Artificial Neural Networks', *Applied Sciences (Switzerland)*, 12(6). doi: 10.3390/app12063134.

Balaji, V. and Rajaji, L. (2013) 'Comparative Study of Pid and Mpc Controller Using Lab View', *International Journal of Advanced Research in Electrical, Electronics and Instrumentation Energy*, pp. 5545–5550.

Barrero, F. *et al.* (2009) 'A proof of concept study of predictive current control for VSI-driven asymmetrical dual three-phase AC machines', *IEEE Transactions on Industrial Electronics*, 56(6), pp. 1937–1954. doi: 10.1109/TIE.2008.2011604.

Bauer, J. (2010) 'Single Phase Voltage Source Inverter Photovoltaic Application', *Acta Polytechnica*, 50(4), pp. 7–11. doi: 10.14311/1217.

Beccuti, A. G. *et al.* (2009) 'Explicit model predictive control of DC-DC switched-mode power supplies with extended kalman filtering', *IEEE Transactions on Industrial Electronics*, 56(6), pp. 1864–1874. doi: 10.1109/TIE.2009.2015748.

Bharanikumar, R., Senthilkumar, R. and Kumar, A. N. (2008) 'Impedance source inverter for wind turbine driven permanent magnet generator', *2008 Joint International Conference on Power System Technology POWERCON and IEEE Power India Conference, POWERCON 2008*. doi: 10.1109/ICPST.2008.4745263.

Bi, C. *et al.* (2022) 'Power optimization control of VSC-HVDC system for electromechanical oscillation suppression and grid frequency control', *Frontiers in Energy Research*, 10. doi: 10.3389/fenrg.2022.1089465.

Blaabjerg, F., Liserre, M. and Ma, K. (2012) 'Power electronics converters for wind turbine systems', *IEEE Transactions on Industry Applications*, 48(2), pp. 708–719. doi: 10.1109/TIA.2011.2181290.

Blaabjerg, F. and Round, S. (2021) 'Power electronics: revolutionizing the world's future energy systems', *Hitachi Energy*. Available at: https://www.hitachienergy.com/es/es/news/perspectives/2021/08/power-electronics-revolutionizing-the-world-s-future-energy-systems.

Bode, G. H. *et al.* (2005) 'An improved robust predictive current regulation algorithm', *IEEE Transactions on Industry Applications*, 41(6), pp. 1720–1733. doi: 10.1109/TIA.2005.858324.

Bordons, C. and Camacho, E. F. (1998) 'A generalized predictive controller for a wide class of industrial processes', *IEEE Transactions on Control Systems Technology*, 6(3), pp. 372–387. doi: 10.1109/87.668038.

Bordry, F. (2004) 'Power converters : definitions , classification and converter topologies', *CAS - CERN Accelerator School and CLRC Daresbury Laboratory : Specialised CAS Course on Power Converters*, (Laboratoire d'Electrotechnique et d'Electronique Industrielle, Toulouse, France), pp. 13–42.

Bordry, F. and Aguglia, D. (2018) 'Definition of Power Converters', *CERN Accelerator School: Power Converters, CAS 2014 - Proceedings*, pp. 15–43. doi: 10.5170/CERN-2015-003.15.

Brahmi, H. and Dhifaoui, R. (2021) 'A Study of a DC/AC Conversion Structure for Photovoltaic System Connected to the Grid with Active and Reactive Power Control', *Complexity*, 2021. doi: 10.1155/2021/9967577.

Buccella, C., Cecati, C. and Latafat, H. (2012) 'Digital control of power converters - A survey', *IEEE Transactions on Industrial Informatics*, 8(3), pp. 437–447. doi: 10.1109/TII.2012.2192280.

Buckner, C. A. *et al.* (2016) 'We are IntechOpen , the world ' s leading publisher of Open Access books Built by scientists , for scientists TOP 1 %', *Intech*, 11(tourism), p. 13. Available at: https://www.intechopen.com/books/advanced-biometric-technologies/liveness-detection-in-biometrics.

Chen, J. *et al.* (2020) 'A Backpropagation Neural Network-Based Explicit Model Predictive Control for DC-DC Converters with High Switching Frequency', *IEEE Journal of Emerging and Selected Topics in Power Electronics*, 8(3), pp. 2124–2142. doi: 10.1109/JESTPE.2020.2968475.

Christensen, V. (2009) 'Fundamentals of wind energy', *WIT Transactions on State of the Art in Science and Engineering*, 34, pp. 1755–8336. doi: 10.2495/978-1-84564.

Clarke, D. W., Mohtadi, C. and Tuffs, P. S. (1987) 'Generalized predictive control-Part I. The basic algorithm', *Automatica*, 23(2), pp. 137–148. doi: 10.1016/0005-1098(87)90087-2.

Correa, P., Pacas, M. and Rodríguez, J. (2007) 'Predictive torque control for inverter-fed induction machines', *IEEE Transactions on Industrial Electronics*, 54(2), pp. 1073–1079. doi: 10.1109/TIE.2007.892628.

Cortes *et al.* (2012) 'Delay compensation in model predictive current control of a three-phase inverter', *IEEE Transactions on Industrial Electronics*, 59(2), pp. 1323–1325. doi: 10.1109/TIE.2011.2157284.

Cortés *et al.* (2009) 'Guidelines for weighting factors design in model predictive control of power converters and drives', *Proceedings of the IEEE International Conference on Industrial Technology*. doi: 10.1109/ICIT.2009.4939742.

Cortes, P. *et al.* (2008) 'Predictive current control strategy with imposed load current spectrum', *EPE-PEMC 2006: 12th International Power Electronics and Motion Control Conference, Proceedings*, 23(2), pp. 612–618. doi: 10.1109/EPEPEMC.2006.283088.

Cortés, P., Rodríguez, J., *et al.* (2008) 'Direct power control of an AFE using predictive control', *IEEE Transactions on Power Electronics*, 23(5), pp. 2516–2523. doi: 10.1109/TPEL.2008.2002065.

Cortés, P., Kazmierkowski, M. P., *et al.* (2008) 'Predictive control in power electronics and drives', *IEEE Transactions on Industrial Electronics*, 55(12), pp. 4312–4324. doi: 10.1109/TIE.2008.2007480.

Cortés, P., Vattuone, L., *et al.* (2009) 'A method of predictive current control with reduced number of calculations for five-phase voltage source inverters', *IECON Proceedings (Industrial Electronics Conference)*, pp. 53–58. doi: 10.1109/IECON.2009.5414805.

Cortés, P., Ortiz, G., *et al.* (2009) 'Model predictive control of an inverter with output LC filter for UPS applications', *IEEE Transactions on Industrial Electronics*, 56(6), pp. 1875–1883. doi: 10.1109/TIE.2009.2015750.

Dahidah, M. S. A. and Agelidis, V. G. (2008) 'Selective harmonic elimination PWM control for cascaded multilevel voltage source converters: A generalized formula', *IEEE Transactions on Power Electronics*, 23(4), pp. 1620–1630. doi: 10.1109/TPEL.2008.925179.

Dahono, P. A. and Dahono, A. (2021) 'New Family of Voltage-Source Converters Derived Using New Basic Cell for Microgrid Applications', pp. 1–5. doi: 10.1109/ichveps53178.2021.9601101.

Dai, N., Lam, C. S. and Zhang, W. (2014) 'Multifunctional voltage source inverter for renewable energy integration and power quality conditioning', *Scientific World Journal*,

2014. doi: 10.1155/2014/421628.

Danial W. Hart (2011) 'Power Electronic', p. 20. Available at: https://d1wqtxts1xzle7.cloudfront.net/34499421/PE-libre.pdf?1408611897=&response-content-disposition=attachment%3B+filename%3DPOWER_ELECTRONIC_CONVERTERS.pdf&Expires=1658140528&Signature=XV7r1FEGA~sRZ1vABoeyENnlKtVNsw-ouWgcnG9HCDsWvUJ4ejGCaUzG7dBeFRT83y2d.

Das, C. K. *et al.* (2018) 'Overview of energy storage systems in distribution networks: Placement, sizing, operation, and power quality', *Renewable and Sustainable Energy Reviews*, 91, pp. 1205–1230. doi: 10.1016/j.rser.2018.03.068.

Davoodnezhad, R., Holmes, D. G. and McGrath, B. P. (2014) 'A novel three-level hysteresis current regulation strategy for three-phase three-level inverters', *IEEE Transactions on Power Electronics*, 29(11), pp. 6100–6109. doi: 10.1109/TPEL.2013.2295597.

Dragičević, T. and Novak, M. (2019) 'Weighting Factor Design in Model Predictive Control of Power Electronic Converters: An Artificial Neural Network Approach', *IEEE Transactions on Industrial Electronics*, 66(11), pp. 8870–8880. doi: 10.1109/TIE.2018.2875660.

Dsa, D., Uma, L. and Bindu, S. (2019) 'Performance Comparison of Two-Level Voltage Source Converter with Sinusoidal PWM and Space Vector PWM for HVDC Application', *2019 International Conference on Nascent Technologies in Engineering, ICNTE 2019 - Proceedings*, (Icnte). doi: 10.1109/ICNTE44896.2019.8945916.

Duran, M. J. *et al.* (2011) 'Predictive current control of dual three-phase drives using restrained search techniques', *IEEE Transactions on Industrial Electronics*, 58(8), pp. 3253–3263. doi: 10.1109/TIE.2010.2087297.

Durna, E. (2018) 'Adaptive fuzzy hysteresis band current control for reducing switching losses of hybrid active power filter', *IET Power Electronics*, 11(5), pp. 937–944. doi: 10.1049/iet-pel.2017.0560.

Effler, S. *et al.* (2008) 'Automated optimization of generalized model predictive control for DC-DC converters', *PESC Record - IEEE Annual Power Electronics Specialists Conference*, pp. 134–139. doi: 10.1109/PESC.2008.4591913.

El-Kholy, E. E. (2005) 'Generalized predictive controller for a boost AC to DC converter fed DC motor', *Proceedings of the International Conference on Power Electronics and Drive Systems*, 2, pp. 1090–1095. doi: 10.1109/peds.2005.1619850.

El-Saady, G., Ibrahim, E. N. A. and Gelany, M. (2017) 'Voltage regulation of stand-alone variable speed wind energy system', *2016 18th International Middle-East Power Systems Conference, MEPCON 2016 - Proceedings*, (1), pp. 360–366. doi: 10.1109/MEPCON.2016.7836916.

Fewson, D. (2015) 'Introduction to Power Electronics', *IEEE Power Engineering Review*, 19(9), p. 44. doi: 10.1109/MPER.1999.785806.

Firdoush, S. *et al.* (2016) 'Reduction of Harmonics in Output Voltage of Inverter', *International Journal of Engineering Research & Technology*, 4(02), pp. 1–6. Available at: www.ijert.org.

Gao, X. *et al.* (2022) 'Model-Predictive Control for Modular Multilevel Converters Operating at Wide Frequency Range with a Novel Cost Function', *IEEE Transactions on Industrial Electronics*, 69(6), pp. 5569–5580. doi: 10.1109/TIE.2021.3090705.

Goodwin, G. C., Seron, M. M. and Dona, J. A. de (2005) 'Constrained Control and

Estimation: an Optimization Approach', *New York: Springer-Verlag*. doi: 10.1177/0261018311403863.

Gu, X. *et al.* (2023) 'Three-Level Inverter-PMSM Model Predictive Current Control Based on the Extended Control Set', *Electronics (Switzerland)*, 12(3). doi: 10.3390/electronics12030557.

Guarnieri, M. (2018) 'Solidifying Power Electronics [Historical]', *IEEE Industrial Electronics Magazine*, 12(1), pp. 36–40. doi: 10.1109/MIE.2018.2791062.

Hamid, F. A. *et al.* (2020) 'Design and simulation of single phase inverter using SPWM unipolar technique', *Journal of Physics: Conference Series*, 1432(1). doi: 10.1088/1742-6596/1432/1/012021.

Han, Jingang *et al.* (2016) 'Simplified Finite Set Model Predictive Control Strategy of Grid-Connected Cascade H-Bridge Converter', *Journal of Control Science and Engineering*, 2016. doi: 10.1155/2016/9478387.

Hannan, M. A. *et al.* (2019) 'Power electronics contribution to renewable energy conversion addressing emission reduction: Applications, issues, and recommendations', *Applied Energy*, 251(May), p. 113404. doi: 10.1016/j.apenergy.2019.113404.

Hassaine, S. *et al.* (2007) 'Robust speed control of PMSM using generalized predictive and direct torque control techniques', *IEEE International Symposium on Industrial Electronics*, pp. 1213–1218. doi: 10.1109/ISIE.2007.4374771.

Hassanein, A. M. *et al.* (2022) 'Active and passive sensitivity analysis for the second-order active RC filter families using operational amplifier: a review', *Analog Integrated Circuits and Signal Processing*, 113(2), pp. 257–286. doi: 10.1007/s10470-022-02079-y.

He, Z. *et al.* (2016) 'Model predictive control of modular multilevel converters', *Zhongguo Dianji Gongcheng Xuebao/Proceedings of the Chinese Society of Electrical Engineering*, 36(5), pp. 1366–1375. doi: 10.13334/j.0258-8013.pcsee.2016.05.023.

Holtz, J. (1994) 'Pulsewidth Modulation for Electronic Power Conversion', *Proceedings of the IEEE*, 82(8), pp. 1194–1214. doi: 10.1109/5.301684.

Holtz, J. and Stadtfeld, S. (1983) 'A predictive controller for the stator current vector of AC machines fed from a switched voltage source', *in International Power Electronics Conference, IPEC, Tokyo,* pp. 1665–1675.

Hsieh, F. H. *et al.* (2012) 'Study on dynamic phenomena in voltage-mode controlled single-phase half-bridge inverters', *Proceedings - International Conference on Machine Learning and Cybernetics*, 5, pp. 1913–1920. doi: 10.1109/ICMLC.2012.6359668.

Hu, J. and Cheng, K. W. E. (2017) 'Predictive control of power electronics converters in renewable energy systems', *Energies*, 10(4). doi: 10.3390/en10040515.

IEA (2021) 'Net Zero by 2050: A Roadmap for the Global Energy Sector', *International Energy Agency*, p. 224. Available at: https://www.iea.org/reports/net-zero-by-2050.

Jalili, S. (2018) 'A novel hybrid model predictive control design with application to a quadrotor helicopter', (November 2017), pp. 1301–1322. doi: 10.1002/oca.2411.

José, R. *et al.* (2009) 'Multilevel converters: An enabling technology for high-poer applications', *Proceedings of the IEEE*, 97(11), pp. 1786–1817. doi: 10.1109/JPROC.2009.2030235.

Katyara, S., Hashmani, A. H. and Chowdhry, B. S. (2020) 'Development and Analysis

of Pulse Width Modulation Techniques for Induction Motor Control', *Mehran University Research Journal of Engineering and Technology*, 39(1), pp. 81–96. doi: 10.22581/muet1982.2001.09.

Kazmierkowski, M. P., Krishnan, R. and Blaabjerg, F. (2002) 'Control in Power Electronics', *Academic Press*.

Kennel, R., Linder, A. and Linke, M. (2001) 'Generalized Predictive Control (GPC) - Ready for use in drive applications?', *PESC Record - IEEE Annual Power Electronics Specialists Conference*, 4, pp. 1839–1844. doi: 10.1109/pesc.2001.954389.

Khan, H. S. *et al.* (2021) 'Improved finite control set model predictive control for distributed energy resource in islanded microgrid with fault-tolerance capability', *Engineering Science and Technology, an International Journal*, 24(3), pp. 694–705. doi: 10.1016/j.jestch.2020.12.015.

Kouro, S. *et al.* (2009) 'Model predictive control - A simple and powerful Method to control power converters', *IEEE Transactions on Industrial Electronics*, 56(6), pp. 1826–1838. doi: 10.1109/TIE.2008.2008349.

Kouro, S. *et al.* (2015) 'Model Predictive Control: MPC's Role in the Evolution of Power Electronics', *IEEE Industrial Electronics Magazine*, 9(4), pp. 8–21. doi: 10.1109/MIE.2015.2478920.

Kukrer, O. (1996) 'Discrete-time current control of voltage-fed three-phase PWM inverters', *IEEE Transactions on Power Electronics*, 11(2), pp. 260–269. doi: 10.1109/63.486174.

Kumar, V. *et al.* (2014) 'High performance predictive current control of a three phase VSI: An experimental assessment', *Sadhana - Academy Proceedings in Engineering Sciences*, 39(6), pp. 1295–1310. doi: 10.1007/s12046-014-0298-6.

Ławryńczuk, M. and Nebeluk, R. (2021) 'Computationally efficient nonlinear model predictive control using the L1 cost-function', *Sensors*, 21(17). doi: 10.3390/s21175835.

Lee, J. H. (2011) 'Model predictive control: Review of the three decades of development', *International Journal of Control, Automation and Systems*, 9(3), pp. 415–424. doi: 10.1007/s12555-011-0300-6.

Lepanov, M. and Rozanov, Y. (2013) 'Multifunctional regulator based on SMES and power electronic converter for increase of power quality and power supply reliability', *International Conference on Power Engineering, Energy and Electrical Drives*, 5, pp. 1387–1391. doi: 10.1109/PowerEng.2013.6635817.

Li, Y. and Quan, Z. (2017) 'Derivation of multilevel voltage source converter topologies for medium voltage drives', *Chinese Journal of Electrical Engineering*, 3(2), pp. 24–31. doi: 10.23919/CJEE.2017.8048409.

Lindblom, H. and Lindblom, H. (2019) 'Design and construction of a voltage source converter for a laboratory setup for a laboratory setup'.

Lipu, M. S. H. *et al.* (2022) 'Power Electronics Converter Technology Integrated Energy Storage Management in Electric Vehicles: Emerging Trends, Analytical Assessment and Future Research Opportunities', *Electronics (Switzerland)*, 11(4). doi: 10.3390/electronics11040562.

Low, K. S. (1998) 'A digital control technique for a single-phase PWM inverter', *IEEE Transactions on Industrial Electronics*, 45(4), pp. 672–674. doi: 10.1109/41.704897.

M. H. Rashid (2007) 'Devices, Circuits, and Applications', *Power Electronics*

Handbook, pp. 245–259.

Maciejowski, J. M. (2002) 'Predictive Control: With Constraints', *Englewood Cliffs, NJ: Prentice Hall,* p. 331. Available at: http://books.google.com/books?id=HV_Y58c7KiwC&pgis=1.

Mantilla Arias, M. P. *et al.* (2021) 'Simulation of the DC-AC Converter Control for an Isolated PV System', *2021 Brazilian Power Electronics Conference, COBEP 2021*. doi: 10.1109/COBEP53665.2021.9684096.

Mariéthoz, S. and Morari, M. (2009) 'Explicit model-predictive control of a PWM inverter with an LCL filter', *IEEE Transactions on Industrial Electronics*, 56(2), pp. 389–399. doi: 10.1109/TIE.2008.2008793.

Mohammed, S. A., A, A.-M. M. and Hasanin, B. (2013) 'A Review of the State-Of-The-Art of Power Electronics For Power System Applications', *Quest Journals Journal of Electronics and Communication Engineering Research Volume1 ~ Issue1*, 1, pp. 43–52. Available at: https://pdfs.semanticscholar.org/3037/a22335e929c7ba266d689339ba7a10de5c54.pdf.

Mohan, N., Undeland, T. M. and Robbins, W. P. (2003) 'Power electronics', *3rd ed. John Wiley & Sons, Inc*.

Moon, H. T., Kim, H. S. and Youn, M. J. (2003) 'A discrete-time predictive current control for PMSM', *IEEE Transactions on Power Electronics*, 18(1 II), pp. 464–472. doi: 10.1109/TPEL.2002.807131.

Morari, M., Garcia, C. E. and Prett, D. M. (1988) 'Model predictive control: Theory and practice', *IFAC Proceedings Volumes*, 21(4), pp. 1–12. doi: 10.1016/b978-0-08-035735-5.50006-1.

Müller, S., Ammann, U. and Rees, S. (2005) 'New time-discrete modulation scheme for matrix converters', *IEEE Transactions on Industrial Electronics*, 52(6), pp. 1607–1615. doi: 10.1109/TIE.2005.858713.

Nascimento, T. P., Dórea, C. E. T. and Gonçalves, L. M. G. (2018) 'Nonlinear model predictive control for trajectory tracking of nonholonomic mobile robots: A modified approach', *International Journal of Advanced Robotic Systems*, 15(1). doi: 10.1177/1729881418760461.

Navpreet, T. *et al.* (2012) 'Voltage Source Converters as the building block of HVDC and FACTS Technology in Power Transmission System: A Simulation based Approach'. Available at: www.pelagiaresearchlibrary.com.

P. Tenca, A. A. Rockhill, T. A. Lipo, and P. T. (2008) 'Current source topology for wind turbines with decreased mains current harmonics, further reducible via functional minimization', *IEEE Trans. Power Electron*, 23(3), pp. 1143–1155.

Pandey, R. K., Purwar, V. and Sharma, N. (2017) 'Hysteresis Current Control Based Shunt Active Power Filter for Six Pulse Ac/Dc Converter', *International Journal of Engineering Research and Applications*, 07(02), pp. 26–30. doi: 10.9790/9622-0702012630.

Parihar, S. *et al.* (2022) 'Model Predictive Control and Its Role in Biomedical Therapeutic Automation: A Brief Review', *Applied System Innovation*, 5(6). doi: 10.3390/asi5060118.

Patel, J. and Sood, V. K. (2018) 'Review of Digital Controllers in Power Converters', *2018 IEEE Electrical Power and Energy Conference, EPEC 2018*, (March), pp. 1–8. doi: 10.1109/EPEC.2018.8598434.

Patel, N. A. and Baria, J. C. (2016) 'A Hysteresis Current Control Technique for Electronics Convertor', pp. 2203–2210. doi: 10.15680/IJIRSET.2016.0502106.

Qian Ping and Zhang Yong (2011) 'Study on Hysteresis Current Control and Its Applications in Power Electronics', pp. 889–895.

Quan, Z. and Li, Y. W. (2019) 'Impact of PWM Schemes on the Common-Mode Voltage of Interleaved Three-Phase Two-Level Voltage Source Converters', *IEEE Transactions on Industrial Electronics*, 66(2), pp. 852–864. doi: 10.1109/TIE.2018.2831195.

Rajagopalan, A. *et al.* (2022) 'Modernized Planning of Smart Grid Based on Distributed Power Generations and Energy Storage Systems Using Soft Computing Methods', *Energies*, 15(23). doi: 10.3390/en15238889.

Raju, M. N. *et al.* (2019) 'Modular multilevel converters technology: A comprehensive study on its topologies, modelling, control and applications', *IET Power Electronics*, 12(2), pp. 149–169. doi: 10.1049/iet-pel.2018.5734.

Rameshkumar, K. *et al.* (2014) 'Performance Analysis of Model Predictive Control for Voltage Source Inverter', *2014 International Conference on Green Computing Com munication and Electrical Engineering (ICGCCEE)*, (1), pp. 1–5. doi: 10.1109/ICGCCEE.2014.6922380.

Rao, R. K. *et al.* (2014) 'Design and Analysis of Various Inverters Using Different Pwm Techniques', *The International Journal Of Engineering And Science (IJES) ISSN*, pp. 2319–1813.

Rivera, M. *et al.* (2017) 'Indirect predictive control techniques for a matrix converter operating at fixed switching frequency', *Proceedings - 2017 IEEE International Symposium on Predictive Control of Electrical Drives and Power Electronics, PRECEDE 2017*, pp. 13–18. doi: 10.1109/PRECEDE.2017.8071101.

Rodriguez and Cortes (2015) *Predictive Control of Power Converters and Electrical Drives*, *Foreign Affairs*. doi: 10.1017/CBO9781107415324.004.

Rodríguez, J. *et al.* (2007) 'Predictive current control of a voltage source inverter', *PESC Record - IEEE Annual Power Electronics Specialists Conference*, 54(1), pp. 495–503.

Rodriguez, J. and Cortes, P. (2012) *Predictive Control of Power Converters and Electrical Drives*, *Predictive Control of Power Converters and Electrical Drives*. doi: 10.1002/9781119941446.

Roselyn *et al.* (2020) 'DEVELOPMENT OF HYSTERESIS CURRENT CONTROLLER FOR POWER QUALITY ENHANCEMENT IN GRID CONNECTED PV', 11(4), pp. 8–21.

Salem, M. *et al.* (2022) 'A Comprehensive Review on Multilevel Inverters for Grid-Tied System Applications', *Energies*, 15(17). doi: 10.3390/en15176315.

Sandre-Hernandez, O., De Jesus Rangel-Magdaleno, J. and Morales-Caporal, R. (2019) 'Modified model predictive torque control for a PMSM-drive with torque ripple minimisation', *IET Power Electronics*, 12(5), pp. 1033–1042. doi: 10.1049/iet-pel.2018.5525.

Schwenzer, M. *et al.* (2021) 'Review on model predictive control: an engineering perspective', *International Journal of Advanced Manufacturing Technology*, 117(5–6), pp. 1327–1349. doi: 10.1007/s00170-021-07682-3.

Scoltock, J., Geyer, T. and Madawala, U. K. (2013) 'A comparison of model predictive control schemes for MV induction motor drives', *IEEE Transactions on Industrial*

Informatics, 9(2), pp. 909–919. doi: 10.1109/TII.2012.2223706.

Seetharamaiah, A. (2008) 'Modeling of Hysteresis Current Control Technique for Three Phase PV Based VSI using MATLAB/Simulink', *International Research Journal of Engineering and Technology*, 9001, p. 1738. Available at: www.irjet.net.

Sener, E. and Ertasgin, G. (2022) 'Design of a Half-Bridge Current-Source Inverter Topology for Avionic Systems', *Aerospace*, 9(7), pp. 1–16. doi: 10.3390/aerospace9070354.

Shanono, I. H., Abdullah, N. R. H. and Muhammad, A. (2018) 'A Survey of Multilevel Voltage Source Inverter Topologies, Controls, and Applications', *International Journal of Power Electronics and Drive Systems (IJPEDS)*, 9(3), p. 1186. doi: 10.11591/ijpeds.v9.i3.pp1186-1201.

Shen, Y. W. *et al.* (2019) 'Finite Control Set Model Predictive Control for Complex Energy System with Large-Scale Wind Power', *Complexity*, 2019. doi: 10.1155/2019/4358958.

Shiravani, F. *et al.* (2022) 'An improved predictive current control for IM drives', *Ain Shams Engineering Journal*. doi: 10.1016/j.asej.2022.102037.

Singh, S. K. *et al.* (2014) 'a Survey and Study of Different Types of Pwm Techniques Used in Induction Motor Drive', (1), pp. 18–22.

Slimani, K. and Viarouge, P. (1994) 'Analysis and Implementation of a Real-Time Predictive Current Controller for Permanent-Magnet Synchronous Servo Drives', *IEEE Transactions on Industrial Electronics*, 41(1), pp. 110–117. doi: 10.1109/41.281616.

Stefanutti, W. *et al.* (2006) 'Digital deadbeat control tuning for dc-dc converters using error correlation', *PESC Record - IEEE Annual Power Electronics Specialists Conference*. doi: 10.1109/PESC.2006.1712130.

Suman, Rishi (2017) 'Finite Set Model Predictive Current Control of a Grid Converter Equipped with an LCL Filter'.

Tamrakar, U. *et al.* (2018) 'Comparative analysis of current control techniques to support virtual inertia applications', *Applied Sciences (Switzerland)*, 8(12). doi: 10.3390/app8122695.

Tang, F. *et al.* (2018) 'An Improved Three-Phase Voltage Source Converter with High-Performance Operation under Unbalanced Conditions', *IEEE Access*, 6, pp. 15908–15918. doi: 10.1109/ACCESS.2018.2814200.

Vargas, R. *et al.* (2007) 'Predictive Control of a Three-Phase', *IEEE Transactions on Industrial Electronics*, 54(5), pp. 2697–2705.

Vargas, R. *et al.* (2008) 'Predictive strategy to control common-mode voltage in loads fed by matrix converters', *IEEE Transactions on Industrial Electronics*, 55(12), pp. 4372–4380. doi: 10.1109/TIE.2008.2007016.

Vargas, R. *et al.* (2010) 'Predictive torque control of an induction machine fed by a matrix converter with reactive input power control', *IEEE Transactions on Power Electronics*, 25(6), pp. 1426–1438. doi: 10.1109/TPEL.2010.2040839.

Vazquez, N. *et al.* (2010) 'A six-switch three-level current source inverter', *International Power Electronics Congress - CIEP*, (August), pp. 145–148. doi: 10.1109/CIEP.2010.5598847.

Vazquez, S. *et al.* (2014) 'Model predictive control: A review of its applications in power electronics', *IEEE Industrial Electronics Magazine*, 8(1), pp. 16–31. doi:

10.1109/MIE.2013.2290138.

Verbytskyi, I. *et al.* (2022) 'Power Converter Solutions for Industrial PV Applications—A Review', *Energies*, 15(9). doi: 10.3390/en15093295.

Walz, S. and Liserre, M. (2020) 'Hysteresis model predictive current control for PMSM with LC filter considering different error shapes', *IEEE Open Journal of Power Electronics*, 1, pp. 190–197. doi: 10.1109/OJPEL.2020.3000466.

Wang, F. *et al.* (2009) 'Voltage source inverter', *IEEE Industry Applications Magazine*, 15(2), pp. 24–33. doi: 10.1109/MIAS.2009.931826.

Wang, H. *et al.* (2021) 'An improved hysteresis current control scheme during grid voltage zero-crossing for grid-connected three-level inverters', *IET Power Electronics*, 14(11), pp. 1946–1959. doi: 10.1049/pel2.12161.

Watson, N. R. and Watson, J. D. (2020) 'An overview of HVDC technology', *Energies*, 13(17). doi: 10.3390/en13174342.

Xu, J. *et al.* (2020) 'Model Predictive Control for the Reduction of DC-link Current Ripple in Two-level Three-phase Voltage Source Inverters', *2020 22nd European Conference on Power Electronics and Applications, EPE 2020 ECCE Europe*, pp. 1–9. doi: 10.23919/EPE20ECCEEurope43536.2020.9215838.

Young, H. A. *et al.* (2020) 'Simple Finite-Control-Set Model Predictive Control of Grid-Forming Inverters with LCL Filters', *IEEE Access*, 8, pp. 81246–81256. doi: 10.1109/ACCESS.2020.2991396.

Zeng, Q. and Chang, L. (2008) 'An advanced SVPWM-based predictive current controller for three-phase inverters in distributed generation systems', *IEEE Transactions on Industrial Electronics*, 55(3), pp. 1235–1246. doi: 10.1109/TIE.2007.907674.

Zhang, D. *et al.* (2022) 'Review and outlook of global energy use under the impact of COVID-19', *Engineering Reports*, (May 2022), pp. 1–23. doi: 10.1002/eng2.12584.

Zhang, G. *et al.* (2018) 'Power electronics converters: Past, present and future', *Renewable and Sustainable Energy Reviews*, 81(June), pp. 2028–2044. doi: 10.1016/j.rser.2017.05.290.

Zhang, W. *et al.* (2003) 'Analysis and implementation of a new PFC digital control method', *PESC Record - IEEE Annual Power Electronics Specialists Conference*, 1, pp. 335–340. doi: 10.1109/pesc.2003.1218315.

Zhang, W. *et al.* (2021) 'A Multiple Open-Circuit Fault Diagnosis Method for Two-Level Three-Phase Voltage Source Converters Based on Average Phase Voltage Model', *IEEE Journal of Emerging and Selected Topics in Power Electronics*, 6777(c). doi: 10.1109/JESTPE.2021.3096851.

Zietsman, M. *et al.* (2022) 'Cost-benefit analysis of wind power integration in distribution networks', *Journal of Energy in Southern Africa*, 33(1), pp. 21–39. doi: 10.17159/2413-3051/2022/v33i1a9344.